

PREMIO TESI DI DOTTORATO

– 66 –

PREMIO TESI DI DOTTORATO
Commissione giudicatrice, anno 2016

Vincenzo Varano, *Presidente della Commissione*

Tito Arecchi, *Area Scientifica*

Aldo Bompani, *Area delle Scienze Sociali*

Franco Cambi, *Area Umanistica*

Mario Caciagli, *Area delle Scienze Sociali*

Paolo Felli, *Area Tecnologica*

Siro Ferrone, *Area Umanistica*

Roberto Genesisio, *Area Tecnologica*

Flavio Moroni, *Area Biomedica*

Adolfo Pazzagli, *Area Biomedica*

Giuliano Pinto, *Area Umanistica*

Vincenzo Schettino, *Area Scientifica*

Luca Uzielli, *Area Tecnologica*

Graziella Vescovini, *Area Umanistica*

Tiberio Uricchio

Image Understanding by Socializing the Semantic Gap

Firenze University Press
2017

Tiberio Uricchio, *Image Understanding by Socializing the Semantic Gap*, ISBN 978-88-6453-576-0 (print), ISBN 978-88-6453-577-7 (online) © 2017 Firenze University Press

Image Understanding by Socializing the Semantic Gap
/ Tiberio Uricchio. – Firenze : Firenze University Press,
2017.

(Premio Tesi di Dottorato ; 66)

<http://digital.casalini.it/9788864535777>

ISBN 978-88-6453-576-0 (print)

ISBN 978-88-6453-577-7 (online)

Front cover design: Alberto Pizarro Fernández, Pagina Maestra snc

Front cover photo: © Italianestro | Dreamstime

Peer Review Process

All publications are submitted to an external refereeing process under the responsibility of the FUP Editorial Board and the Scientific Committees of the individual series. The works published in the FUP catalogue are evaluated and approved by the Editorial Board of the publishing house. For a more detailed description of the refereeing process we refer to the official documents published on the website and in the online catalogue of the FUP (www.fupress.com).

Consiglio editoriale Firenze University Press

A. Dolfi (Presidente), M. Boddi, A. Bucelli, R. Casalbuoni, M. Garzaniti, M.C. Grisolia, P. Guarnieri, R. Lanfredini, A. Lenzi, P. Lo Nostro, G. Mari, A. Mariani, P.M. Mariano, S. Marinai, R. Minuti, P. Nanni, G. Nigro, A. Perulli, M.C. Torricelli.

This work is licensed under a Creative Commons Attribution 4.0 International License
(CC BY 4.0: <https://creativecommons.org/licenses/by/4.0/legalcode>)

This book is printed on acid-free paper

CC 2017 Firenze University Press
Università degli Studi di Firenze
Firenze University Press
via Cittadella, 7, 50144 Firenze, Italy
www.fupress.com
Printed in Italy

Ai miei genitori

Table of contents

Chapter 1	
Introduction	11
1.1 The goal	11
1.2 Contributions and Organization	14
Chapter 2	
Literature review of Assignment, Renement and Retrieval	17
2.1 Problems and Tasks	18
2.2 Scope and Aims	18
2.3 Foundations	20
2.4 Media for tag relevance	21
2.4.1 Tag based	22
2.4.2 Tag + Image based	23
2.4.3 Tag + Image + User information based	23
2.5 Learning for tag relevance	25
2.5.1 Instance-based	25
2.5.2 Model-based	27
2.5.3 Transduction-based	28
2.6 Auxiliary components	30
2.7 Conclusions	32
Chapter 3	
A new Experimental Protocol	33
3.1 Introduction	33
3.2 Datasets	34
3.3 Implementation and Evaluation	36
3.3.1 Evaluating tag assignment	37
3.3.2 Evaluating tag refinement	37
3.3.3 Evaluating tag retrieval	38
3.4 Methods under analysis	39
3.4.1 SemanticField	39
3.4.2 TagRanking	40
3.4.3 KNN	40
3.4.4 TagVote	41

Image Understanding by Socializing the Semantic Gap

3.4.5 TagProp	41
3.4.6 TagCooccur	42
3.4.7 TagCooccur+	42
3.4.8 TagFeature	42
3.4.9 RelExample	43
3.4.10 RobustPCA	44
3.4.11 TensorAnalysis	45
3.4.12 Considerations	45
3.5 Evaluation	47
3.5.1 Tag assignment	47
3.5.2 Tag refinement	49
3.5.3 Tag retrieval	52
3.5.4 Flickr versus ImageNet	60
3.6 Conclusions	63
Chapter 4	
A Cross Modal Approach for Tag Assignment	65
4.1 Introduction	65
4.1.1 Contribution	68
4.2 Related Work	68
4.3 Approach	69
4.3.1 Visual and Tags Views	70
4.3.2 Kernel Canonical Correlation Analysis	72
4.3.3 Tag Assignment Using Nearest Neighbor Models in the Semantic Space	73
4.4 Experiments	77
4.4.1 Datasets	77
4.4.2 Evaluation Measures	79
4.4.3 Results	79
4.5 Conclusions	82
Chapter 5	
Evaluating Temporal Information in Social Images	85
5.1 Introduction	85
5.2 Data Analysis Method	87
5.2.1 Datasets	87
5.2.2 Temporal features	88
5.2.3 Flickr Popularity Model	89
5.2.4 Processing	90
5.2.5 Correlation analysis	91
5.3 Experiments and Discussion	92
5.3.1 Temporal Evaluation	92
5.3.2 Correlation Analysis	94
5.4 Conclusions	96

Chapter 6	
Multimodal Feature Learning for Sentiment Analysis	99
6.1 Introduction	99
6.2 Previous Work	101
6.3 The Proposed Method	103
6.3.1 Textual information	104
6.3.2 Textual and Visual Information	107
6.4 Experiments	110
6.5 Conclusions	116
Chapter 7	
Popularity Prediction with Sentiment and Context Features	119
7.1 Introduction	119
7.2 Related work	121
7.3 The Proposed Method	122
7.3.1 Measuring Popularity	122
7.3.2 Visual Sentiment Features	122
7.3.3 Object Features	123
7.3.4 Context Features	123
7.3.5 User Features	124
7.3.6 Popularity prediction	124
7.4 Experiments	124
7.4.1 Results	125
7.4.2 Qualitative Analysis	127
7.5 Conclusions	127
Chapter 8	
Conclusion	129
8.1 Summary of Contribution	129
8.2 Direction of future work	130
Appendix A	
Publications	133
Bibliography	137

Chapter 1

Introduction

Sharing images is an essential experience. Be it a drawing carved in rock, a painting exposed in a museum, or a photo capturing a special moment, it is the sharing that relives the experience stored in the image. Several technological developments have spurred the sharing of images in unprecedented volumes. The first is the ease with which images can be captured in a digital format by cameras, cellphones and other wearable sensory devices. The second is the Internet that allows transfer of digital image content to anyone, anywhere in the world. Finally, and most recently, the sharing of digital imagery has reached new heights by the massive adoption of social network platforms. All of a sudden images came with tags, and tagging, commenting, and rating of any digital image has become a common habit. The sharing paradigm is lead by users interactions with each other, like forming groups of shared interests, sharing messages that convey sentiments, and by commenting the photos that have been shared. And consequently, in the huge quantity of available media, some of these images are going to become very popular, while others are going to be totally unnoticed and end up in oblivion.

1.1 The goal

Our ultimate goal is to extract *information* from image collections in social networks. In particular, we aim at obtaining tags, i.e. human interpretable labels associated to the content at a global level. These can be related to objective aspects such as the presence of things, properties and activities, or subjective ones such as the sentiments aroused in a viewer or the attractiveness of an image.

Being able to extract this information can have a great impact in several applications. First, the retrieval of images from collections can be improved. Current image search engines (such as Google or Yahoo), that traditionally rely on the associated text data, have recently exploited the visual content to improve performance. Similarly, in social networks, they mostly rely on user provided metadata in form of tags or textual description. Second,

it can ease the browsing of large collections. For instance, through selection or summarization of the most attractive and significative photos. In particular, sentiments aroused in the viewer can play a role in producing significative output. Third, the distribution and enjoyment of contents can be improved. Advertising and distribution of content can be more efficient when matching content to user preferences. Moreover, to the aim of minimizing storage costs, images may be replicated according to popularity and still maintaining a low latency for unpopular content. For these reasons, image retrieval and understanding receive a lot of attention from both the scientific community and industry.

Machine understanding of media is still very poor. While their data processing capabilities are continuously improving (e.g. Moore’s law (Moore, 1965)), stemming information from unannotated multimedia is a challenging task. The main hindrance is that machines are able to compute only low level features of the data, hardly correlated to the semantics. Tasks such as recognizing things, understanding the sentiment induced in the viewer or predicting the expected attractiveness of an image, require high level features. This is a well-known problem in the literature, formalized as the **semantic gap** (Smeulders et al., 2000): “The semantic gap is the lack of coincidence between the information that machines can extract from the visual data and the interpretations the user may give to the data.”. Hence the ensuing question is:

How can we fill the semantic gap for multimedia understanding?

We believe that Social Networks are promising frameworks that can fill the gap. Comparing to the classic multimedia databases, social networks provide a dilated context where the user is king. Users can contribute by providing photos with attached metadata (such as tags, description, location) or by expressing interest in others content (e.g. likes, comments). In Figures 1.1 and 1.2 we show two examples of such contributions in two different social networks.

Social network contributions are provided by common users. They often cannot meet high quality standards related to content association, in particular for accurately describing objective aspects of the visual content according to some expert’s opinion (Dodge et al., 2012). Moreover, when subjective components are considered (e.g. sentiments), different users may read images differently.

The most historically exploited pieces of metadata are the social tags associated to the images. These tags tend to follow context, trends and events in the real world. They are often used to describe both the situation and the entity represented in the visual content. So tagging deviations due to spatial and temporal correlation to external factors, including user



Figure 1.1: Example of a user generated content on social network Instagram. An image of a bracelet is associated with a little description and several tags. Several users have commented the content.

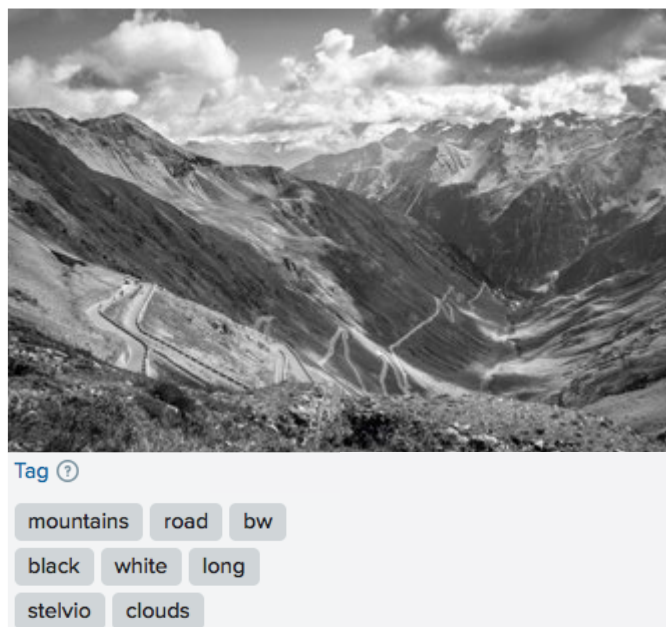


Figure 1.2: Example of a user generated content on social network Flickr. Tags are associated to an image of a panoramic view of a mountain.

influence, semantics of activity and relationships between tags, are common phenomena. Social tags tend to be imprecise, ambiguous, incomplete and biased towards personal perspectives (Golder and Huberman, 2006; Sen et al., 2006; Sigurbjörnsson and van Zwol, 2008; Kennedy et al., 2006).

Quite a few researchers have proposed solutions for image annotation and retrieval in social frameworks (Li et al., 2015), although the peculiarities of this domain have been only partially addressed.

1.2 Contributions and Organization

In this thesis we show that the tagged images shared in social media platforms are promising to resolve the semantic gap. In particular, we focus on image annotation and provide a structured survey of methods in social networks with a thorough empirical evaluation of several key methods. Then we describe four novel state-of-the-art methods for extracting information, that explicitly take into account the social context.

Two themes can be highlighted. The first one is related to the task of objective analysis of images (i.e. recognize things), while the second one relates to the tasks of subjective analysis (i.e. recognize the sentiment induced in viewers, predict the expected popularity of images). In spite of the two themes, the underlying idea of our work is the exploitation of social images through the design of features that comprises both the visual observation *and* their tags. Learned or handcrafted, these features provide a robust global representation of the content and context.

The thesis is organized as follows¹. Considering the absence of a comprehensive review of annotation and retrieval in social networks, we start in Chapter 2 with a structured survey of related work. Although image annotation and retrieval in social networks are a relatively recent direction of research, several tasks have been addressed by the multimedia community. We survey three linked semantic tasks (i.e. tag assignment, tag refinement and tag-based image retrieval) that have seen the most contributions to date. Figure 1.3 shows an example of tag refinement of an image and its associated user tags. Recognizing a lack of a structured survey in the literature, we aimed at giving a reference contribution for future researchers in this field. We organize the rich literature of tagging and retrieval in a taxonomy to highlight the ingredients of the main works and recognize their advantages and limitations. In particular, we structure our survey along the line of understanding how a specific method constructs the underlying tag relevance function.

Witnessing the absence of a thorough empirical comparison in the lit-

¹Note that each chapter is written in a self-contained fashion and can be read on its own.

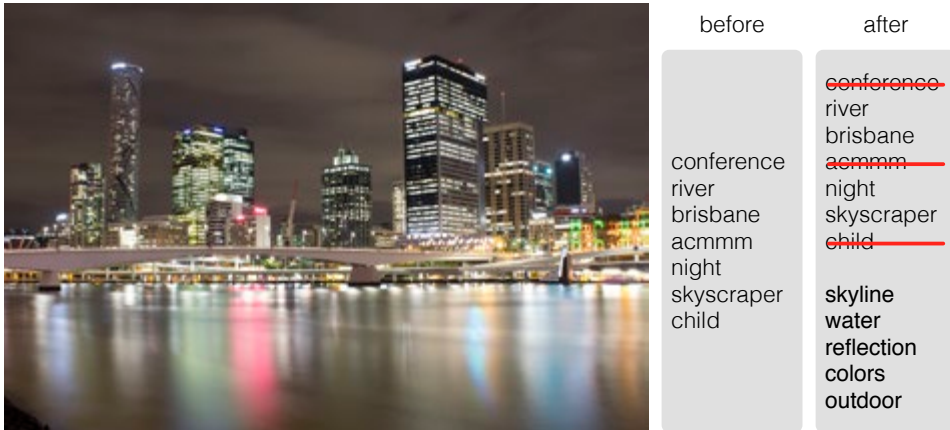


Figure 1.3: An example of an image processed with an algorithm of tag refinement. Not relevant tags are removed and additional relevant tags are added.

erature for the three semantic tasks, in Chapter 3 we establish a common experimental protocol and successively exert it in the evaluation of key methods. Our proposed protocol contains training data of varied scales extracted from social frameworks. This permits to evaluate the methods under analysis with data that reflect the specificity of the social domain. We made the data and source code public so that new proposals for tag assignment, tag refinement, and tag retrieval can be evaluated rigorously and easily. Taken together with Chapter 2, these efforts should provide an overview of the field’s past and foster progress for the near future.

Chapters 4 builds on ideas from the previous chapters to propose a novel approach for tag assignment. By considering visual content and the tags associated with an image, novel features are automatically learned. A cross-model method is proposed to capture the intricate dependencies between image content and annotations. We propose a learning procedure based on Kernel Canonical Correlation Analysis which finds a mapping between visual and textual words by projecting them into a latent meaning space. The learned mapping is then used to annotate new images using advanced nearest neighbor voting methods. We evaluate our approach on three popular datasets, and show clear improvements over several approaches relying on more standard representations.

Chapter 5 gives an evaluation of the temporal information in web images. The idea is to use the temporal gist of annotations to improve tasks such as annotation, indexing and retrieval. While visual content, text and metadata, are typically used to improve these tasks, here we look at the temporal aspect of social media production and tagging. The correlation of the time series of the tags with Google searches shows that, for certain concepts, web information sources may be beneficial to the annotation of

social media.

Chapters 6 and 7 deal with the non semantic problems of image sentiment analysis and popularity prediction. In particular, Chapter 6 investigate the use of a multimodal feature learning approach using neural network based models such as Skip-gram and Denoising Autoencoders. The task is to perform sentiment analysis of micro-blogging content, such as Twitter short messages, that are composed by a short text and, possibly, an image. A novel architecture that incorporates these models is proposed and tested on several standard Twitter datasets. We show that the approach is efficient and obtains good classification results.

By considering that attractiveness of images is related to popularity, in Chapter 7 we propose to use visual sentiment features together with three novel context features to predict a concise popularity score of social images. Experiments on large scale datasets show the benefits of proposed features on the performance of image popularity prediction. Moreover, exploiting state-of-the-art sentiment features, we report a qualitative analysis of which sentiments seem to be related to good or poor popularity.

Finally, Chapter 8 summarizes the contribution of the thesis and discusses avenues for future research. Notice also that the full-list of published papers from this thesis is provided in Appendix A.

Chapter 2

Literature review of Assignment, Refinement and Retrieval

*This chapter gives an unified survey of related work on the three closely linked problems of Tag Assignment, Tag Refinement and Tag-based Image Retrieval. While existing works vary in terms of their targeted tasks and methodology, they rely on the key functionality of tag relevance, i.e., estimating the relevance of a specific tag with respect to the visual content of a given image and its social context. A taxonomy is introduced to structure the growing literature, understand the ingredients of the main works, clarify their connections and difference, and recognize their merits and limitations.*¹

Excellent surveys on content-based image retrieval have been published in the past. In their seminal work, Smeulders *et al.* review the early years up to the year 2000 by focusing on what can be seen in an image and introducing the main scientific problem of the field: the semantic gap as “the lack of coincidence between the information that one can extract from the visual data and the interpretation that the same data have for a user in a given situation” (Smeulders *et al.*, 2000). Datta *et al.* continue along this line and describe the coming-of-age of the field, highlighting the key theoretical and empirical contributions of recent years (Datta *et al.*, 2008). These reviews completely ignore social platforms and socially generated images, which is not surprising as the phenomenon only became apparent after these reviews were published.

In this chapter, we survey the state-of-the-art of content-based image retrieval in the context of social image platforms, with a comprehensive treatise of the closely linked problems of image tag assignment, image tag refinement and tag-based image retrieval. Similar to (Smeulders *et al.*, 2000) and (Datta *et al.*, 2008), the focus of this survey is on visual information, but we explicitly take into account *and* quantify the value of social tagging.

¹Parts of this chapter previously appeared in Li, X., Uricchio, T., Ballan, L., Bertini, M., Snoek, C. G. and Del Bimbo, A. (2016). “Socializing the semantic gap: A comparative survey on image tag assignment, refinement, and retrieval”. ACM Computing Surveys (CSUR), 49(1), 14. The publication is available at <http://dx.doi.org/10.1145/2906152>

2.1 Problems and Tasks

Social tags are provided by common users. They often cannot meet high quality standards related to content association, in particular for accurately describing objective aspects of the visual content according to some expert’s opinion (Dodge et al., 2012). Social tags tend to follow context, trends and events in the real world. They are often used to describe both the situation and the entity represented in the visual content. So tagging deviations due to spatial and temporal correlation to external factors, including user influence, semantics of activity and relationships between tags, are common phenomena. Social tags tend to be imprecise, ambiguous, incomplete and biased towards personal perspectives (Golder and Huberman, 2006; Sen et al., 2006; Sigurbjörnsson and van Zwol, 2008; Kennedy et al., 2006). Quite a few researchers have proposed solutions for image annotation and retrieval in social frameworks, although the peculiarities of this domain have been only partially addressed. We categorize existing works into three different main tasks and structure our survey along these tasks:

- **Tag Assignment.** Given an unlabeled image, tag assignment strives to assign a (fixed) number of tags related to the image content (Makadia et al., 2010; Guillaumin et al., 2009; Verbeek et al., 2010; Tang et al., 2011).
- **Tag Refinement.** Given an image associated with some initial tags, tag refinement aims to remove irrelevant tags from the initial tag list and enrich it with novel, yet relevant, tags (Liu et al., 2010; Wu et al., 2013; Znaidia et al., 2013; Lin et al., 2013; Feng et al., 2014).
- **Tag Retrieval.** Given a tag and a collection of images labeled with the tag (and possibly other tags), the goal of tag retrieval is to retrieve images relevant with respect to the tag of interest (Li et al., 2009*b*; Duan et al., 2011; Sun et al., 2011; Gao et al., 2013; Wu et al., 2013).

Other related tasks such as tag filtering (Zhu et al., 2010; Liu, Yan, Hua and Zhang, 2011; Zhu et al., 2012) and tag suggestion (Sigurbjörnsson and van Zwol, 2008; Li et al., 2009*b*; Wu et al., 2009) have also been studied. As these tasks focus on either cleaning existing tags or expanding them, we view them as variants of tag refinement.

2.2 Scope and Aims

Existing works in tag assignment, refinement, and retrieval vary in terms of their targeted tasks and methodology, making it non-trivial to interpret

them within a unified framework. Nonetheless, we reckon that all works rely on the key functionality of *tag relevance*, i.e., estimating the relevance of a specific tag with respect to the visual content of a given image and its social context. In general terms, relevance should be evaluated considering the complementarity of tags. They may be of low interest alone but become interesting if in conjunction with others. However in the literature, only few methods consider multi-tag relevance evaluation and only for the task of multi-tag retrieval (Li et al., 2012; Nie et al., 2012; Borth et al., 2013). Hence, we focus on methods that implement the unique-tag relevance model.

We survey papers that learn from images tagged in social contexts. We do not cover traditional image classification that is grounded on carefully labeled data. For a state-of-the-art overview in that direction, we refer the interested reader to (Everingham et al., 2015; Russakovsky et al., 2015). Nonetheless, one may question the necessity of using socially tagged examples as training data, given that a number of labeled resources are already publicly accessible. An exemplar of such resources is ImageNet (Deng et al., 2009), providing crowd-sourced positive examples for over 20k classes. Since ImageNet employs several web image search engines to obtain candidate images, its positive examples tend to be biased by the search results. As observed by (Vreeswijk et al., 2012), the positive set of vehicles mainly consists of car and buses, although vehicles can be tracks, watercraft and aircraft. Moreover, controversial images are discarded upon vote disagreement during the crowd sourcing. All this reduces diversity in visual appearance. We empirically show in Chapter 3 the advantage of socially tagged examples against ImageNet for tag relevance learning.

Reviews on social tagging exist. The work by Gupta *et al.* discusses papers on why people tag, what influences the choice of tags, and how to model the tagging process, but its discussion on content-based image tagging is limited (Gupta et al., 2010). The focus of (Jabeen et al., 2015) is on papers about adding semantics to tags by exploiting varied knowledge sources such as Wikipedia, DBpedia, and WordNet. Again, it leaves the visual information untouched.

Several reviews that consider socially tagged images have appeared recently. In (Liu, Hua and Zhang, 2011), technical achievements in content-based tag processing for social images are briefly surveyed. Sawant *et al.* (Sawant et al., 2011), Wang *et al.* (Wang, Ni, Hua and Chua, 2012) and Mei *et al.* (Mei et al., 2014) present extended reviews of particular aspects, i.e., collaborative media annotation, assistive tagging, and visual search re-ranking, respectively. In (Sawant et al., 2011), papers that propose collaborative image labeling games and tagging in social media networks are reviewed. In (Wang, Ni, Hua and Chua, 2012) the authors survey papers where computers assist humans in tagging either by organizing data for

manual labelling, improving quality of human-provided tags or recommending tags for manual selection, instead of applying purely automatic tagging. In (Mei et al., 2014) the authors review techniques that aim for improving initial search results, typically returned by a text based visual search engine, by visual search re-ranking. These reviews offer resumes of the methods and interesting insights on particular aspects of the domain, without giving an experimental comparison between the varied methods.

We notice efforts in empirical evaluations of social media annotation and retrieval (Sun et al., 2011; Uricchio et al., 2013; Ballan, Bertini, Uricchio and Del Bimbo, 2014). In (Sun et al., 2011), the authors analyze different dimensions to compute the relevance score between a tagged image and a tag. They evaluate varied combinations of these dimensions for tag-based image retrieval on NUS-WIDE, a leading benchmark set for social image retrieval (Chua et al., 2009). However, their evaluation focuses only on tag-based image ranking features, without comparing content-based methods. Moreover, tag assignment and refinement are not covered. In (Uricchio et al., 2013; Ballan, Bertini, Uricchio and Del Bimbo, 2014), the authors compared three algorithms for tag refinement on the NUS-WIDE and MIR-Flickr, a popular benchmark set for tag assignment and refinement (Huiskes et al., 2010). However, the two reviews lack a thorough comparison between different methods under the umbrella of a common experimental protocol. Moreover, they fail to assess the high-level connection between image tag assignment, refinement, and retrieval.

2.3 Foundations

Our key observation is that the essential component, which measures the relevance between a given image and a specific tag, stands at the heart of the three tasks. In order to describe this component in a more formal way, we first introduce some notation.

We use x , t , and u to represent the three basic elements in social images, namely image, tag, and user. An image x is shared on social media by its user u . A user u can choose a specific tag t to label x . By sharing and tagging images, a set of users \mathcal{U} contribute a set of n socially tagged images \mathcal{X} , wherein \mathcal{X}_t denotes the set of images tagged with t . Tags used to describe the image set form a vocabulary of m tags \mathcal{V} . The relationship between images and tags can be represented by an image-tag association matrix $D \in \{0, 1\}^{n \times m}$, where $D_{ij} = 1$ means the i -th image is labeled with the j -th tag, and 0 otherwise.

Given an image and a tag, we introduce a real-valued function that computes the relevance between x and t based on the visual content and an optional set of user information Θ associated with the image:

$$f_{\Phi}(x, t; \Theta)$$

We use Θ in a broad sense, making it refer to any type of social context provided by or referring to the user like associated tags, where and when the image was taken, personal profile, and contacts. The subscript Φ specifies how the tag relevance function is constructed. We can easily interpret each of the three tasks: assignment and refinement can be done by sorting \mathcal{V} in descending order by $f_{\Phi}(x, t; \Theta)$, while retrieval can be achieved by sorting the labeled image set \mathcal{X}_t in descending order in terms of $f_{\Phi}(x, t; \Theta)$. Note that this formalization does not necessarily imply that the same implementation of tag relevance is applied for all the three tasks. For example, for retrieval relevance is intended to obtain image ranking (Li, 2015) while tag ranking for each single image is the goal of assignment (Wu et al., 2009) and refinement (Qian et al., 2014).

Fig. 2.1 presents a unified framework, illustrating the main data flow of varied approaches to tag relevance learning. Compared to traditional methods that rely on expert-labeled examples, a novel characteristic of a social media based method is its capability to learn from socially tagged examples with unreliable annotations. Such a training media is marked as \mathcal{S} in the framework. Optionally, in order to obtain a refined training media $\hat{\mathcal{S}}$, one might consider designing a filter to remove unwanted tags and images. In addition, prior information such as tag statistics, tag correlations, and image affinities in the training media are independent of a specific image-tag pair. They can be precomputed for the sake of efficiency. As the filter and the precomputation appear to be a choice of implementation, they are positioned as auxiliary components in Fig. 2.1.

A number of implementations of the relevance function are described and compared in Chapter 3, with regard to their use for tag assignment, refinement and retrieval. Depending on how $f_{\Phi}(x, t; \Theta)$ is composed internally, we propose a taxonomy which organizes existing works along two dimensions, namely *media* and *learning*. As shown in Table 2.1, the media dimension characterizes *what* essential information $f_{\Phi}(x, t; \Theta)$ exploits, while the learning dimension depicts *how* such information is exploited. We explore the taxonomy along the media dimension in Section 2.4 and the learning dimension in Section 2.5, followed by a discussion on the two auxiliary components in Section 2.6.

2.4 Media for tag relevance

Different sources of information may play a role in determining the relevance between an image and a social tag. For instance, the position of a tag

Image Understanding by Socializing the Semantic Gap

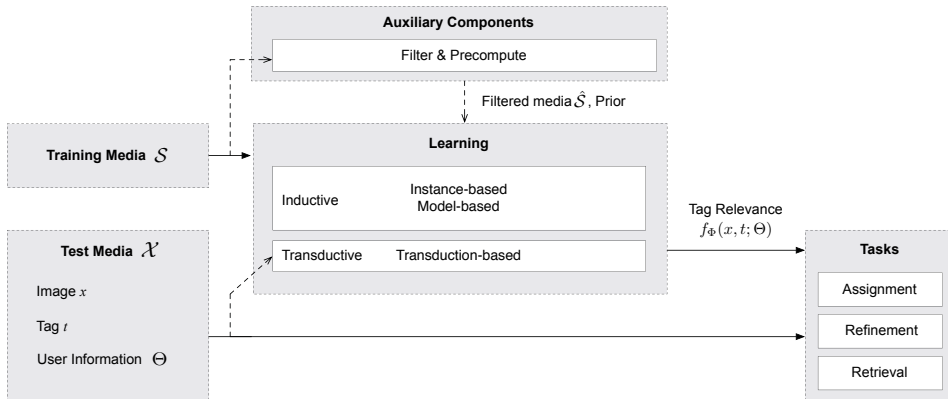


Figure 2.1: **Dataflow to structure the literature on tag relevance learning for image tag assignment, refinement and retrieval.** We follow the input data as it flows through the process of the tag relevance function $f_{\Phi}(x, t; \Theta)$ to higher level tasks, complete with common internal activities and surrounding auxiliary components. Dashed lines indicate optional processes such as the auxiliary components and transduction-based algorithms.

appearing in the tag list might reflect a user’s tagging priority to some extent (Sun et al., 2011). Knowing what other tags are assigned to the image (Zhu et al., 2012) or what other users label about similar images (Li et al., 2009b; Kennedy et al., 2009) can also be helpful for judging whether the tag under examination is appropriate or not. Depending on what modalities in \mathcal{S} are utilized, we divide existing works into the following three groups: 1) tag based, 2) tag + image based and 3) tag + image + user information based, ordered in light of the amount of information they utilize. Table 2.1 shows this classification for several papers that appeared in the literature on the subject.

2.4.1 Tag based

These methods build $f_{\Phi}(x, t; \Theta)$ purely based on tag information. Tag position is considered in (Sun et al., 2011), where a tag appearing top in the tag list is regarded as more relevant. To find tags that are semantically close to the majority of the tags assigned to the test image, tag co-occurrence is considered in (Sigurbjörnsson and van Zwol, 2008; Zhu et al., 2012), while topic modeling is employed in (Xu et al., 2009). As the tag based methods presume that the test image has been labeled with some initial tags, i.e. the initial tags are taken as the user information Θ , they are inapplicable for tag assignment.

2.4.2 Tag + Image based

Works in this group develop $f_{\Phi}(x, t; \Theta)$ on the base of visual information and associated tags. The main rationale behind them is visual consistency, i.e. visually similar images shall be labeled with similar tags. Implementations of this intuition can be grouped in three conducts. One, leverage images visually close to the test image (Li et al., 2009b; Li, Snoek and Worring, 2010; Verbeek et al., 2010; Ma et al., 2010; Wu et al., 2011; Feng et al., 2012). Two, exploit relationships between images labeled with the same tag (Liu, Hua, Yang, Wang and Zhang, 2009; Richter et al., 2012; Liu, Yan, Hua and Zhang, 2011; Kuo et al., 2012; Gao et al., 2013). Three, learn visual classifiers from socially tagged examples (Wang et al., 2009a; Chen et al., 2012; Li and Snoek, 2013; Yang, Gao, Zhang, Shao and Chua, 2014). By propagating tags based on the visual evidence, the above works exploit the image modality and the tag modality in a sequential way. By contrast, there are works that concurrently exploit the two modalities. This can be approached by generating a common latent space upon the image-tag association (Srivastava and Salakhutdinov, 2014; Niu et al., 2014; Duan et al., 2014), so that a cross media similarity can be computed between images and tags (Zhuang and Hoi, 2011; Qi et al., 2012; Liu et al., 2013). In (Pereira et al., 2014), the latent space is constructed by Canonical Correlation Analysis, finding two matrices which separately project feature vectors of image and tag into the same subspace. In (Ma et al., 2010), a random walk model is used on a unified graph composed from the fusion of an image similarity graph with an image-tag connection graph. In (Wu et al., 2013; Xu et al., 2014; Zhu et al., 2010), predefined image similarity and tag similarity are used as two constraint terms to enforce that similarities induced from the recovered image-tag association matrix will be consistent with the two predefined similarities.

Although late fusion has been actively studied for multimedia data analysis (Atrey et al., 2010), improving tag relevance estimation by late fusion is not much explored. There are some efforts in that direction, among which interesting performance has been reported in (Qian et al., 2014) and more recently in (Li, 2015).

2.4.3 Tag + Image + User information based

In addition to tags and images, this group of works exploit user information, motivated from varied perspectives. With the hypothesis that a specific tag chosen by many users to label visually similar images is more likely to be relevant with respect to the visual content, (Li et al., 2009b) utilizes user identities to ensure that learning examples come from distinct users. A similar idea is reported in (Kennedy et al., 2009), finding visually similar image

pairs with matching tags from different users. (Ginsca et al., 2014) improves image retrieval by favoring images uploaded by users with good credibility estimates. In (Sawant et al., 2010; Li, Gavves, Snoek, Worring and Smeulders, 2011), personal tagging preference is considered in the form of tag statistics computed from images a user has uploaded in the past. These past images are used in (Liu et al., 2014) to learn a user-specific embedding space. In (Sang, Xu and Liu, 2012), user affinities, measured in terms of the number of common groups users are sharing, is considered in a tensor analysis framework. Similarly, tensor based low-rank data reconstruction is employed in (Qian et al., 2015) to discover latent associations between users, images, and tags. Photo timestamps are exploited for time-sensitive image retrieval (Kim and Xing, 2013), where the connection between image occurrence and various temporal factors is modeled. In (McParlane et al., 2013a), time-constrained tag co-occurrence statistics are considered to refine the output of visual classifiers for tag assignment. In their follow-up work (McParlane et al., 2013b), location-constrained tag co-occurrence computed from images taken in a specific continent is further included. User interactions in social networks are exploited in (Sawant et al., 2010), computing local interaction networks from the comments left by other users. Social-network metadata such as group memberships of images and contacts of users is employed in (Wang et al., 2009b; McAuley and Leskovec, 2012; Johnson et al., 2015) for image classification.

Comparing the three groups, tag + image appears to be the mainstream, as evidenced by the imbalanced distribution in Table 2.1. Intuitively, using more media from \mathcal{S} would typically increase the reliability of tag relevance estimation. We attribute the imbalance among the groups, in particular the relatively few works in the third group, to the following two reasons. First, no publicly available dataset with expert annotations was built to gather representative and adequate user information, e.g. MIRFlickr has nearly 10k users for 25k images, while in NUS-WIDE only 6% of the users have at least 15 images. As a consequence, current works that leverage user information are forced to use a minimal subset to alleviate sample insufficiency (Sang, Xu and Liu, 2012; Sang, Xu and Lu, 2012) or homemade collections with social tags as ground truth instead of benchmark sets (Sawant et al., 2010; Li, Gavves, Snoek, Worring and Smeulders, 2011). Second, adding more media often results in a substantial increase in terms of both computation and memory, e.g. the cubic complexity for tensor factorization in (Sang, Xu and Liu, 2012). As a trade-off, one has to use \mathcal{S} of a much smaller scale. The dilemma is whether one should use large data with less media or more media but less data.

It is worth noting that the above groups are not exclusive. The output of some methods can be used as a refined input of some other methods.

In particular, we observe a frequent usage of tag-based methods by others for their computational efficiency. For instance, tag relevance measured in terms of tag similarity is used in (Zhuang and Hoi, 2011; Gao et al., 2013; Li and Snoek, 2013) before applying more advanced analysis, while nearest neighbor tag propagation is a pre-process used in (Zhu et al., 2010). The number of tags per image is embedded into image retrieval functions in (Liu, Hua, Yang, Wang and Zhang, 2009; Xu et al., 2009; Zhuang and Hoi, 2011; Chen et al., 2012).

Given the varied sources of information one could leverage, the subsequent question is how the information is exactly utilized, which will be made clear next.

2.5 Learning for tag relevance

This section presents the second dimension of the taxonomy, elaborating on various algorithms for tag relevance learning. Depending on whether the tag relevance learning process is transductive, i.e., producing tag relevance scores without distinction as training and testing, we divide existing works into transduction-based and induction-based. Since the latter produces rules or models that are directly applicable to a novel instance (Michalski, 1983), it has a better scalability for large-scale data compared to its transductive counterpart. Depending on whether an explicit model, let it be discriminative or generative, is built, a further division for the induction-based methods can be made: instance-based algorithms and model-based algorithms. Consequently, we divide existing works into the following three exclusive groups: 1) instance-based, 2) model-based, and 3) transduction-based.

2.5.1 Instance-based

This class of methods does not perform explicit generalization but, instead, compares new test images with training instances. It is called instance-based because it constructs hypotheses directly from the training instances themselves. These methods are non parametric and the complexity of the learned hypotheses grows as the amount of training data increases. The neighbor voting algorithm (Li et al., 2009b) and its variants (Kennedy et al., 2009; Li, Snoek and Worring, 2010; Truong et al., 2012; Lee et al., 2013; Zhu et al., 2014) estimate the relevance of a tag t with respect to an image x by counting the occurrence of t in annotations of the visual neighbors of x . The visual neighborhood is created using features obtained from early-fusion of global features (Li et al., 2009b), distance metric learning to combine local and global features (Verbeek et al., 2010; Wu et al., 2011), cross modal learning of tags and image features (Qi et al., 2012; Ballan, Uricchio, Seidenari

Image Understanding by Socializing the Semantic Gap

Table 2.1: The taxonomy of methods for tag relevance learning, organized along the *Media* and *Learning* dimensions of Fig. 2.1. Methods for which we provide an experimental evaluation in the next chapter are indicated in **bold font**.

<i>Media</i>	<i>Learning</i>	
	<i>Instance-based</i>	<i>Model-based</i>
<i>tag</i>	<p>Sigurbjörnsson et al. (Sigurbjörnsson and van Zwol, 2008)</p> <p>Sam et al. (Sam et al., 2011)</p> <p>Zhu et al. (Zhu et al., 2012)</p>	<p>Xu et al. (Xu et al., 2009)</p>
	<p>Lin et al. (Lin, Hua, Yang, Wang and Zhang, 2009)</p> <p>Makadia et al. (Makadia et al., 2010)</p> <p>Tang et al. (Tang et al., 2011)</p> <p>Wu et al. (Wu et al., 2011)</p> <p>Yang et al. (Yang et al., 2011)</p> <p>Truong et al. (Truong et al., 2012)</p> <p>Qi et al. (Qi et al., 2012)</p> <p>Lin et al. (Lin et al., 2013)</p> <p>Lee et al. (Lee et al., 2013)</p> <p>Uricchio et al. (Uricchio et al., 2013)</p> <p>Zhu et al. (Zhu et al., 2014)</p> <p>Ballan et al. (Ballan, Uricchio, Sedewart and Bimbo, 2014)</p> <p>Pereira et al. (Pereira et al., 2014)</p>	<p>Wu et al. (Wu et al., 2009)</p> <p>Guillaumin et al. (Guillaumin et al., 2009)</p> <p>Verbeek et al. (Verbeek et al., 2010)</p> <p>Lin et al. (Lin et al., 2010)</p> <p>Ma et al. (Ma et al., 2010)</p> <p>Lin et al. (Lin, Yan, Hua and Zhang, 2011)</p> <p>Duan et al. (Duan et al., 2011)</p> <p>Feng et al. (Feng et al., 2012)</p> <p>Shrivastava et al. (Shrivastava and Szeliski, 2014)</p> <p>Chen et al. (Chen et al., 2012)</p> <p>Lan et al. (Lan and Mori, 2013)</p> <p>Li et al. (Li and Snoek, 2013)</p> <p>Li et al. (Li, Lin and Lu, 2013)</p> <p>Wang et al. (Wang, Zhou, Xu, Mei, Hua and Li, 2014)</p> <p>Niu et al. (Niu et al., 2014)</p>
<i>tag + image + user</i>	<p>Li et al. (Li et al., 2009b)</p> <p>Kennedy et al. (Kennedy et al., 2009)</p> <p>Li et al. (Li, Snoek and Worring, 2010)</p> <p>Zanidia et al. (Zanidia et al., 2013)</p> <p>Lin et al. (Lin et al., 2014)</p>	<p>Sawant et al. (Sawant et al., 2010)</p> <p>Li et al. (Li, Garves, Snoek, Worring and Smeynders, 2011)</p> <p>McAuley et al. (McAuley and Leskovec, 2012)</p> <p>Kim et al. (Kim and Xing, 2013)</p> <p>McParlane et al. (McParlane et al., 2013b)</p> <p>Ginsca et al. (Ginsca et al., 2014)</p> <p>Ballan et al. (Johnson et al., 2015)</p>
		<p>Sang et al. (Sang, Xu and Lin, 2012)</p> <p>Sang et al. (Sang, Xu and Lin, 2012)</p> <p>Qian et al. (Qian et al., 2015)</p>

and Bimbo, 2014; Pereira et al., 2014), and fusion of multiple single-feature learners (Li, Snoek and Worring, 2010). While the standard neighbor voting algorithm (Li et al., 2009b) simply let the neighbors vote equally, efforts have been made to (heuristically) weight neighbors in terms of their importance. For instance, in (Truong et al., 2012; Lee et al., 2013) the visual similarity is used as the weights. As an alternative to such a heuristic strategy, (Zhu et al., 2014) models the relationships among the neighbors by constructing a directed voting graph, wherein there is a directed edge from image x_i to image x_j if x_i is in the k nearest neighbors of x_j . Subsequently an adaptive random walk is conducted over the voting graph to estimate the tag relevance. However, the performance gain obtained by these weighting strategies appears to be limited (Zhu et al., 2014). The kernel density estimation technique used in (Liu, Hua, Yang, Wang and Zhang, 2009) can be viewed as another form of weighted voting, but the votes come from images labeled with t instead of the visual neighbors. (Yang et al., 2011) further considers the distance of the test image to images not labeled with t . In order to eliminate semantically unrelated samples in the neighborhood, sparse reconstruction from a k -nearest neighborhood is used in (Tang et al., 2009, 2011). In (Lin et al., 2013), with intention of recovering missing tags by matrix reconstruction, the image and tag modalities are separately exploited in parallel to produce a new candidate image-tag association matrix each. Then, the two resultant tag relevance scores are linearly combined to produce the final tag relevance scores. To address the incompleteness of tags associated with the visual neighbors, (Znaidia et al., 2013) proposes to enrich these tags by exploiting tag co-occurrence in advance to neighbor voting.

2.5.2 Model-based

This class of tag relevance learning algorithms puts their foundations on parameterized models learned from the training media. Notice that the models can be tag-specific or holistic for all tags. As an example of holistic modeling, a topic model approach is presented in (Wang, Zhou, Xu, Mei, Hua and Li, 2014) for tag refinement, where a hidden topic layer is introduced between images and tags. Consequently, the tag relevance function is implemented as the dot product between the topic vector of the image and the topic vector of the tag. In particular, the authors extend the Latent Dirichlet Allocation model (Blei et al., 2003) to force images with similar visual content to have similar topic distribution. According to their experiments (Wang, Zhou, Xu, Mei, Hua and Li, 2014), however, the gain of such a regularization appears to be marginal compared to the standard Latent Dirichlet Allocation model. (Li, Liu and Lu, 2013) first finds embedding vectors of training images and tags using the image-tag association matrix

of \mathcal{S} . The embedding vector of a test image is obtained by a convex combination of the embedding vectors of its neighbors retrieved in the original visual feature space. Consequently, the relevance score is computed in terms of the Euclidean distance between the embedding vectors of the test image and the tag.

For tag-specific modeling, linear SVM classifiers trained on features augmented by pre-trained classifiers of popular tags are used in (Chen et al., 2012) for tag retrieval. Fast intersection kernel SVMs trained on selected relevant positive and negative examples are used in (Li and Snoek, 2013). A bag-based image reranking framework is introduced in (Duan et al., 2011), where pseudo relevant images retrieved by tag matching are partitioned into clusters by using visual and textual features. Then, by treating each cluster as a bag and images within the cluster as its instances, multiple instance learning (Andrews et al., 2003) is employed to learn multiple-instance SVMs per tag. Viewing the social tags of a test image as ground truth, a multi-modal tag suggestion method based on both tags and visual correlation is introduced in (Wu et al., 2009). Each modality is used to generate a ranking feature, and the tag relevance function is a combination of these ranking features, with the combination weights learned online by the RankBoost algorithm (Freund et al., 2003). In (Guillaumin et al., 2009; Verbeek et al., 2010), logistic regression models are built per tag to promote rare tags. In a similar spirit to (Li and Snoek, 2013), (Zhou et al., 2015) learns an ensemble of SVMs by treating tagged images as positive training examples and untagged images as candidate negative training examples. Using the ensemble to classify image regions generated by automated image segmentation, the authors assign tags at the image level and the region level simultaneously.

2.5.3 Transduction-based

This class of methods consists in procedures that evaluate tag relevance for a given image-tag pair of a set of images by minimizing some specific cost function. Given an initial image-tag association matrix D , the output of the procedure is a new matrix \hat{D} the elements of which are taken as tag relevance scores. Due to this formulation, no explicit form of the tag relevance function exists nor any distinction between training and test sets (Joachims, 1999). If novel images are added to the initial set, minimization of the cost function needs to be re-computed.

The majority of transduction-based approaches are founded on matrix factorization (Zhu et al., 2010; Sang, Xu and Liu, 2012; Liu et al., 2013; Wu et al., 2013; Kalayeh et al., 2014; Feng et al., 2014; Xu et al., 2014). In (Zhuang and Hoi, 2011) the objective function is a linear combination of the difference between \hat{D} and the matrix of image similarity, the distortion between \hat{D} and the matrix of tag similarity, and the difference between \hat{D}

and D . A stochastic coordinate descent optimization is applied to a randomly chosen row of \hat{D} per iteration. In (Zhu et al., 2010), considering the fact that D is corrupted with noise derived by missing or over-personalized tags, robust principal component analysis with laplacian regularization is applied to recover \hat{D} as a low-rank matrix. In (Wu et al., 2013), \hat{D} is regularized such that the image similarity induced from \hat{D} is consistent with the image similarity computed in terms of low-level visual features, and the tag similarity induced from \hat{D} is consistent with the tag correlation score computed in terms of tag co-occurrence. In (Xu et al., 2014), it is proposed to re-weight the penalty term of each image-tag pair by their relevance score, which is estimated by a linear fusion of tag-based and content-based relevance scores. To incorporate the user element, (Sang, Xu and Liu, 2012) extends D to a three-way tensor with tag, image, and user as each of the ways. A core tensor and three matrices representing the three media, obtained by Tucker decomposition (Tucker, 1966), are multiplied to construct \hat{D} .

As an alternative approach, in (Feng et al., 2014) it is assumed that the tags of an image are drawn independently from a fixed but unknown multinomial distribution. Estimation of this distribution is implemented by maximum likelihood with low-rank matrix recovery and laplacian regularization like (Zhu et al., 2010).

Graph-based label propagation is another type of transduction-based methods. In (Richter et al., 2012; Wang et al., 2010; Kuo et al., 2012), the image-tag pairs are represented as a graph in which each node corresponds to a specific image and the edges are weighted according to a multi-modal similarity measure. Viewing the top ranked examples in the initial search results as positive instances, tag refinement is implemented as a semi-supervised labeling process by propagating labels from the positive instances to the remaining examples using random walk. While the edge weights are fixed in the above works, (Gao et al., 2013) argues that fixing the weights could be problematic, because tags found to be discriminative in the learning process should adaptively contribute more to the edge weights. In that regard, the hypergraph learning algorithm (Zhou et al., 2006) is exploited and weights are optimized by minimizing a joint loss function which considers both the graph structure and the divergence between the initial labels and the learned labels. In (Liu, Wu, Zhang, Shao and Zhuang, 2011), the hypergraph is embedded into a lower-dimension space by hypergraph Laplacian.

Comparing the three groups of methods for learning tag relevance, an advantage of instance-based methods against the other two groups is their flexibility to adapt to previously unseen images and tags. They may simply add new training images into \mathcal{S} or remove outdated ones. The advantage

however comes with a price that \mathcal{S} has to be maintained, a non-trivial task given the increasing amount of training data available. Also, the computational complexity and memory footprint grow linearly with respect to the size of \mathcal{S} . In contrast, model-based methods could be more swift, especially when linear classifiers are used, as the training data is compactly represented by a fixed number of models. As the imagery of a given tag may evolve, re-training is required to keep the models up-to-date.

Different from instance-based and model-based learning where individual tags are considered independently, transduction-based learning methods via matrix factorization can favorably exploit inter-tag and inter-image relationships. However, their ability to deal with the extremely large number of social images is a concern. For instance, the use of Laplacian graphs results in a memory complexity of $O(|\mathcal{S}|^2)$. The accelerated proximal gradient algorithm used in (Zhu et al., 2010) requires Singular Value Decomposition, which is known to be an expensive operation. The Tucker decomposition used in (Sang, Xu and Liu, 2012) has a cubic computational complexity with respect to the number of training samples. We notice that some engineering tricks have been considered in these works, which alleviate the scalability issue to some extent. In (Zhuang and Hoi, 2011), for instance, clustering is conducted in advance to divide \mathcal{S} into much smaller subsets, and the algorithm is applied to these subsets, separately. By making the Laplacian more sparse by retaining only the k nearest neighbors (Zhu et al., 2010; Sang, Xu and Liu, 2012), the memory footprint can be reduced to $O(k \cdot |\mathcal{S}|)$, with the cost of performance degeneration. Perhaps due to the scalability concern, works resorting to matrix factorization tend to experiment with a dataset of relatively small scale.

2.6 Auxiliary components

The *Filter* and the *Precompute* component are auxiliary components that may sustain and improve tag relevance learning.

Filter. As social tags are known to be subjective and overly personalized, removing personalized tags appears to be a natural and simple way to improve the tagging quality. This is usually the first step performed in the framework for tag relevance learning. Although there is a lack of golden criteria to determine which tags are personalized, a popular strategy is to exclude tags which cannot be found in the WordNet ontology (Zhu et al., 2010; Li, Gavves, Snoek, Worring and Smeulders, 2011; Chen et al., 2012; Zhu et al., 2012) or a Wikipedia thesaurus (Liu, Hua, Yang, Wang and Zhang, 2009). Tags with rare occurrence, say appearing less than 50 times, are discarded in (Verbeek et al., 2010; Zhu et al., 2010). For methods that directly work on the image-tag association matrix (Zhu et al., 2010; Sang,

Xu and Liu, 2012; Wu et al., 2013; Lin et al., 2013), reducing the size of the vocabulary in terms of tag occurrence is an important prerequisite to keep the matrix in a manageable scale. Observing that images tagged in a batch manner are often nearly duplicate and of low tagging quality, batch-tagged images are excluded in (Li et al., 2012). Since relevant tags may be missing from user annotations, the negative tags that are semantically similar or co-occurring with positive ones are discarded in (Sang, Xu and Liu, 2012). As the above strategies do not take the visual content into account, they cannot handle situations where an image is incorrectly labeled with a valid and frequently used tag, say ‘dog’. In (Li et al., 2009a), tag relevance scores are assigned to each image in \mathcal{S} by running the neighbor voting algorithm (Li et al., 2009b), while in (Li and Snoek, 2013), the semantic field algorithm (Zhu et al., 2012) is further added to select relevant training examples. In (Qian et al., 2015), the annotation of the training media is enriched by a random walk.

Precompute. The precompute component is responsible for the generation of the prior information that is jointly used with the refined training media $\hat{\mathcal{S}}$ in learning. For instance, global statistics and external resources can be used to synthesize new prior knowledge useful in learning. The prior information commonly used is tag statistics in \mathcal{S} , including tag occurrence and tag co-occurrence. Tag occurrence is used in (Li et al., 2009b) as a penalty to suppress overly frequent tags. Measuring the semantic similarity between two tags is important for tag relevance learning algorithms that exploit tag correlations. While linguistic metrics as those derived from WordNet were used before the proliferation of social media (Jin et al., 2005; Wang et al., 2006), they do not directly reflect how people tag images. For instance, tag ‘sunset’ and tag ‘sea’ are weakly related according to the WordNet ontology, but they often appear together in social tagging as many of the sunset photos are shot around seashores. Therefore, similarity measures that are based on tag statistics computed from many socially tagged images are in dominant use. Sigurbjörnsson and van Zwol utilized the Jaccard coefficient and a conditional tag probability in their tag suggestion system (Sigurbjörnsson and van Zwol, 2008), while Liu *et al.* used normalized tag co-occurrence (Liu et al., 2013). To better capture the visual relationship between two tags, Wu *et al.* proposed the Flickr distance (Wu et al., 2008). The authors represent each tag by a visual language model, trained on bag of visual words features of images labeled with this tag. The Flickr distance between two tags is computed as the Jensen-Shannon divergence between the corresponding models. Later, Jiang *et al.* introduced the Flickr context similarity, which also captures the visual relationship between two tags, but without the need of the expensive visual modeling (Jiang et al., 2009). The trick is to compute the Normalized Google Distance (Cilibrasi and Vitanyi,

2004) between two tags, but with tag statistics acquired from Flickr image collections instead of Google indexed web pages. For its simplicity and effectiveness, we observe a prevalent use of the Flickr context similarity in the literature (Liu, Hua, Yang, Wang and Zhang, 2009; Zhu et al., 2010; Wang et al., 2010; Zhuang and Hoi, 2011; Zhu et al., 2012; Gao et al., 2013; Li and Snoek, 2013; Qian et al., 2014).

2.7 Conclusions

We presented a survey on image tag assignment, refinement and retrieval, with the hope of illustrating connections and difference between the many methods and their applicabilities, and consequently helping the interested audience to either pick up an existing method or devise a method of their own given the data at hand. As the topics are being actively studied, inevitably this survey will miss some papers. Nevertheless, it provides a unified view of many existing works, and consequently eases the effort of placing future works in a proper context, both theoretically and experimentally. Based on the key observation that all works rely on tag relevance learning as the common ingredient, exiting works, which vary in terms of their methodologies and target tasks, are interpreted in a unified framework. Consequently, a two-dimensional taxonomy has been developed, allowing us to structure the growing literature in light of what information a specific method exploits and how the information is leveraged in order to produce their tag relevance scores.

Chapter 3

A new Experimental Protocol

*In this chapter we propose an evaluation test-bed for the three linked tasks of Assignment, Refinement and Retrieval. Training sets of varying sizes and three test datasets are considered to evaluate methods of varied learning complexity. A selected set of eleven representative works have been implemented and evaluated. Several overall patterns are recognized. To highlight the advantages of socially tagged training sets, an empirical evaluation between ImageNet and the proposed Flickr-based training sets is reported.*¹

3.1 Introduction

In spite of the expanding literature, there is a lack of consensus on the performance of the individual methods. This is largely due to the fact that existing works either use homemade data, see (Liu, Hua, Yang, Wang and Zhang, 2009; Wang et al., 2010; Chen et al., 2012; Gao et al., 2013), which are not publicly accessible, or use selected subsets of benchmark data, e.g. as in (Zhu et al., 2010; Sang, Xu and Liu, 2012; Feng et al., 2014). As a consequence, the performance scores reported in the literature are not comparable across the papers.

Benchmark data with manually verified labels is crucial for an objective evaluation. As Flickr has been well recognized as a profound manifestation of social image tagging, Flickr images act as a main source for benchmark construction. MIRFlickr from the Leiden University (Huiskes et al., 2010) and NUS-WIDE from the National University of Singapore (Chua et al., 2009) are the two most popular Flickr-based benchmark sets for social image tagging and retrieval, as demonstrated by the number of citations. On the use of the benchmarks, one typically follows a single-set protocol, that is,

¹Parts of this chapter previously appeared in Li, X., Uricchio, T., Ballan, L., Bertini, M., Snoek, C. G. and Del Bimbo, A. (2016). "Socializing the semantic gap: A comparative survey on image tag assignment, refinement, and retrieval". ACM Computing Surveys (CSUR), 49(1), 14. The publication is available at <http://dx.doi.org/10.1145/2906152>

learning the underlying tag relevance function from the training part of a chosen benchmark set, and evaluating it on the test part. Such a protocol is inadequate given the dynamic nature of social media, which could easily make an existing benchmark set outdated. For any method targeting at social images, a cross-set evaluation is necessary to test its generalization ability, which is however overlooked in the literature.

Another desirable property is the capability to learn from the increasing amounts of socially tagged images. While existing works mostly use training data of a fixed scale, this property has not been well evaluated.

Following these considerations, we present a new experimental protocol, wherein training and test data from distinct research groups are chosen for evaluating a number of representative works in the cross-set scenario. Training sets with their size ranging from 10k to one million images are constructed to evaluate methods of varied complexity. To the best of our knowledge, such a comparison between many methods on varied scale datasets with a common experimental setup has not been conducted before. For the sake of experimental reproducibility, all data and code is made available online at www.micc.unifi.it/tagssurvey/.

3.2 Datasets

We describe the training media \mathcal{S} and the test media \mathcal{X} as follows, with basic data characteristics and their usage summarized in Table 3.1.

Training media \mathcal{S} . We use a set of 1.2 million Flickr images collected by the University of Amsterdam (Li et al., 2012), by using over 25,000 nouns in WordNet as queries to uniformly sample images uploaded between 2006 and 2010. Based on our observation that batch-tagged images, namely those labeled with the same tags by the same user, tend to be near duplicate, we have excluded these images beforehand. Other than this, we do not perform near-duplicate image removal. To meet with methods that cannot handle large data, we created two random subsets from the entire training sets, resulting in three training sets of varied sizes, termed as Train10k, Train100k, and Train1m, respectively.

Test media \mathcal{X} . We use MIRFlickr (Huiskes et al., 2010) and NUS-WIDE (Chua et al., 2009) for tag assignment and refinement, as in (Verbeek et al., 2010; Zhu et al., 2010; Uricchio et al., 2013) and (Tang et al., 2011; McAuley and Leskovec, 2012; Zhu et al., 2010; Uricchio et al., 2013) respectively. We use NUS-WIDE for evaluating tag retrieval as in (Sun et al., 2011; Li, Duan, Xu and Tsang, 2011). In addition, for retrieval we collected another test set namely Flickr51 contributed by Microsoft Research Asia (Wang et al., 2010; Gao et al., 2013). The MIRFlickr set contains 25,000 images with ground truth available for 14 tags. The NUS-WIDE set contains 259,233 images,

Table 3.1: Our proposed experimental protocol instantiates the *Media* and *Tasks* dimensions of Fig. 2.1 with three training sets and three test sets for tag assignment, refinement and retrieval. Note that the training sets are socially tagged, they have no ground truth available for any tag.

Media	Media characteristics				Tasks		
	# images	# tags	# users	# test tags	assignment	refinement	retrieval
<i>Training media S:</i>							
Train10k	10,000	41,253	9,249	–	✓	✓	✓
Train100k	100,000	214,666	68,215	–	✓	✓	✓
Train1m (Li et al., 2012)	1,198,818	1,127,139	347,369	–	✓	✓	✓
<i>Test media X:</i>							
MIRFlickr (Huiskes et al., 2010)	25,000	67,389	9,862	14	✓	✓	–
Flickr51 (Wang et al., 2010)	81,541	66,900	20,886	51	–	–	✓
NUS-WIDE (Chua et al., 2009)	259,233	355,913	51,645	81	✓	✓	✓

Table 3.2: Data overlap between Train1M and the three test sets, measured in terms of the number of shared images, tags, and users, respectively. Tag overlap is counted on the top 1,000 most frequent tags. As the original photo ids of MIRFlickr have been anonymized, we cannot check image overlap between this dataset and Train1M.

Test media	Overlap with Train1M		
	# images	# tags	# users
MIRFlickr	–	693	6,515
Flickr51	730	538	14,211
NUS-WIDE	7,975	718	38,481

with ground truth available for 81 tags. The Flickr51 set consists of 81,541 Flickr images with partial ground truth provided for 55 test tags. Among the 55 tags, there are 4 tags which either have zero occurrence in our training data or have no correspondence in WordNet, so we ignore them. Differently from the binary judgments in NUS-WIDE, Flickr51 provides graded relevance, with 0, 1, and 2 to indicate irrelevant, relevant, and very relevant, respectively. Moreover, the set contains several ambiguous tags such as ‘apple’ and ‘jaguar’, where relevant instances could exhibit completely different imagery, e.g., Apple computers versus fruit apples. Following the original intention of the datasets, we use MIRFlickr and NUS-WIDE for evaluating tag assignment and tag refinement, and Flickr51 and NUS-WIDE for tag retrieval. For all the three test sets, we use the full dataset for testing.

Although the training and test media are all from Flickr, they were collected independently, and consequently they have a relatively small amount of images overlapped with each other, as shown in Table 3.2.

3.3 Implementation and Evaluation

This section describes common implementations applicable to all the three tasks, including the choice of visual features and tag preprocessing. Implementations that are applied uniquely to single tasks will be described in the coming sections.

Visual features. Two types of features are extracted to provide insights of the performance improvement achievable by appropriate feature selection: the classical bag of visual words (BoVW) and the current state of the art deep learning based features extracted from Convolutional Neural Networks (CNN). The BoVW feature is extracted by the color descriptor software (van de Sande et al., 2010). SIFT descriptors are computed at dense sampled points, at every 6 pixels for two scales. A codebook of size 1,024 is created by K-means clustering. The SIFTs are quantized by the codebook using hard assignment, and aggregated by sum pooling. In addition, we extract a compact 64-d global feature (Li, 2007), combining a 44-d color correlogram, a 14-d texture moment, and a 6-d RGB color moment, to compensate the BoVW feature. The CNN feature is extracted by the pre-trained VGGNet (Simonyan and Zisserman, 2015). In particular, we adopt the 16-layer VGGNet, and take as feature vectors the last fully connected layer of ReLU activation, resulting in a feature vector of 4,096 dimensions per image. The BoVW feature is used with the l_1 distance and the CNN feature is used with the cosine distance for their good performance.

Vocabulary \mathcal{V} . As what tags a person may use is meant to be open, the need of specifying a tag vocabulary is merely an engineering convenience. For a tag to be meaningfully modeled, there has to be a reasonable amount of training images with respect to that tag. For methods where tags are processed independently from the others, the size of the vocabulary has no impact on the performance. In the other cases, in particular for transductive methods that rely on the image-tag association matrix, the tag dimension has to be constrained to make the methods runnable. In our case, for these methods a three-step automatic cleaning procedure is performed on the training datasets. First, all the tags are lemmatized to their base forms by the NLTK software (Bird et al., 2009). Second, tags not defined in WordNet are removed. Finally, in order to avoid insufficient sampling, we remove tags that cannot meet a threshold on tag occurrence. The thresholds are empirically set as 50, 250, and 750 for Train10k, Train100k, and Train1m, respectively, in order to have a linear increase in vocabulary size versus a logarithmic increase in the number of labeled images. This results in a final vocabulary of 237, 419, and 1,549 tags, respectively, with all the test tags included. Note that these numbers of tags are larger than the number of tags that can be actually evaluated. This allows to build a unified learning

method that is more handy for cross-dataset evaluation and exploit inter-tag relationships.

3.3.1 Evaluating tag assignment

Evaluation criteria. A good method for tag assignment shall rank relevant tags before irrelevant tags for a given test image. Moreover, with the assigned tags, relevant images shall be ranked before irrelevant images for a given test tag. We therefore use the image-centric Mean image Average Precision (MiAP) to measure the quality of tag ranking, and the tag-centric Mean Average Precision (MAP) to measure the quality of image ranking. Let m_{gt} be the number of ground-truthed test tags, which is 14 for MIR-Flickr and 81 for NUS-WIDE. The image-centric Average Precision of a given test image x is computed as

$$iAP(x) := \frac{1}{R} \sum_{j=1}^{m_{gt}} \frac{r_j}{j} \delta(x, t_j), \quad (3.1)$$

where R is the number of relevant tags of the given image, r_j is the number of relevant tags in the top j ranked tags, and $\delta(x_i, t_j) = 1$ if tag t_j is relevant and 0 otherwise. MiAP is obtained by averaging $iAP(x)$ over the test images.

The tag-centric Average Precision of a given test tag t is computed as

$$AP(t) := \frac{1}{R} \sum_{i=1}^n \frac{r_i}{i} \delta(x_i, t), \quad (3.2)$$

where R is the number of relevant images for the given tag, and r_i is the number of relevant images in the top i ranked images. MAP is obtained by averaging $AP(t)$ over the test tags.

The two metrics are complementary to some extent. Since MiAP is averaged over images, each test image contributes equally to MiAP, as opposed to MAP where each tag contributes equally. Consequently, MiAP is biased towards frequent tags, while MAP can be easily affected by the performance of rare tags, especially when m_{gt} is relatively small.

Baseline. Any method targeting at tag assignment shall be better than a random guess, which simply returns a random set of tags. The RandomGuess baseline is obtained by computing MiAP and MAP given the random prediction, which is run 100 times with the resulting scores averaged.

3.3.2 Evaluating tag refinement

Evaluation criteria. As tag refinement is also meant for improving tag ranking and image ranking, it is evaluated by the same criteria, i.e., MiAP

and MAP, as used for tag assignment.

Baseline. A natural baseline for tag refinement is the original user tags assigned to an image, which we term as UserTags.

3.3.3 Evaluating tag retrieval

Evaluation criteria. To compare methods for tag retrieval, for each test tag we first conduct tag-based image search to retrieve images labeled with that tag, and then sort the images by the tag relevance scores. We use MAP to measure the quality of the entire image ranking. As users often look at the top ranked results and hardly go through the entire list, we also report Normalized Discounted Cumulative Gain (NDCG), commonly used to evaluate the top few ranked results of an information retrieval system (Järvelin and Kekäläinen, 2002). Given a test tag t , its NDCG at a particular rank position h is defined as:

$$NDCG_h(t) := \frac{DCG_h(t)}{IDCG_h(t)}, \quad (3.3)$$

$$DCG_h(t) = \sum_{i=1}^h \frac{2^{rel_i} - 1}{\log_2(i + 1)}, \quad (3.4)$$

where rel_i is the graded relevance of the result at position i , and $IDCG_h$ is the maximum possible DCG till position h . We set h to be 20, which corresponds to a typical number of search results presented on the first two pages of a web search engine. Similar to MAP, $NDCG_{20}$ of a specific method on a specific test set is averaged over the test tags of that test set.

Baselines. When searching for relevant images for a given tag, it is natural to ask how much a specific method gains compared to a baseline system which simply returns a random subset of images labeled with that tag. Similar to the refinement baseline, we also denote this baseline as UserTags, as both of them purely use the original user tags. For each test tag, the test images labeled with this tag are sorted at random, and MAP and $NDCG_{20}$ are computed accordingly. The process is executed 100 times, and the average score over the 100 runs is reported.

The number of tags per image is often included for image ranking in previous works (Liu, Hua, Yang, Wang and Zhang, 2009; Xu et al., 2009). Hence, we build another baseline system, denoted as TagNum, which sort images in ascending order by the number of tags per image. The third baseline, denoted as TagPosition, is from (Sun et al., 2011), where the relevance score of a tag is determined by its position in the original tag list uploaded by the user. More precisely, the score is computed as $1 - position(t)/l$, where l is the tag number.

3.4 Methods under analysis

Despite the rich literature, most works do not provide code. An exhaustive evaluation covering all published methods is impractical. We have to leave out methods that do not show significant improvements or novelties w.r.t. the seminal papers in the field, and methods that are difficult to replicate with the same mathematical preciseness as intended by their developers. We drive our choice by the intention to cover methods that aim for each of the three tasks, exploiting varied modalities by distinct learning mechanisms. Eventually we evaluate 11 representative methods. For each method we analyze its scalability in terms of both computation and memory. Our analysis leaves out operations that are independent of specific tags and thus only need to be executed once in an offline manner, such as visual feature extraction, tag preprocessing, prior information precomputing, and filtering. Main properties of the methods are summarized in table 3.3. Concerning the choices of parameters, we adopt what the original papers recommend. When no recommendation is given for a specific method, we try a range of values to our best understanding, and choose the parameters that yield the best overall performance.

3.4.1 SemanticField

SemanticField (Zhu et al., 2012) measures tag relevance in terms of an averaged semantic similarity between the tag and the other tags assigned to the image:

$$f_{SemField}(x, t) := \frac{1}{l_x} \sum_{i=1}^{l_x} sim(t, t_i), \quad (3.5)$$

where $\{t_1, \dots, t_{l_x}\}$ is a list of l_x social tags assigned to the image x , and $sim(t, t_i)$ denotes a semantic similarity between two tags. SemanticField explicitly assumes that several tags are associated to visual data and their coexistence is accounted in the evaluation of tag relevance. Following (Zhu et al., 2012), the similarity is computed by combining the Flickr context similarity and the WordNet Wu-Palmer similarity (Wu and Palmer, 1994). The WordNet based similarity exploits path length in the WordNet hierarchy to infer tag relatedness. We make a small revision of (Zhu et al., 2012), i.e. combining the two similarities by averaging instead of multiplication, because the former strategy produces slightly better results. SemanticField requires no training except for computing tag-wise similarity, which can be computed offline and is thus omitted. Having all tag-wise similarities in memory, applying Eq. (3.5) requires l_x table lookups per tag. Hence, the computational complexity is $O(m \cdot l_x)$, and $O(m^2)$ for memory.

3.4.2 TagRanking

The tag ranking algorithm (Liu, Hua, Yang, Wang and Zhang, 2009) consists of two steps. Given an image x and its tags, the first step produces an initial tag relevance score for each of the tags, obtained by (Gaussian) kernel density estimation on a set of $\bar{n} = 1,000$ images labeled with each tag, separately. Secondly, a random walk is performed on a tag graph where the edges are weighted by a tag-wise similarity. We use the same similarity as in SemanticField. Notice that when applied for tag retrieval, the algorithm uses the rank of t instead of its score, i.e.,

$$f_{\text{TagRanking}}(x, t) = -\text{rank}(t) + \frac{1}{l_x}, \quad (3.6)$$

where $\text{rank}(t)$ returns the rank of t produced by the tag ranking algorithm. The term $\frac{1}{l_x}$ is a tie-breaker when two images have the same tag rank. Hence, for a given tag t , TagRanking cannot distinguish relevant images from irrelevant images if t is the sole tag assigned to them. It explicitly exploits the coexistence of several tags per image. TagRanking has no learning stage. To derive tag ranks for Eq. 3.6, the main computation is the kernel density estimation on \bar{n} socially-tagged examples for each tag, followed by an L iteration random walk on the tag graph of m nodes. All this results in a computation cost of $O(m \cdot d \cdot \bar{n} + L \cdot m^2)$ per test image. Because the two steps are executed sequentially, the corresponding memory cost is $O(\max(d\bar{n}, m^2))$.

3.4.3 KNN

This algorithm (Makadia et al., 2010) estimates the relevance of a given tag with respect to an image by first retrieving k nearest neighbors from \mathcal{S} based on a visual distance d , and then counting the tag occurrence in associated tags of the neighborhood. In particular, KNN builds $f_{\Phi}(x, t; \Theta)$ as:

$$f_{\text{KNN}}(x, t) := k_t, \quad (3.7)$$

where k_t is the number of images with t in the visual neighborhood of x . The instance-based KNN requires no training. The main computation of f_{KNN} is to find k nearest neighbors from \mathcal{S} , which has a complexity of $O(d \cdot |\mathcal{S}| + k \cdot \log |\mathcal{S}|)$ per test image, and a memory footprint of $O(d \cdot |\mathcal{S}|)$ to store all the d -dimensional feature vectors. It is worth noting that these complexities are drawn from a straightforward implementation of k -nn search, and can be substantially reduced by employing more efficient search techniques, c.f. (Jégou et al., 2011). Accelerating KNN by the product quantization technique (Jégou et al., 2011) imposes an extra training step, where

one has to construct multiple vector quantizers by K-means clustering, and further use the quantizers to compress the original feature vector into a few codes.

3.4.4 TagVote

The TagVote (Li et al., 2009b) algorithm estimates the relevance of a tag t w.r.t. an image x by counting the occurrence frequency of t in social annotations of the visual neighbors of x . Differently from KNN, TagVote exploits the user element in the social framework and introduces a unique-user constraint on the neighbor set to make the voting result more objective. Each user has at most one image in the neighbor set. Moreover, TagVote also takes into account tag prior frequency to suppress over frequent tags. In particular, the TagVote algorithm builds $f_{\Phi}(x, t; \Theta)$ as

$$f_{\text{TagVote}}(x, t) := k_t - k \frac{n_t}{|\mathcal{S}|}, \quad (3.8)$$

where n_t is the number of images labeled with t in \mathcal{S} . Following (Li et al., 2009b), we set k to be 1,000 for both KNN and TagVote. TagVote has the same order of complexity as KNN.

3.4.5 TagProp

TagProp (Guillaumin et al., 2009; Verbeek et al., 2010) employs neighbor voting plus distance metric learning. A probabilistic framework is proposed where the probability of using images in the neighborhood is defined based on rank or distance-based weights. TagProp builds $f_{\Phi}(x, t; \Theta)$ as:

$$f_{\text{TagProp}}(x, t) := \sum_j^k \pi_j \cdot \mathbf{I}(x_j, t), \quad (3.9)$$

where π_j is a non-negative weight indicating the importance of the j -th neighbor x_j , and $\mathbf{I}(x_j, t)$ returns 1 if x_j is labeled with t , and 0 otherwise. Following (Verbeek et al., 2010), we use $k = 1,000$ and the rank-based weights, which showed similar performance to the distance-based weights. Differently from TagVote that uses tag prior to penalize frequent tags, TagProp promotes rare tags and penalizes frequent ones by training a logistic model per tag upon $f_{\text{TagProp}}(x, t)$. The use of the logistic model makes TagProp a model-based method. In contrast to KNN and TagVote wherein visual neighbors are treated equally, TagProp employs distance metric learning to re-weight the neighbors, yielding a learning complexity of $O(l \cdot m \cdot k)$ where l is the number of gradient descent iterations it needs (typically less than 10). TagProp maintains $2m$ extra parameters for the logistic models, though their storage cost is ignorable compared to the visual features.

Therefore, running Eq. (3.9) has the same order of complexity as KNN and TagVote.

3.4.6 TagCooccur

While both SemanticField and TagCooccur are tag-based, the main difference lies in how they compute the contribution of a specific tag to the test tag’s relevance score. Different from SemanticField which uses tag similarities, TagCooccur (Sigurbjörnsson and van Zwol, 2008) uses the test tag’s rank in the tag ranking list created by sorting all tags in terms of their co-occurrence frequency with the tag in a social framework. In addition, TagCooccur takes into account the stability of the tag, measured by its frequency. The method is implemented as

$$f_{tagcooccur}(x, t) = \text{descript}(t) \sum_{i=1}^{l_x} \text{vote}(t_i, t) \cdot \text{rank-promo}(t_i, t) \cdot \text{stability}(t_i), \quad (3.10)$$

where $\text{descript}(t)$ is to damp the contribution of tags with a very high-frequency, $\text{rank-promo}(t_i, t)$ measures the rank-based contribution of t_i to t , $\text{stability}(t_i)$ for promoting tags for which the statistics are more stable, and $\text{vote}(t_i, t)$ is 1 if t is among the top 25 ranked tags of t_i , and 0 otherwise. TagCooccur has the same order of complexity as SemanticField.

3.4.7 TagCooccur+

TagCooccur+ (Li et al., 2009b) is proposed to improve TagCooccur by adding the visual content. This is achieved by multiplying $f_{tagcooccur}(x, t)$ with a content-based term, i.e.,

$$f_{tagcooccur+}(x, t) = f_{tagcooccur}(x, t) \cdot \frac{k_c}{k_c + r_c(t) - 1}, \quad (3.11)$$

where $r_c(t)$ is the rank of t when sorting the vocabulary by $f_{TagVote}(x, t)$ in descending order, and k_c is a positive weighting parameter, which is empirically set to 1. While TagCooccur+ is grounded on TagCooccur and TagVote, the complexity of the former is ignorable compared to the latter, so the complexity of TagCooccur+ is the same as KNN.

3.4.8 TagFeature

The basic idea of TagFeature (Chen et al., 2012) is to enrich image features by adding an extra tag feature. It thus relies on the possible presence of several tags per image in the training set. In particular, a tag vocabulary that consists of d' most frequent tags in \mathcal{S} is constructed first. Then, for

each tag a two-class linear SVM classifier is trained using LIBLINEAR (Fan et al., 2008). The positive training set consists of p images labeled with the tag in \mathcal{S} , and the same amount of negative training examples are randomly sampled from images not labeled with the tag. The probabilistic output of the classifier, obtained by the Platt’s scaling (Lin et al., 2007), corresponds to a specific dimension in the tag feature. By concatenating the tag and visual features, an augmented feature of $d + d'$ dimension is obtained. For a test tag t , its tag relevance function $f_{\text{TagFeature}}(x, t)$ is obtained by re-training an SVM classifier using the augmented feature. The linear property of the classifier allows us to first sum up all the support vectors into a single vector and consequently to classify a test image by the inner product with this vector. That is,

$$f_{\text{TagFeature}}(x, t) := b + \langle x_t, x \rangle, \quad (3.12)$$

where x_t is the weighted sum of all support vectors and b the intercept. To build meaningful classifiers, we use tags that have at least 100 positive examples. While d' is chosen to be 400 in (Chen et al., 2012), the two smaller training sets, namely Train10k and Train100k, have 76 and 396 tags satisfying the above requirement. We empirically set p to 500, and do a random down-sampling if the amount of images for a tag exceeds this number. For TagFeature, learning a linear classifier for each tag from p positive and p negative examples requires $O((d + d')p)$ in computation and $O((d + d')p)$ in memory (Fan et al., 2008). Running Eq. (3.12) for all the m tags and n images needs $O(nm(d + d'))$ in computation and $O(m(d + d'))$ in memory.

3.4.9 RelExample

Different from TagFeature (Chen et al., 2012) that learns from tagged images, RelExample (Li and Snoek, 2013) exploits positive and negative training examples which are deemed to be more relevant with respect to the test tag t . In particular, relevant positive examples are selected from \mathcal{S} by combining SemanticField and TagVote in a late fusion manner. For negative training example acquisition, they leverage Negative Bootstrap (Li, Snoek, Worring, Koelma and Smeulders, 2013), a negative sampling algorithm which iteratively selects negative examples deemed most relevant for improving classification. A T -iteration Negative Bootstrap will produce T meta classifiers. The corresponding tag relevance function is written as

$$f_{\text{RelExample}}(x, t) := \frac{1}{T} \sum_{l=1}^T (b_l + \sum_{j=1}^{n_l} \alpha_{l,j} \cdot y_{l,j} \cdot \mathcal{K}(x, x_{l,j})), \quad (3.13)$$

where $\alpha_{l,j}$ is a positive coefficient of support vector $x_{l,j}$, $y_{l,j} \in \{-1, 1\}$ is class label, and n_l the number of support vectors in the l -th classifier. For

the sake of efficiency, the kernel function \mathcal{K} is instantiated with the fast intersection kernel (Maji et al., 2008). RelExample uses the same amount of positive training examples as TagFeature. The number of iterations T is empirically set to 10. For the SVM classifiers used in TagFeature and RelExample, the Platt’s scaling (Lin et al., 2007) is employed to convert prediction scores into probabilistic output. In RelExample, for each tag learning a histogram intersection kernel SVM has a computation cost of $O(dp^2)$ per iteration, and $O(Tdp^2)$ for T iterations. By jointly using the fast intersection kernel with a quantization factor of q (Maji et al., 2008) and model compression (Li, Snoek, Worring, Koelma and Smeulders, 2013), an order of $O(dq)$ is needed to keep all learned meta classifiers in memory. Since learning a new classifier needs a memory of $O(dp)$, the overall memory cost for training RelExample is $O(dp+dq)$. For each tag, model compression is applied to its learned ensemble in advance to running Eq. (3.13). As a consequence, the compressed classifier can be cached in an order of $O(dq)$ and executed in an order of $O(d)$.

3.4.10 RobustPCA

RobustPCA (Zhu et al., 2010) has been explicitly modeled to deal with a social framework, including noisy tags and several tags per image. On the base of robust principal component analysis (Candès et al., 2011), it factorizes the image-tag matrix D by a low rank decomposition with error sparsity. That is,

$$D = \hat{D} + E, \quad (3.14)$$

where the reconstructed \hat{D} has a low rank constraint based on the nuclear norm, and E is an error matrix with a ℓ_1 -norm sparsity constraint. Notice that the decomposition is not unique. So for a better solution, the decomposition process takes into account image affinities and tag affinities, by adding two extra penalties with respect to a Laplacian matrix L_i from the image affinity graph and another Laplacian matrix L_t from the tag affinity graph. Consequently, two hyper-parameters λ_1 and λ_2 are introduced to balance the error sparsity and the two Laplacian strengths. We follow the original paper and set the two parameters by performing a grid search on the very same proposed range. As user tags are usually missing, the authors proposed a pre-processing step where D is reinitialized by a weighted KNN propagation based on the visual similarity. RobustPCA requires an iterative procedure based on the accelerated proximal gradient method with a quadratic convergence rate (Zhu et al., 2010). Each iteration spends the majority of the required time performing Singular Value Decomposition that, according to (Golub and Van Loan, 2012), has a well known complexity of $O(cm^2n + c'n^3)$ where c, c' are constants. Regarding memory, it has a

requirement of $O(cn \cdot m + c' \cdot (n^2 + m^2))$ as it needs to process a full copy of D and Laplacians of images and labels.

3.4.11 TensorAnalysis

This method (Sang, Xu and Liu, 2012) has been explicitly designed for social frameworks. It explicitly considers ternary relationships between images, tags and user. User relationships are exploited by extending the image-tag association matrix to a binary user-image-tag tensor $F \in \{0, 1\}^{|\mathcal{X}| \times |\mathcal{V}| \times |\mathcal{U}|}$. The tensor is factorized by Tucker decomposition into a dense core C and three low rank matrices U , I , T , which correspond to the user, image, and tag modalities, respectively:

$$F = C \times_u U \times_i I \times_t T, \quad (3.15)$$

Here \times_k is the tensor product between a tensor and a matrix along dimension k . The idea is that C contains the interactions between modalities, while each low rank matrix represent the main components of each modality. Every modality has to be sized manually or by energy retention, adding three needed parameters $R = (r_I, r_T, r_U)$. The eventual tag relevance function is obtained after the optimization process by computing $\hat{D} = C \times_i I \times_t T \times_u \mathbf{1}_{r_u}$. Similar to RobustPCA, the decomposition in Eq. (3.15) is not unique and a better solution may be found regularizing the problem with a Laplacian built on a similarity graph for each modality, i.e., L_i , L_t , and L_u , and a ℓ_2 regularizer on each factor i.e. C , U , I and T . For TensorAnalysis, the complexity is $O(|P_1| \cdot (r_T \cdot m^2 + r_U \cdot r_I \cdot r_T))$, proportional to the number P_1 of tags asserted in D and the dimension of low rank r_U, r_I, r_T factors. The memory required is $O(n^2 + m^2 + u^2)$ because of Laplacians of images, tags and users.

3.4.12 Considerations

An overview of the methods analyzed is given Table 3.3. Among them, SemanticField, counting solely on the tag modality, has the best scalability with respect to both computation and memory. Among the instance-based methods, TagRanking, which works on selected subsets of \mathcal{S} rather than the entire collection, has the lowest memory request. When the number of tags to be modeled m is substantially smaller than the size of \mathcal{S} , the model-based methods require less memory and run faster in the test stage, but at the expense of SVM model learning in the training stage. The two transduction-based methods have limited scalability, and can operate only on small sized \mathcal{S} .

Image Understanding by Socializing the Semantic Gap

Table 3.3: Main properties of the eleven methods evaluated in this survey following the dimensions of Fig. 2.1. The computational and memory complexity of each method is based on processing n test images and m test tags by exploiting the training set \mathcal{S} .

Methods	Test Media	Task	Learning			
			Train Computation	Test Computation	Train Memory	Test Memory
Instance-based:						
SemanticField	tag	Retrieval	–	$O(nmL_x)$	–	$O(m^2)$
TagCooccur	tag	Refinement	–	$O(nmL_x)$	–	$O(m^2)$
		Retrieval	–	$O(nmL_x)$	–	$O(m^2)$
TagRanking	tag + image	Retrieval	–	$O(n(md\bar{n} + Lm^2))$	–	$O(\max(d\bar{n}, m^2))$
KNN	tag + image	Assignment	–	$O(n(d \mathcal{S} + k \log \mathcal{S}))$	–	$O(d \mathcal{S})$
		Retrieval	–	$O(n(d \mathcal{S} + k \log \mathcal{S}))$	–	$O(d \mathcal{S})$
TagVote	tag + image	Assignment	–	$O(n(d \mathcal{S} + k \log \mathcal{S}))$	–	$O(d \mathcal{S})$
		Retrieval	–	$O(n(d \mathcal{S} + k \log \mathcal{S}))$	–	$O(d \mathcal{S})$
TagCooccur+	tag + image	Refinement	–	$O(n(d \mathcal{S} + k \log \mathcal{S}))$	–	$O(d \mathcal{S})$
		Retrieval	–	$O(n(d \mathcal{S} + k \log \mathcal{S}))$	–	$O(d \mathcal{S})$
Model-based:						
TagProp	tag + image	Assignment	$O(l \cdot m \cdot k)$	$O(n(d \mathcal{S} + k \log \mathcal{S}))$	$O(d \mathcal{S} + 2m)$	$O(d \mathcal{S} + 2m)$
		Retrieval	$O(l \cdot m \cdot k)$	$O(n(d \mathcal{S} + k \log \mathcal{S}))$	$O(d \mathcal{S} + 2m)$	$O(d \mathcal{S} + 2m)$
TagFeature	tag + image	Assignment	$O(m(d + d')p)$	$O(nm(d + d'))$	$O((d + d')p)$	$O(m(d + d'))$
		Retrieval	$O(m(d + d')p)$	$O(nm(d + d'))$	$O((d + d')p)$	$O(m(d + d'))$
RelExample	tag + image	Assignment	$O(mTdp^2)$	$O(dp + dq)$	$O(nmd)$	$O(mdq)$
		Retrieval	$O(mTdp^2)$	$O(dp + dq)$	$O(nmd)$	$O(mdq)$
Transduction-based:						
RobustPCA	tag + image	Refinement Retrieval	$O(cm^2n + c'n^3)$		$O(cnm + c' \cdot (n^2 + m^2))$	
TensorAnalysis	tag + image + user	Refinement	$O(P_1 \cdot (r_T \cdot m^2 + r_U \cdot r_I \cdot r_T))$		$O(n^2 + m^2 + u^2)$	

3.5 Evaluation

This section presents our evaluation of the 11 methods according to their applicability to the three tasks using the proposed experimental protocol, that is, KNN, TagVote, TagProp, TagFeature and RelExample for tag assignment (Section 3.5.1), TagCooccur, TagCooccur+, RobustPCA, and TensorAnalysis for tag refinement (Section 3.5.2), and all for tag retrieval (Section 3.5.3). For TensorAnalysis we were able to evaluate only tag refinement with BovW features on MIRFlickr with Train10k and Train100k. The reason for this exception is that our implementation of TensorAnalysis performs worse than the baseline. Consequently, the results of TensorAnalysis were kindly provided by the authors in the form of tag ranks. Since the provided tag ranks cannot be converted to image ranks, we could not compute MAP scores. Finally a comparison between our Flickr based training data and ImageNet is given in Section 3.5.4.

3.5.1 Tag assignment

Table 3.4 shows the tag assignment performance of KNN, TagVote, TagProp, TagFeature and RelExample. Their superior performance against the RandomGuess baseline shows that learning purely from social media is meaningful. TagVote and TagProp are the two best performing methods on both test sets. Substituting CNN for BovW consistently brings improvements for all methods.

In more detail, the following considerations hold. TagProp has higher MAP performance than KNN and TagVote in almost all the cases under analysis. As discussed in Section 3.4.5, TagProp is built upon KNN, but it weights the neighbor images by rank and applies a logistic model per tag. Since the logistic model does not affect the image ranking, the superior performance of TagProp should be ascribed to rank-based neighbor weighting. A per-tag comparison on MIRFlickr is given in Fig. 3.1. TagProp is almost always ahead of KNN and TagVote. Concerning TagVote and KNN, recall that their main difference is that TagVote applies the unique-user constraint on the neighborhood and it employs tag prior as a penalty term. The fact that the training data contains no batch-tagged images minimizes the influence of the unique-user constraint. While the penalty term does not affect image ranking for a given tag, it affects tag ranking for a given image. This explains why KNN and TagVote have mostly the same MAP. Also, the result suggests that the tag prior based penalty is helpful for doing tag assignment by neighbor voting.

We observe that RelExample has a better MAP than TagFeature in every case. The absence of a filtering component makes TagFeature more likely to overfit to training examples irrelevant to the test tags. For the other two

Image Understanding by Socializing the Semantic Gap

Table 3.4: Evaluating methods for tag assignment. Given the same feature, bold values indicate top performers on individual test sets.

Method	MIRFlickr			NUS-WIDE		
	Train10k	Train100k	Train1m	Train10k	Train100k	Train1m
<i>MiAP scores:</i>						
RandomGuess	0.147	0.147	0.147	0.061	0.061	0.061
BovW + KNN	0.232	0.286	0.312	0.171	0.217	0.248
BovW + TagVote	0.276	0.310	0.328	0.183	0.231	0.259
BovW + TagProp	0.276	0.299	0.314	0.230	0.249	0.268
BovW + TagFeature	0.278	0.294	0.298	0.244	0.221	0.214
BovW + RelExample	0.284	0.309	0.303	0.257	0.233	0.245
CNN + KNN	0.326	0.366	0.379	0.315	0.343	0.376
CNN + TagVote	0.355	0.378	0.389	0.340	0.370	0.396
CNN + TagProp	0.373	0.384	0.392	0.366	0.376	0.380
CNN + TagFeature	0.359	0.378	0.383	0.367	0.338	0.373
CNN + RelExample	0.309	0.385	0.373	0.365	0.354	0.388
<i>MAP scores:</i>						
RandomGuess	0.072	0.072	0.072	0.023	0.023	0.023
BovW + KNN	0.231	0.282	0.336	0.094	0.139	0.185
BovW + TagVote	0.228	0.280	0.334	0.093	0.137	0.184
BovW + TagProp	0.245	0.293	0.342	0.102	0.149	0.193
BovW + TagFeature	0.200	0.199	0.201	0.090	0.096	0.098
BovW + RelExample	0.284	0.303	0.310	0.119	0.155	0.172
CNN + KNN	0.564	0.613	0.639	0.271	0.356	0.400
CNN + TagVote	0.561	0.613	0.638	0.257	0.358	0.402
CNN + TagProp	0.586	0.619	0.641	0.305	0.376	0.397
CNN + TagFeature	0.444	0.554	0.563	0.262	0.310	0.326
CNN + RelExample	0.538	0.603	0.584	0.300	0.346	0.373

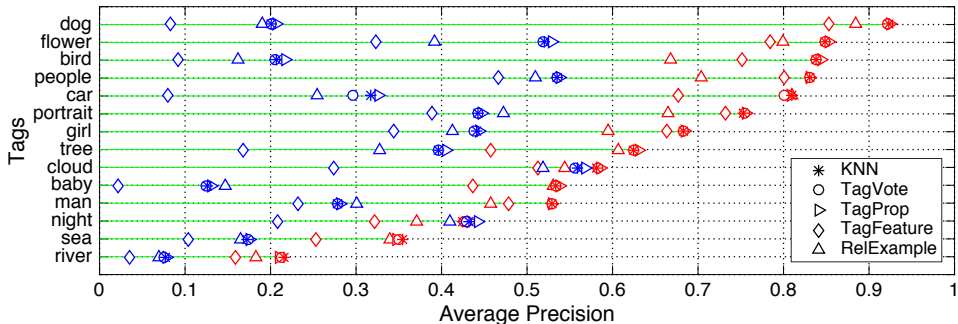


Figure 3.1: **Per-tag comparison of methods for tag assignment on MIRFlickr**, trained on Train1m. The colors identify the features used: **blue** for BovW, **red** for CNN. The test tags have been sorted in descending order by the performance of CNN + TagProp.

model-based methods, the overfit issue is alleviated by different strategies: RelExample employs a filtering component to select more relevant training examples, while TagProp has less parameters to tune.

A per-image comparison on NUS-WIDE is given in Fig. 3.2. The test images are put into disjoint groups so that images within the same group have the same number of ground truth tags. For each group, the area of the colored bars is proportional to the number of images on which the corresponding methods score best. The first group, i.e., images containing only one ground-truth tag, has the most noticeable change as the training set grows. There are 75,378 images in this group, and for 39% of the images, their single label is ‘person’. When Train1m is used, RelExample beats KNN, TagVote, and TagProp for this frequent label. This explains the leading position of RelExample in the first group. The result also confirms our earlier discussion in Section 3.3.1 that MiAP is likely to be biased by frequent tags.

In summary, as long as enough training examples are provided, instance-based methods are on par with model-based methods for tag assignment. Model-based methods are more suited when the training data is of limited availability. However, they are less resilient to noise, and consequently a proper filtering strategy for refining the training data becomes essential.

3.5.2 Tag refinement

Table 3.5 shows the performance of different methods for tag refinement. We were unable to complete the table. In particular, RobustPCA could not go over 350k images due to its high demand in both CPU time and memory (see Table 3.3), while TensorAnalysis was provided by the authors only on MIRFlickr with Train10k, Train100k, and the BovW feature.

Image Understanding by Socializing the Semantic Gap

Table 3.5: Evaluating methods for tag refinement. The asterisk (*) indicates results provided by the authors of the corresponding methods, while the dash (–) means we were unable to produce results. Given the same feature, bold values indicate top performers on individual test sets per performance metric.

Method	MIRFlickr			NUS-WIDE		
	Train10k	Train100k	Train1m	Train10k	Train100k	Train1m
<i>MiAP scores:</i>						
UserTags	0.204	0.204	0.204	0.255	0.255	0.255
TagCooccur	0.213	0.242	0.253	0.269	0.305	0.317
BovW + TagCooccur+	0.217	0.262	0.286	0.245	0.297	0.324
BovW + RobustPCA	0.271	0.310	–	0.332	0.323	–
BovW + TensorAnalysis	*0.298	*0.297	–	–	–	–
CNN + TagCooccur+	0.234	0.277	0.310	0.305	0.359	0.387
CNN + RobustPCA	0.368	0.376	–	0.424	0.419	–
CNN + TensorAnalysis	–	–	–	–	–	–
<i>MAP scores:</i>						
UserTags	0.263	0.263	0.263	0.338	0.338	0.338
TagCooccur	0.266	0.298	0.313	0.223	0.321	0.308
BovW + TagCooccur+	0.294	0.343	0.377	0.231	0.345	0.353
BovW + RobustPCA	0.225	0.337	–	0.229	0.234	–
BovW + TensorAnalysis	–	–	–	–	–	–
CNN + TagCooccur+	0.330	0.381	0.420	0.264	0.391	0.406
CNN + RobustPCA	0.566	0.627	–	0.439	0.440	–
CNN + TensorAnalysis	–	–	–	–	–	–

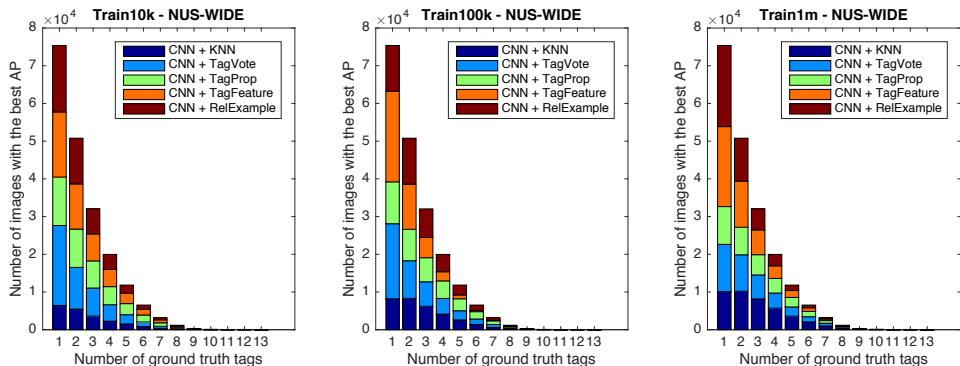


Figure 3.2: **Per-image comparison of methods for tag assignment on NUS-WIDE.** Test images are grouped in terms of their number of ground truth tags. The area of a colored bar is proportional to the number of images that the corresponding method scores best.

RobustPCA outperforms the competitors on both test sets, when provided with the CNN feature. Fig. 3.3 presents a per-tag comparison on MIRFlickr. RobustPCA has the best scores for 9 out of the 14 tags with BovW, and wins all the tags when CNN is used.

Concerning the influence of the media dimension, the tag + image based methods (RobustPCA and TagCooccur+) are in general better than the tag based method (TagCooccur). As shown in Fig. 3.3, except for 3 out of 14 MIRFlickr test tags with BovW, using the image media is beneficial. As in the tag assignment task, the use of the CNN feature strongly improves the performance.

Concerning the learning methods, TensorAnalysis has the potential to leverage tag, image, and user simultaneously. However, due to its relatively poor scalability, we were able to run this method only with Train10k and Train100k on MIRFlickr. For Train10k, TensorAnalysis yielded higher MiAP than RobustPCA, probably thanks to its capability of modeling user correlations. It is outperformed by RobustPCA when more training data is used.

As more training data is used, the performance of TagCooccur, TagCooccur+, and RobustPCA on MIRFlickr consistently improves. Since these three methods rely on data-driven tag affinity, image affinity, or tag and image affinity, a small set of 10k images is generally inadequate to compute these affinities. The effect of increasing the training set size is clearly visible if we compare scores corresponding to Train10k and Train100k. The results on NUS-WIDE show some inconsistency. For TagCooccur, MiAP improves from Train100k to Train1m, while MAP drops. This is presumably due to the fact that in the experiments we used the parameters recommended in the original paper, appropriately selected to optimize tag ranking.

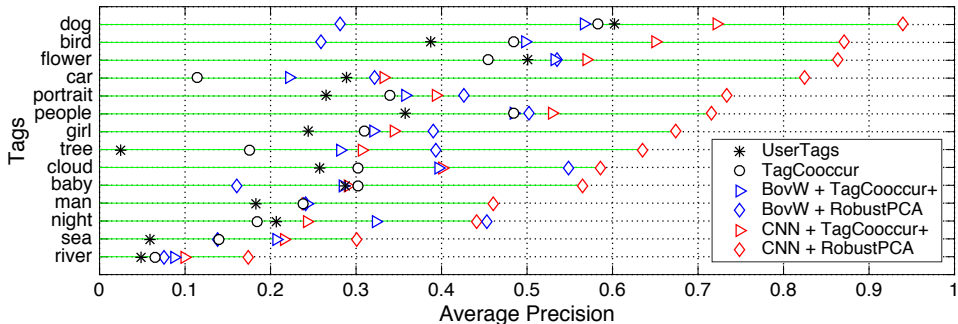


Figure 3.3: **Per-tag comparison of methods for tag refinement on MIRFlickr**, trained on Train100k. The colors identify the features used: **blue** for BovW, **red** for CNN. The test tags have been sorted in descending order by the performance of CNN + RobustPCA.

Hence, they might be suboptimal for image ranking. BovW + RobustPCA scores a lower MAP than BovW + TagCooccur+. This is probably due to the fact that the low-rank matrix factorization technique, while being able to jointly exploit tag and image information, is more sensitive to the content-based representation.

A per-image comparison is given in Fig. 3.4. As for tag assignment, the test images have been grouped according to the number of ground truth tags associated. The size of the colored areas is proportional to the number of images where the corresponding method scores best. For the majority of test image, the three tag refinement methods have higher average precision than UserTags. This means more relevant tags are added, so the tags are refined. It should be noted that the success of tag refinement depends much on the quality of the original tags assigned to the test images. Examples are shown in Table 3.7: in row 6, although the tag ‘earthquake’ is irrelevant to the image content, it is ranked at the top by RobustPCA. To what extent a tag refinement method shall count on the existing tags is tricky.

To summarize, the tag + image based methods outperform the tag based method for tag refinement. RobustPCA is the best, and improves as more training data is employed. Nonetheless, implementing RobustPCA is challenging for both computation and memory footprint. In contrast, TagCooccur+ is more scalable and it can learn from large-scale data.

3.5.3 Tag retrieval

Tables 3.8 and 3.9 show the performance of different methods for tag retrieval. Recall that when retrieving images for a specific test tag, we consider only images that are labeled with this tag. Hence, MAP scores here are higher than their counterpart in Table 3.5.

Tiberio Uricchio

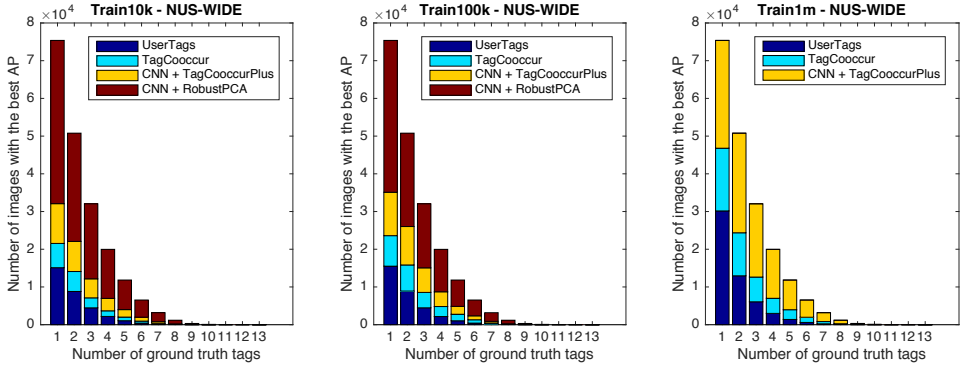


Figure 3.4: **Per-image comparison of methods for tag refinement on NUS-WIDE.** Test images are grouped in terms of their number of ground truth tags. The area of a colored bar is proportional to the number of images that the corresponding method scores best.

Image Understanding by Socializing the Semantic Gap

Table 3.6: Selected tag assignment results on NUS-WIDE. Visual feature: BovW. The top five ranked tags are shown, with correct prediction marked by the *bold italic* font.




Test image	Ground truth	User tags	Tag assignment			
			KNN	TagVote	TagProp	RelExample
	sign	<i>sign</i> reptile zoo red white	animal flower car horse street	dog house bird <i>sign</i> bear	<i>sign</i> street flower dog bird	soccer whale book toy moon
	animal dog person	colour color <i>dog</i> hound	flower garden horse tree <i>dog</i>	garden flower food cat <i>dog</i>	flower <i>dog</i> garden car tree	garden <i>dog</i> fish fox <i>animal</i>
	cloud grass sky	<i>cloud</i> <i>grass</i>	<i>cloud</i> <i>sky</i> beach water snow	<i>cloud</i> <i>sky</i> water beach mountain	<i>cloud</i> <i>sky</i> beach water lake	<i>cloud</i> ocean surf <i>sky</i> beach
	animal bear water	brown <i>bear</i> salmon national park	snow beach <i>animal</i> <i>water</i> tree	snow <i>animal</i> waterfall tree <i>water</i>	snow beach sand <i>bear</i> <i>water</i>	<i>water</i> sand rock surf ocean
	airplane cloud military sky	flag great	<i>sky</i> <i>cloud</i> snow bird <i>airplane</i>	snow <i>cloud</i> <i>sky</i> mountain bird	<i>airplane</i> <i>sky</i> snow bird airport	snow frost bird <i>airplane</i> tattoo
	cloud garden sky water	china earthquake people hangzhou summer westlake	car beach <i>water</i> street tree	grass tree <i>water</i> road bridge	car road street <i>sky</i> bird	house road grass bird sand
	police road vehicle window	farmer dog motorcycle <i>police</i> train	car street <i>police</i> <i>vehicle</i> <i>road</i>	car street <i>police</i> <i>vehicle</i> sport	<i>police</i> car street <i>road</i> sport	<i>police</i> <i>vehicle</i> street car sport

Table 3.7: Selected tag refinement results on NUS-WIDE. Visual feature: BovW. The top five ranked tags are shown, with correct prediction marked by the *bold italic* font.

Test image	Ground truth	User tags	Tag refinement		
			TagCooccur	TagCooccur+	RobustPCA
	sign	<i>sign</i> reptile zoo red white	animal street <i>sign</i> water car	<i>sign</i> bird dog animal toy	<i>sign</i> bird flower animal street
	animal dog person	colour color <i>dog</i> hound	<i>dog</i> <i>animal</i> car beach flower	<i>dog</i> flower <i>animal</i> cat food	<i>dog</i> flower <i>animal</i> water garden
	cloud grass sky	<i>cloud</i> <i>grass</i>	<i>grass</i> <i>sky</i> tree flower water	<i>cloud</i> <i>sky</i> water beach tree	<i>cloud</i> <i>grass</i> <i>sky</i> water mountain
	animal bear water	brown <i>bear</i> salmon national park	waterfall <i>water</i> tree <i>bear</i> <i>animal</i>	waterfall <i>water</i> <i>animal</i> snow tree	<i>water</i> waterfall <i>bear</i> <i>animal</i> snow
	airplane cloud military sky	flag great	car street snow water <i>sky</i>	snow <i>sky</i> <i>cloud</i> mountain bird	flag <i>sky</i> snow <i>cloud</i> bird
	cloud garden sky water	china earthquake people hangzhou summer westlake	<i>water</i> flower street temple tree	tree <i>water</i> street <i>garden</i> car	earthquake <i>water</i> tree <i>cloud</i> <i>sky</i>
	police road vehicle window	farmer dog motorcycle <i>police</i> train	street car animal train bird	car street <i>police</i> food horse	<i>police</i> train dog bird car

We start our analysis by comparing the three baselines, namely UserTags, TagNum, and TagPosition, which retrieve images simply by the original tags. As it can be noticed, TagNum and TagPosition are more effective than UserTags, TagNum outperforms TagPosition on Flickr51, and the latter has better scores on NUS-WIDE. The effectiveness of such metadata based features depend much on datasets, and are unreliable for tag retrieval.

All the methods considered have higher MAP than the three baselines. All the methods have better performance than the baselines on Flickr51 and performance increases with the size of the training set. On NUS-WIDE, SemanticField, TagCooccur, and TagRanking, are less effective than TagPosition. We attribute this result to the fact that, for these methods, the tag relevance functions favor images with fewer tags. So they closely follow similar performance and dataset dependency.

Concerning the influence of the media dimension, the tag + image based methods (KNN, TagVote, TagProp, TagCooccur+, TagFeature, RobustPCA, RelExample) are in general better than the tag based method (SemanticField and TagCooccur). Fig. 3.5 shows the per-tag retrieval performance on Flickr51. For 33 out of the 51 test tags, RelExample exhibits average precision higher than 0.9. By examining the top retrieved images, we observe that the results produced by tag + image based methods and tag based methods are complementary to some extent. For example, consider ‘military’, one of the test tags of NUS-WIDE. RelExample retrieves images with strong visual patterns such as military vehicles, while SemanticField returns images of military personnel. Since the visual content is ignored, the results of SemanticField tend to be visually different, so making it possible to handle tags with visual ambiguity. This fact can be observed in Fig. 3.6, which shows the top 10 ranked images of ‘jaguar’ by TagPosition, SemanticField, BovW + RelExample, and CNN + RelExample. Although their results are all correct, RelExample finds jaguar-brand cars only, while SemanticField covers both cars and animals. However, for a complete evaluation of the capability of managing ambiguous tags, fine-grained ground truth beyond what we currently have is required.

Concerning the learning methods, TagVote consistently performs well as in the tag assignment experiment. KNN is comparable to TagVote, due to the reason we have discussed in Section 3.5.1. Given the CNN feature, the two methods even outperform their model-based variant TagProp. Similar to the tag refinement experiment, the effectiveness of RobustPCA for tag retrieval is sensitive to the choice of visual features. While BovW + RobustPCA is worse than the majority on Flickr51, the performance of CNN + RobustPCA is more stable, and performs well. For TagFeature, its gain from using larger training data is relatively limited due to the absence of denoising. In contrast, RelExample, by jointly using SemanticField and

Table 3.8: Evaluating methods for tag retrieval, MAP scores. Given the same feature, bold values indicate top performers on individual test sets per performance metric.

Method	Flickr51			NUS-WIDE		
	Train10k	Train100k	Train1m	Train10k	Train100k	Train1m
<i>MAP scores:</i>						
UserTags	0.595	0.595	0.595	0.489	0.489	0.489
TagNum	0.664	0.664	0.664	0.520	0.520	0.520
TagPosition	0.640	0.640	0.640	0.557	0.557	0.557
SemanticField	0.687	0.707	0.713	0.565	0.584	0.584
TagCooccur	0.625	0.679	0.704	0.534	0.576	0.588
BovW + TagCooccur+	0.640	0.732	0.764	0.560	0.622	0.643
BovW + TagRanking	0.685	0.686	0.708	0.557	0.574	0.578
BovW + KNN	0.678	0.742	0.770	0.587	0.632	0.658
BovW + TagVote	0.678	0.741	0.769	0.587	0.632	0.659
BovW + TagProp	0.671	0.748	0.772	0.585	0.636	0.657
BovW + TagFeature	0.689	0.726	0.737	0.589	0.602	0.606
BovW + RelExample	0.706	0.756	0.783	0.609	0.645	0.663
BovW + RobustPCA	0.697	0.701	–	0.650	0.650	–
BovW + TensorAnalysis	–	–	–	–	–	–
CNN + TagCooccur+	0.654	0.781	0.821	0.572	0.653	0.674
CNN + TagRanking	0.744	0.735	0.747	0.589	0.590	0.590
CNN + KNN	0.811	0.859	0.880	0.683	0.722	0.734
CNN + TagVote	0.808	0.859	0.881	0.675	0.724	0.738
CNN + TagProp	0.824	0.867	0.879	0.689	0.727	0.731
CNN + TagFeature	0.827	0.853	0.859	0.675	0.700	0.703
CNN + RelExample	0.838	0.863	0.878	0.689	0.717	0.734
CNN + RobustPCA	0.811	0.839	–	0.725	0.726	–
CNN + TensorAnalysis	–	–	–	–	–	–

Image Understanding by Socializing the Semantic Gap

Table 3.9: Evaluating methods for tag retrieval, NDCG₂₀ scores. Given the same feature, bold values indicate top performers on individual test sets per performance metric.

Method	Flickr51			NUS-WIDE		
	Train10k	Train100k	Train1m	Train10k	Train100k	Train1m
<i>NDCG₂₀ scores:</i>						
UserTags	0.432	0.432	0.432	0.487	0.487	0.487
TagNum	0.522	0.522	0.522	0.541	0.541	0.541
TagPosition	0.511	0.511	0.511	0.623	0.623	0.623
SemanticField	0.591	0.623	0.645	0.596	0.622	0.624
TagCooccur	0.482	0.527	0.631	0.529	0.602	0.614
BovW + TagCooccur+	0.503	0.625	0.686	0.590	0.681	0.734
BovW + TagRanking	0.530	0.568	0.571	0.557	0.572	0.572
BovW + KNN	0.577	0.699	0.756	0.638	0.734	0.799
BovW + TagVote	0.573	0.701	0.754	0.629	0.734	0.804
BovW + TagProp	0.570	0.715	0.759	0.666	0.750	0.809
BovW + TagFeature	0.547	0.626	0.646	0.622	0.615	0.618
BovW + RelExample	0.614	0.722	0.748	0.692	0.736	0.776
BovW + RobustPCA	0.549	0.548	–	0.768	0.781	–
BovW + TensorAnalysis	–	–	–	–	–	–
CNN + TagCooccur+	0.504	0.615	0.724	0.571	0.705	0.738
CNN + TagRanking	0.577	0.607	0.597	0.578	0.594	0.583
CNN + KNN	0.709	0.830	0.897	0.773	0.832	0.863
CNN + TagVote	0.722	0.826	0.899	0.740	0.837	0.879
CNN + TagProp	0.768	0.857	0.865	0.764	0.839	0.845
CNN + TagFeature	0.755	0.813	0.818	0.704	0.807	0.787
CNN + RelExample	0.764	0.843	0.879	0.773	0.814	0.866
CNN + RobustPCA	0.733	0.821	–	0.865	0.862	–
CNN + TensorAnalysis	–	–	–	–	–	–

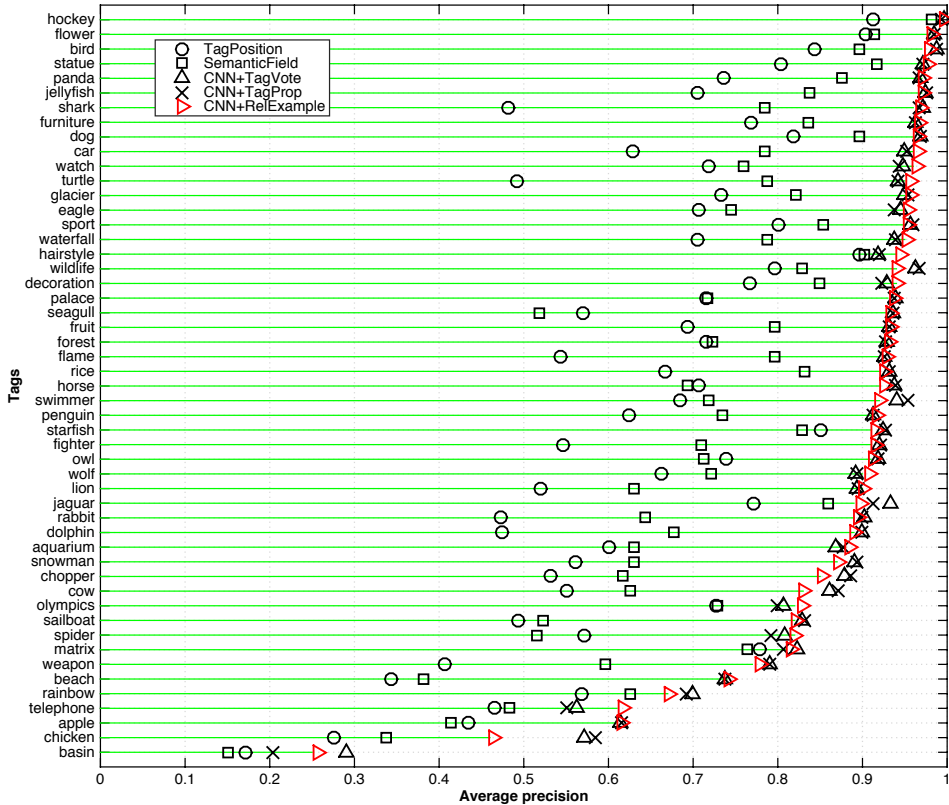


Figure 3.5: **Per-tag comparison between TagPosition, SemanticField, TagVote, TagProp, and RelExample on Flickr51**, with Train1m as the training set. The 51 test tags have been sorted in descending order by the performance of RelExample.

TagVote in its denoising component, is consistently better than TagFeature.

The performance of individual methods consistently improves as more training data is used. As the size of the training set increases, the performance gap between the best model-based method (RelExample) and the best instance-based method (TagVote) reduces. This suggests that large-scale training data diminishes the advantage of model-based methods against the relatively simple instance-based methods.

In summary, even though the performance of the methods evaluated varies over datasets, common patterns have been observed. First, the more social data for training are used the better performance is obtained. Since the tag relevance functions are learned purely from social data without any extra manual labeling, and social data are increasingly growing, this result promises that better tag relevance functions can be learned. Second, given small-scale training data, tag + image based methods that conducts model-based learning with denoised training examples turn out to be the most effective solution, This however comes with a price of reducing the visual

Image Understanding by Socializing the Semantic Gap

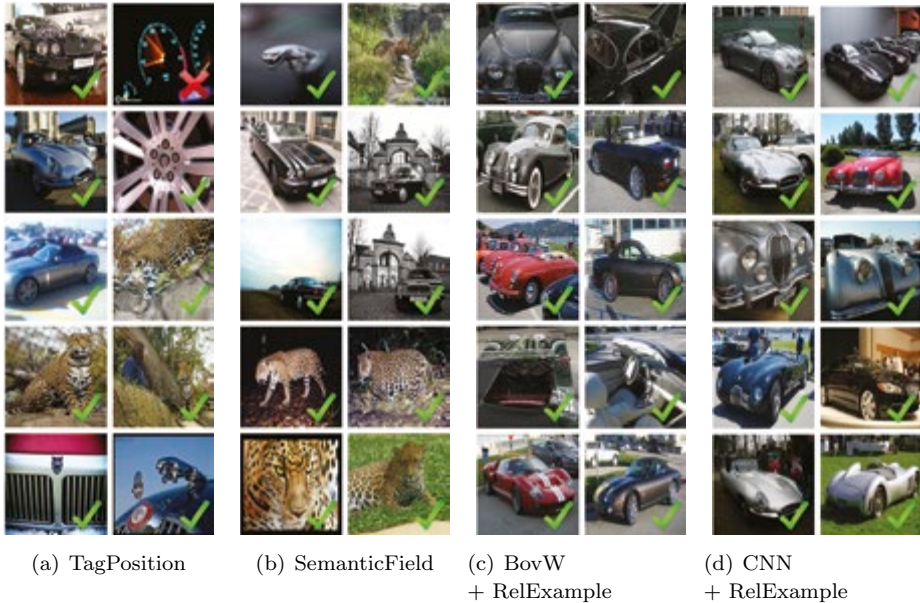


Figure 3.6: **Top 10 ranked images of ‘jaguar’, by (a) TagPosition, (b) SemanticField, (c) BovW + RelExample, and (d) CNN + RelExample.** Checkmarks (✓) indicate relevant results. While both RelExample and SemanticField outperform the TagPosition baseline, the results of SemanticField show more diversity for this ambiguous tag. The difference between (c) and (d) suggests that the results of RelExample can be diversified by varying the visual feature in use.

diversity in the retrieval results. Moreover, the advantage of model-based learning vanishes as more training data and the CNN feature are used, and TagVote performs the best.

3.5.4 Flickr versus ImageNet

To address the question of whether one shall resort to an existing resource such as ImageNet for tag relevance learning, this section presents an empirical comparison between our Flickr based training data and ImageNet. A number of methods do not work with ImageNet or require modifications. For instance, tag + image + user information based methods must be able to remove their dependency on user information, as such information is unavailable in ImageNet. Tag co-occurrences are also strongly limited, because an ImageNet example is annotated with a single label. Because of these limitations, we evaluate only the two best performing methods, TagVote and TagProp. TagProp can be directly used since it comes from classic image annotation, while TagVote is slightly modified by removing the unique user constraint. The CNN feature is used for its superior performance against

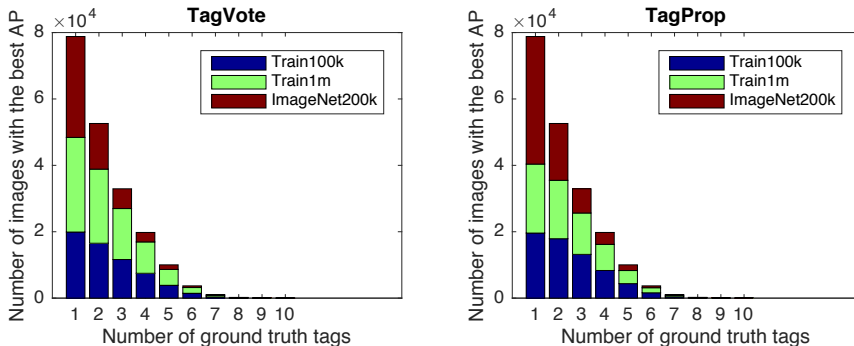


Figure 3.7: **Per-image comparison of TagVote/TagProp learned from different training datasets**, tested on NUS-WIDE. Test images are grouped in terms of the number of ground truth tags. Within each group, the area of a colored bar is proportional to the number of images that (the method derived from) the corresponding training dataset scores the best. ImageNet200k is less effective for assigning multiple labels to an image.

the BoVW feature.

To construct a customized subset of ImageNet that fits the three test sets, we take ImageNet examples whose labels precisely match with the test tags. Notice that some test tags, e.g., ‘portrait’ and ‘night’, have no match, while some other tags, e.g, ‘car’ and ‘dog’, have more than one matches. In particular, MIRFlickr has 2 missing tags, while the number of missing tags on Flickr51 and NUS-WIDE is 9 and 15. For a fair comparison these missing tags are excluded from the evaluation. Putting the remaining test tags together, we obtain a subset of ImageNet, containing 166 labels and over 200k images, termed ImageNet200k. For a fair comparison, we considered only Train100k and Train1m training sets of socially tagged images.

The left half of Table 3.10 shows the performance of tag assignment. TagVote/TagProp trained on the ImageNet data are less effective than their counterparts trained on the Flickr data. For a better understanding of the result, we employ the same visualization technique as used in Section 3.5.1, i.e., grouping the test images in terms of the number of their ground truth tags, and subsequently checking the performance per group. As shown in Fig. 3.7, while ImageNet200k performs better on the first group, i.e., images with a single relevant tag, it is outperformed by Train100k and Train1M on the other groups. For its single-label nature, ImageNet is less effective for assigning multiple labels to an image.

For tag retrieval, as shown in the right half of Table 3.10, TagVote/TagProp learned from ImageNet200k in general have higher MAP and NDCG scores than their counterparts learned from the Flickr data. By comparing the performance difference per concept, we find that the gain is largely contributed by a relatively small amount of concepts. Consider for instance

Image Understanding by Socializing the Semantic Gap

Table 3.10: Flickr versus ImageNet. Notice that the numbers on Train100k and Train1M are different from Tables 3.4, 3.8 and 3.9 due to the use of a reduced set of test tags. Bold values indicate top performers on a specific test set per performance metric.

Tag Assignment				
Training Set	MIRFlickr		NUS-WIDE	
	TagVote	TagProp	TagVote	TagProp
<i>MiAP scores:</i>				
Train100k	0.377	0.383	0.392	0.389
Train1M	0.389	0.392	0.414	0.393
ImageNet200k	0.345	0.304	0.325	0.368
<i>MAP scores:</i>				
Train100k	0.641	0.647	0.386	0.405
Train1M	0.664	0.668	0.429	0.420
ImageNet200k	0.532	0.532	0.363	0.362
Tag Retrieval				
Training Set	Flickr51		NUS-WIDE	
	TagVote	TagProp	TagVote	TagProp
<i>MAP scores:</i>				
Train100k	0.854	0.860	0.742	0.745
Train1M	0.874	0.871	0.753	0.745
ImageNet200k	0.873	0.873	0.762	0.762
<i>NDCG₂₀ scores:</i>				
Train100k	0.838	0.863	0.849	0.856
Train1M	0.894	0.851	0.891	0.853
ImageNet200k	0.920	0.898	0.843	0.847

TagVote + ImageNet200k and TagVote + Train1M on NUS-WIDE. The former outperforms the latter for 25 out of the 66 tested concepts. By sorting the concepts according to their absolute performance gain, the top three winning concepts of TagVote + ImageNet200k are ‘sand’, ‘garden’, and ‘rainbow’, with AP gain of 0.391, 0.284, and 0.176, respectively. Here, the lower performance of TagVote + Train1M is largely due to the subjectiveness of social tagging. For instance, Flickr images labeled with ‘sand’ tend to be much more diverse, showing a wide range of things visually irrelevant to sand. Interestingly, the top three losing concepts of TagVote + ImageNet200k are ‘running’, ‘valley’, and ‘building’, with AP loss of 0.150, 0.107, and 0.090, respectively. For these concepts, we observe that their ImageNet examples lack diversity. E.g., ‘running’ in ImageNet200k mostly shows a person running on a track. In contrast, the subjectiveness of social tagging now has a positive effect on generating diverse training examples.

In summary, for tag assignment social media examples are a preferred resource of training data. For tag retrieval ImageNet yields better performance, yet the performance gain is largely due to a few tags where social tagging is very noisy. In such a case, controlled manual labeling seems indispensable. In contrast, with clever tag relevance learning algorithms, social training data demonstrate competitive or even better performance for many of the tested tags. Nevertheless, where the boundary between the two cases is precisely located remains unexplored.

3.6 Conclusions

Having established the common ground between methods, a new experimental protocol was introduced for a head-to-head comparison between the state-of-the-art. A selected set of eleven representative works were implemented and evaluated for tag assignment, refinement, and/or retrieval. The evaluation justifies the state-of-the-art on the three tasks. For tag assignment, TagProp and TagVote perform best. For tag refinement, RobustPCA is the choice. For tag retrieval, TagVote achieves the best overall performance. Concerning what media is essential for tag relevance learning, tag + image is consistently found to be better than tag alone. While the joint use of tag, image, and user information (via TensorAnalysis) demonstrates its potential on small-scale datasets, it becomes computationally prohibitive as the dataset size increases to 100k and beyond. Comparing the three learning strategies, instance-based and model-based methods are found to be more reliable and scalable than their transduction-based counterparts. As model-based methods are more sensitive to the quality of social image tagging, a proper filtering strategy for refining the training media is crucial for their success. Despite their leading performance on the small training

Image Understanding by Socializing the Semantic Gap

dataset, we find that the performance gain over the instance-based alternatives diminishes as more training data is used. Finally, the CNN feature used as a substitute for the BoVW feature brings considerable improvements for all the tasks.

Chapter 4

A Cross Modal Approach for Tag Assignment

*Tag assignment is still an important open problem in multimedia and computer vision. Many approaches previously proposed in the literature do not accurately capture the intricate dependencies between image content and annotations. We propose a learning procedure based on Kernel Canonical Correlation Analysis which finds a mapping between visual and textual words by projecting them into a latent meaning space. The learned mapping is then used to annotate new images using advanced nearest neighbor methods. We evaluate our approach on three popular datasets, and show clear improvements over several approaches relying on more standard representations.*¹

4.1 Introduction

The exponential growth of media sharing websites, such as Flickr or Picasa, and social networks such as Facebook, has led to the availability of large collections of images tagged with human-provided labels. These tags reflect the image content and can thus be exploited as a loose form of labels and context. Several researchers have explored ways to use images with associated labels as a source to build classifiers or to transfer their tags to similar images (Duygulu et al., 2002; Makadia et al., 2008; Guillaumin et al., 2009; Li et al., 2009b; Li and Fei-Fei, 2010; Znaidia et al., 2013). Image annotation is therefore a very active subject of research (Metzler and Manmatha, 2004; Yavlinsky et al., 2005; Carneiro et al., 2007; Liu, Li, Liu, Lu and Ma, 2009; Zhang et al., 2010; Verma and Jawahar, 2012) since we can clearly increase performance of search and indexing over image collections that are machine enriched with a set of meaningful labels. In this chapter we tackle the problem of assigning a finite number of relevant tags to an image, given

¹Parts of the work presented in this chapter have been published in Ballan, L., Uricchio, T., Seidenari, L., and Del Bimbo, A. (2014, April). "A cross-media model for automatic image annotation". In Proceedings of International Conference on Multimedia Retrieval (p. 73). ACM. The publication is available at <http://dx.doi.org/10.1145/2578726.2578728>.

the image appearance and some prior knowledge on the joint distribution of visual features and tags based on some weakly and noisy annotated data.

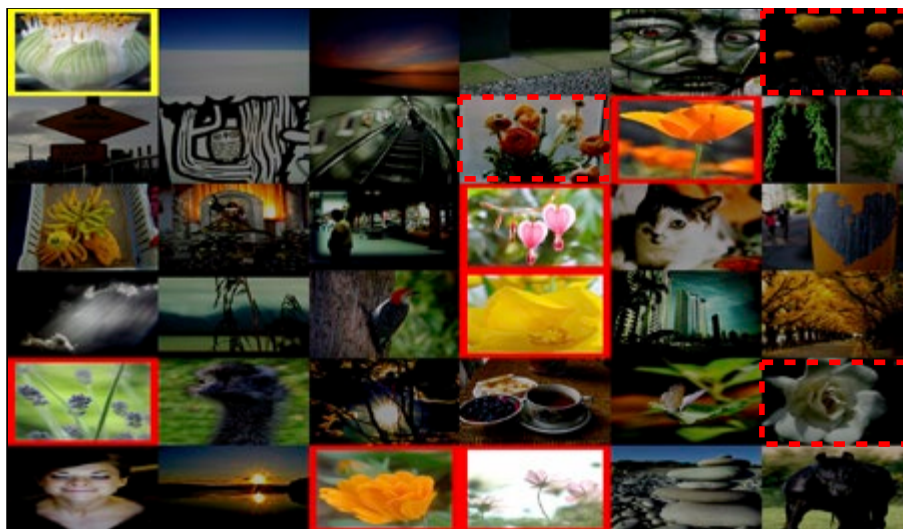
The main shortcomings of previous works in the field are twofold. The first is the aforementioned *semantic gap* problem, which points to the fact that it is hard to extract semantically meaningful entities using just low level visual features. The second shortcoming arises from the fact that many parametric models, previously presented in the literature, are not rich enough to accurately capture the intricate dependencies between image content and annotations. Recently, nearest neighbor based methods have attracted much attention since they have been found to be quite successful for tag prediction (Makadia et al., 2008; Guillaumin et al., 2009; Li et al., 2009b; Uricchio et al., 2013; Znaidia et al., 2013) (see also Chapter 2 and 3). This is mainly due to their flexibility and capacity to adapt to the patterns in the data as more training data is available. The base ingredient for a vote based tagging algorithm is of course the source of votes: the set of K nearest neighbors. In challenging real world data it is often the case that the vote casting neighbors do not contain enough statistics to obtain reliable predictions. This is mainly due to the fact that certain tags are much more frequent than others and can cancel out less frequent but relevant tags (Guillaumin et al., 2009; Li et al., 2009b). It is obvious that all voting schemes can benefit from a better set of neighbors. We believe that the main bottleneck in obtaining such ideal neighbors set is the semantic gap. We address this problem using a cross-modal approach to learn a representation that maximizes the correlation between visual features and tags in a common semantic subspace.

In Figure 4.1 we show our intuition with an example provided by real data. We compare for the same query, a flower close-up, the first thirty-five most similar examples provided by the visual features and by our representation. The first thing to notice is the large visual and semantic difference between the sets of retrieved neighbors by the two approaches. Note also that some flower pictures, which we highlight with a dashed red rectangle, were not tagged as such. Second, note how the result presented in Figure 4.1(b) have more and better ranked *flower* images than the one in Figure 4.1(a). Indeed with the result set in Figure 4.1(a) it is not possible to obtain a sufficient amount of meaningful neighbors and the correct tag *flower* is canceled by others such as *dog* or *people*.

In this chapter we present a cross-media approach that relies on Kernel Canonical Correlation Analysis (KCCA) (Hardoon and Shawe-Taylor, 2003; Hardoon et al., 2004) to connect visual and textual modalities through a common latent meaning space (called *semantic space*). Visual features and labels are mapped to this space using feature similarities that are observable inside the respective domains. If mappings are close in this semantic



(a) Baseline



(b) Our Method

Figure 4.1: Nearest neighbors found with baseline representation (a) and with our proposed method (b) for a flower image (first highlighted in yellow in both figures) from the MIRFlickr-25K dataset. Training images with ground truth tag *flower* are highlighted with a red border. Nearest neighbors are sorted by decreasing similarity and arranged in a matrix using a row-major convention. Dashed red lines indicate flower pictures not tagged as such.

space, the images are likely to be instances of the same underlying semantic concept. The learned mapping is then used to annotate new images using a nearest-neighbor voting approach. We present several experiments using different voting schemes. First, the simple KNN voting of Makadia *et al.* (Makadia et al., 2008), and second three advanced NN models such as TagVote (Li et al., 2009b), TagProp (Guillaumin et al., 2009) and 2PKNN (Verma and Jawahar, 2012).

4.1.1 Contribution

Other existing approaches learn from both words and images, including previous uses of CCA (Hardoon and Shawe-Taylor, 2003; Rasiwasia et al., 2010; Hwang and Grauman, 2012; Gong et al., 2013). In contrast, we are the first to propose an approach that combines an effective cross-modal representation with advanced nearest-neighbor models for the specific task of tag assignment.

In the following we show that, if combined with advanced NN schemes able to deal with the class-imbalance (i.e. large variations in the frequency of different labels), our cross-media model achieves high performance without requiring heavy computation such as in the case of metric learning frameworks with many parameters (as in (Guillaumin et al., 2009; Verma and Jawahar, 2012)).

We present experimental results for two standard datasets, Corel5K (Duygulu et al., 2002) and IAPR-TC12 (Grubinger et al., 2006), obtaining highly competitive results. We report also experiments on a challenging dataset collected from Flickr, i.e. the MIRFlickr-25K dataset (Huiskes and Lew, 2008), and our results show that the performance of the proposed method is boosted even further in a realistic and more interesting scenario such as the one provided by weakly-labeled images.

4.2 Related Work

In the multimedia and computer vision communities, jointly modeling images and text has been an active research area in the recent years. A first group of methods uses mixture models to define a joint distribution over image features and labels. The training images are used by these models as components to define a mixture model over visual features and tags (Lavrenko et al., 2003; Feng et al., 2004; Carneiro et al., 2007). They can be interpreted as non-parametric density estimators over the co-occurrence of images and labels. In another group of methods based on topic models (such as LDA and pLSA), each topic represents a distribution over image features and labels (Barnard et al., 2003; Monay and Gatica-Perez, 2004).

These kind of generative models may be criticized because they maximize the generative data likelihood, which is not optimal for predictive performance. Another main criticism of these models is their need for simplifying assumptions in order to do tractable learning and inference.

Discriminative models such as support vector machines have also been proposed (Grangier and Bengio, 2008; Verma and Jawahar, 2013). These methods learn a classifier for each label, and use them to predict whether a test image belongs to the class of images that are annotated with a particular label. A main criticism of these works resides in the necessity to define in advance the number of labels and to train individual classifiers for each of them. This is not feasible in a realistic scenario like the one of web images. Despite their simplicity, nearest-neighbor based methods for image annotation have been found to give state-of-the-art results (Makadia et al., 2008; Guillaumin et al., 2009; Verma and Jawahar, 2012). The intuition is that similar images share common labels. The common procedure of the existing nearest-neighbor methods is to search for a set of visually similar images and then to select a set of relevant associated tags based on a tag transfer procedure (Makadia et al., 2008; Li et al., 2009b; Guillaumin et al., 2009). In all these previous approaches, this similarity is determined only using image visual features.

4.3 Approach

The proposed method is based on KCCA which provides a common representation for the visual and tag features. We refer to this common representation as *semantic space*. Similarly to (Hardoon and Shawe-Taylor, 2003; Hwang and Grauman, 2012) we use KCCA to connect visual and textual modalities, but our method is designed to effectively tackle the particular problem of image auto-annotation. In Section 4.3.1 we present our visual and text features with their respective kernels; next we briefly describe KCCA (Section 4.3.2) and the different NN schemes (Section 4.3.3). In Figure 4.2 we show an embedding computed with ISOMAP (Tenenbaum et al., 2000) of the visual data and its semantic projection. We randomly pick three tags to show how the semantic projection that we learn with KCCA better suits the actual distribution of tags with respect to the visual representation. The semantic projection improves the separation of the classes, allowing a better manifold reconstruction and, as our experiments will confirm, an improvement on precision and recall on different datasets.

4.3.1 Visual and Tags Views

Visual Feature Representation and Kernels

We directly use the 15 features provided by the authors of (Guillaumin et al., 2009; Verbeek et al., 2010)². These are different types of global and local features commonly used for image retrieval and categorization. In particular we use two types of global descriptors: Gist and color histograms with 16 bins in each channel for RGB, LAB, HSV color spaces. Local features include SIFT and robust hue descriptors, both extracted densely on a multi-scale grid or for Harris-Laplacian interest points. The local feature descriptors are quantized using k-means and then all the images are represented as bag-of-(visual)words histograms. The histograms are also computed in a spatial arrangement over three horizontal regions of the image, and then concatenated to form a new global descriptor that encodes some information of the global spatial layout.

In this work we use χ^2 exponential kernels for all visual features $f \in \mathcal{F}$:

$$K_{\chi^2}(h_i, h_j) = \exp\left(-\frac{1}{2A} \sum_{k=1}^d \frac{(h_i(k) - h_j(k))^2}{(h_i(k) + h_j(k))}\right), \quad (4.1)$$

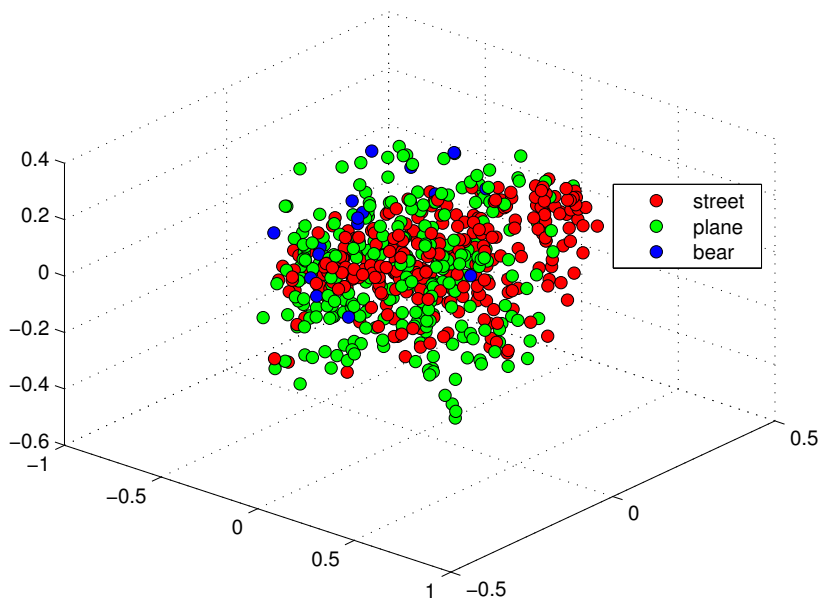
where A is the mean of the χ^2 distances among all the training examples, d is the dimensionality of a particular feature descriptor and h_i is its respective histogram representation. It has to be noticed that all the feature descriptors are L1-normalized. Finally, all the different visual kernels are averaged to obtain the final visual representation. We obtain the kernel between two images I_i, I_j via kernel averaging:

$$K_v(I_i, I_j) = \frac{1}{|\mathcal{F}|} \sum_{f \in \mathcal{F}} K_{\chi^2}(h_i^f, h_j^f). \quad (4.2)$$

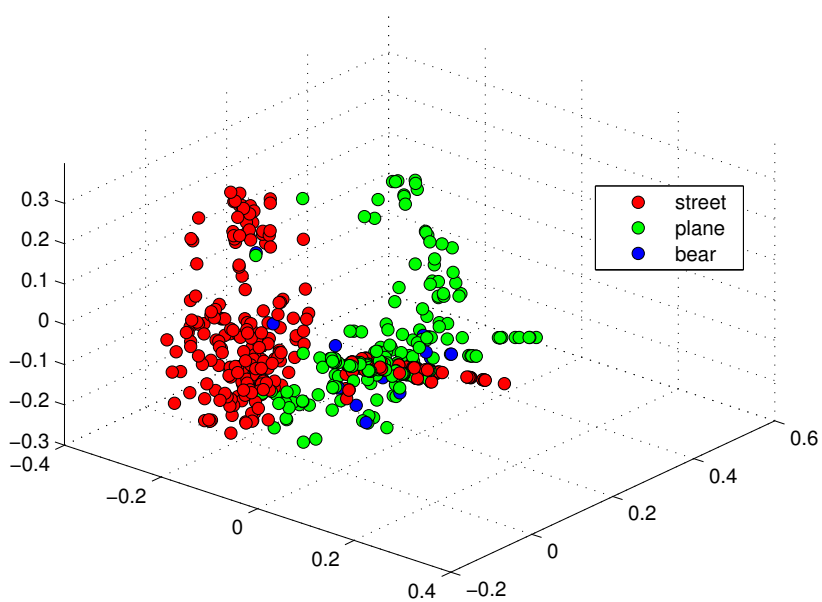
Tag Feature Representation and Kernel

We use as tag features the traditional bag-of-words which records which labels are named in the image, and how many times. Supposing V is our vocabulary size, i.e. the total possible words used for annotation, each tag-list is mapped to an V -dimensional feature vector $h = [w_1, \dots, w_V]$, where w_i counts the number of times the i -th word is mentioned in the tag list. In our case this representation is highly sparse and often counts are simply 0 or 1 values. We use these features to compute a linear kernel that corresponds

²These features are available at: <http://lear.inrialpes.fr/people/guillaumin/data.php>.



(a) Visual Space



(b) Semantic Space

Figure 4.2: Visualization of three labels (Corel5K): (a) distribution of image features in the visual space (b) distribution of the same images after projecting into the semantic space learned using KCCA. Note the clearer distinction of the clusters in the semantic space.

to counting the number of tags in common between two images:

$$K_t(h_i, h_j) = \langle h_i, h_j \rangle = \sum_k^V h_i(k)h_j(k). \quad (4.3)$$

4.3.2 Kernel Canonical Correlation Analysis

Given two views of the data, such as the ones provided by visual and textual modalities, we can construct a common representation. Canonical Correlation Analysis (CCA) seeks to utilize data consisting of paired views to simultaneously find projections from each feature space such that the correlation between the projected representations is maximized. In the literature, the CCA method has often been used in cross-language information retrieval, where one queries a document in a particular language to retrieve relevant documents in another language. In our case, the algorithm learns two semantic projection bases, one per each modality (i.e. the v view is the visual cue while the t view is the tag-list cue).

More formally, given N samples from a paired dataset $\{(v_1, t_1), \dots, (v_N, t_N)\}$, where $v_i \in \mathbb{R}^n$ and $t_i \in \mathbb{R}^m$ are the two views of the data, the goal is to simultaneously find directions w_v^* and w_t^* that maximize the correlation of the projections of v onto w_v and t onto w_t . This is expressed as:

$$w_v^*, w_t^* = \arg \max_{w_v, w_t} \frac{\hat{E}[\langle v, w_v \rangle \langle t, w_t \rangle]}{\sqrt{\hat{E}[\langle v, w_v \rangle^2] \hat{E}[\langle t, w_t \rangle^2]}} = \arg \max_{w_v, w_t} \frac{w_v^T C_{vt} w_t}{\sqrt{w_v^T C_{vv} w_v w_t^T C_{tt} w_t}}, \quad (4.4)$$

where \hat{E} denotes the empirical expectation, C_{vv} and C_{tt} respectively denote the auto-covariance matrices for v and t data, and C_{vt} denotes the between-sets covariance matrix. The solution can be found via a generalized eigenvalue problem (Hardoon et al., 2004).

The common CCA algorithm can only recover linear relationships, it is therefore useful to kernelize it by projecting the data into a higher-dimensional feature space by using the kernel trick. Kernel Canonical Correlation Analysis (KCCA) is the kernelized version of CCA. To this end, we define kernel functions over v and t as $K_v(v_i, v_j) = \phi_v(v_i)^T \phi_v(v_j)$ and $K_t(t_i, t_j) = \phi_t(t_i)^T \phi_t(t_j)$. Here, the idea is to search for solutions of w_v, w_t that lie in the span of the N training instances $\phi_v(v_i)$ and $\phi_t(t_i)$:

$$w_v = \sum_i \alpha_i \phi_v(v_i), \\ w_t = \sum_i \beta_i \phi_t(t_i), \quad (4.5)$$

where $i \in \{1, \dots, N\}$. The objective of KCCA is thus to identify the weights $\alpha, \beta \in \mathbb{R}^N$ that maximize:

$$\alpha^*, \beta^* = \arg \max_{\alpha, \beta} \frac{\alpha^T K_v K_t \beta}{\sqrt{\alpha^T K_v^2 \alpha \beta^T K_t^2 \beta}}, \quad (4.6)$$

where K_v and K_t denote the $N \times N$ kernel matrices over a sample of N pairs. As shown by Hardoon (Hardoon et al., 2004), learning may need to be regularized in order to avoid trivial solutions. Hence, we penalize the norms of the projection vectors and obtain the standard eigenvalue problem:

$$(K_v + \kappa I)^{-1} K_t (K_t + \kappa I)^{-1} K_v \alpha = \lambda^2 \alpha. \quad (4.7)$$

The top D eigenvectors of this problem yield basis $A = [\alpha^{(1)} \dots \alpha^{(D)}]$ and $B = [\beta^{(1)} \dots \beta^{(D)}]$ that we use to compute the semantic projections of any vector v_i, t_i .

Implementation Details

In order to avoid degeneracy with non-invertible Gram matrices and to increase computational efficiency we approximate the Gram matrices using the Partial Gram-Schmidt Orthogonalization (PGSO) algorithm provided by Hardoon *et al.* (Hardoon et al., 2004). As suggested in (Hardoon et al., 2004) the regularization parameter κ is found by maximizing the difference between projections obtained by correctly and randomly paired views of the data on the training set. In the experiments we have optimized both the parameters of the PGSO algorithm (i.e. κ and T); however, we found as a good starting configuration the setting $T = 30$ and $\kappa = 0.1$. We also found important swapping the use of visual and textual spaces as Hardoon (Hardoon et al., 2004) fixes A to be unit vectors while computing B on the basis of the two kernels.

4.3.3 Tag Assignment Using Nearest Neighbor Models in the Semantic Space

The intuition underlying the use of nearest-neighbor methods for tag assignment is that similar images share common labels. Following this key idea, we have investigated and applied several NN schemes to our semantic space in order to automatically annotate images. We briefly describe these models below and refer the interested reader to the Chapter 3.

For all baseline methods the K neighbors of a test image I_i are selected as the training images I_j for which our averaged test kernel value $K_v(I_i, I_j)$, defined in Eq. 4.2, scores higher. In case the semantic space projection is

used, the K neighbors are computed using:

$$d(\psi(I_i), \psi(I_j)) = 1 - \frac{\psi(I_i)^T \cdot \psi(I_j)}{\|\psi(I_i)\|_2 \cdot \|\psi(I_j)\|_2} \quad (4.8)$$

where $\psi(I_i)$ is the semantic projection of a test image I_i . The projection of I_i is defined as $\psi(I_i) = K_v(I_i, \cdot)^T A$, where $K_v(I_i, \cdot)$ is the vector of kernel values of a sample I_i and all the training samples. Note that we only use the *visual* view of our data both for training and test samples.

KNN

Given a test image, we project onto the semantic space and identify its K Nearest-Neighbors. Then we merge their labels to create a tag-list by counting all tag occurrences on the K retrieved images, and finally we reorder the tags by their frequency. If we fix K to a very small number (e.g. $K = 2$) this approach is similar to the ad-hoc nearest neighbor tag transfer mechanism proposed by Makadia *et al.* (Makadia et al., 2008).

TagVote

Li *et al.* (Li et al., 2009b) proposed a tag relevance measure based on the consideration that if different persons label visually similar images using the same tags, then these tags are more likely to reflect objective aspects of the visual content. Following this idea it can be assumed that, given a query image, the more frequently the tag occurs in the neighbor set, the more relevant it might be. However, some frequently occurring tags are unlikely to be relevant to the majority of images. To account for this fact the proposed tag relevance measurement takes into account both the distribution of a tag t in the neighbor set for an image I and in the entire collection:

$$\text{tagVote}(l, I, K) := n_t[N(I, K)] - \text{Prior}(t), \quad (4.9)$$

where n_t is an operator counting the occurrences of t in the neighborhood $N(I, K)$ of K similar images, and $\text{Prior}(t)$ is the occurrence frequency of t in the entire collection.

TagProp

Guillaumin *et al.* (Guillaumin et al., 2009) proposed an image annotation algorithm in which the main idea is to learn a weighted nearest neighbor model, to automatically find the optimal combination of multiple feature distances. Using $y_{it} \in \{-1, +1\}$ to represent if tag t is relevant or not for the test image I_i , the probability of being relevant given a neighborhood of

K images $I_j \in N(I_i, K) = \{I_1, I_2, \dots, I_K\}$ is:

$$p(y_{it} = +1) = \sum_{I_j \in N(I_i, K)} \pi_{ij} p(y_{it} = +1 | N(I_i, K)), \quad (4.10)$$

$$p(y_{it} = +1 | N(I_i, K)) = \begin{cases} 1 - \epsilon & \text{for } y_{it} = +1, \\ \epsilon & \text{otherwise} \end{cases} \quad (4.11)$$

$$\pi_{ij} \geq 0, \quad \sum_{I_j \in N(I_i, K)} \pi_{ij} = 1, \quad (4.12)$$

where π_{ij} is the weight of a training image I_j of the neighborhood $N(I, K)$ and $p(y_{it} = +1 | N(I_i, K))$ is the prediction of tag t according to each neighbor in the weighted sum.

The model can be used with rank-based (RK) or distance-based weighting; the latter can be learnt by using a single distance (referred to as the SD variant) or using metric learning (ML) over multiple distances. Furthermore, to compensate for varying frequencies of tags, a tag-specific sigmoid is used to scale the predictions, to boost the probability for rare tags and decrease that of frequent ones. Sigmoids and metric parameters can be learned by maximizing the log-likelihood $\sum_{I_i, t} \ln p(y_{it})$.

2PKNN

Verma and Jawahar (Verma and Jawahar, 2012) proposed a two phase method: a first pass is employed to address the class-imbalance by constructing a balanced neighborhood for each test image and then a second pass, where the actual tag importance is assigned based on image similarity.

The problem of image annotation is formulated similarly as Guillaumin *et al.* (Guillaumin et al., 2009), by finding the posterior probabilities:

$$P(y_{it} | I_i) = \frac{P(I_i | y_{it}) P(y_{it})}{P(I_i)} \quad (4.13)$$

Given a test image I_i , and a vocabulary $Y = \{t_1, t_2, \dots, t_M\}$, the first phase collects a set neighborhoods T_{it} for each tag $t \in Y$ by selecting at least the nearest M training images annotated with t . The neighborhood of image I_i is then given by $N(I_i) = \bigcup_{t \in Y} T_{it}$. It should be noticed that a tag can have less than M training image and therefore $N(I_i)$, may still be a lightly unbalanced set of tags.

On the second phase of 2PKNN, given a tag $t \in Y$, the probability $P(I_i | t)$ is estimated by the neighborhood defined in phase one for image I :

$$P(I_i | t) = \sum_{I_j \in N(I_i)} \exp(-D(I_i, I_j)) p(y_{it} = +1 | N(I_i)) \quad (4.14)$$

Image Understanding by Socializing the Semantic Gap

(a) Core5K

	NN-voting		TagVote		TagProp		2PKNN	
	Baseline	KCCA	Baseline	KCCA	Baseline	KCCA	Baseline	KCCA
P	26	37	25	36	29	35	36	42
R	30	36	35	37	35	40	38	46
N+	135	139	151	144	144	149	169	179

(b) IAPR-TC12

	NN-voting		TagVote		TagProp		2PKNN	
	Baseline	KCCA	Baseline	KCCA	Baseline	KCCA	Baseline	KCCA
P	32	56	27	57	37	58	46	59
R	21	25	26	28	22	26	29	30
N+	235	213	258	246	225	235	272	259

(c) MIRFlickr-25K

	NN-voting		TagVote		TagProp		2PKNN	
	Baseline	KCCA	Baseline	KCCA	Baseline	KCCA	Baseline	KCCA
P	34	51	38	50	37	55	16	56
R	26	35	22	37	26	36	6	25
N+	17	18	18	18	18	18	16	18

Table 4.1: This table shows the results of several configurations of our method based on KCCA and baselines on the Core5K , IAPR-TC12 and MIRFlickr-25K datasets.

where $p(y_{it} = +1|N(I_i))$ is the presence of tag t for image I_i as in Guillaumin *et al.* (Guillaumin et al., 2009) and $D(I_i, I_j)$ is the distance between image I_i and I_j .

In the simplest version of this algorithm $D(I_i, I_j)$ is just a scaled version of the distance $wD(I_i, I_j)$, where w is a scalar. Authors in (Verma and Jawahar, 2012) also propose a more complex version where $D(I_i, I_j)$ can be parameterized as a Mahalanobis distance where the weight matrix can be learned in a way that the resulting metric will pull the neighbors from the T_t belonging to ground-truth tags closer and push far the remaining ones.

4.4 Experiments

We evaluate the performance of our cross-media model for tag assignment on three popular datasets and we compare it to closely related work.

	Previously reported results														ML		
	CRM (Lavrenko et al., 2003)	InfNet (Metzler and Manmatha, 2004)	NPDE (Yavinsky et al., 2005)	MBRM (Feng et al., 2004)	SML (Carneiro et al., 2007)	TGLM (Lin, Li, Liu, Lu and Ma, 2009)	GS (Zhang et al., 2010)	JEC-15 (Guillaumin et al., 2009)	TagProp σ RK (Guillaumin et al., 2009)	TagProp σ SD (Guillaumin et al., 2009)	RF-opt (Fu et al., 2012)	K SVM-VT (Verma and Jawahar, 2013)	2PKNN (Verma and Jawahar, 2012)	TagProp σ ML (Guillaumin et al., 2009)	2PKNN ML (Verma and Jawahar, 2012)		
P	16	17	18	24	23	25	30	28	26	28	29	32	39	33	44		42
R	19	24	21	25	29	29	33	33	34	35	40	42	40	42	46		46
N+	107	112	114	122	137	131	146	140	143	145	157	179	177	160	191		179

Table 4.2: This table shows the results of our method and related work on the Corel5K dataset (as reported in the literature). JEC-15 refers to the JEC (Makadia et al., 2008) implementation of (Guillaumin et al., 2009) that uses our 15 visual features.

4.4.1 Datasets

Corel5K. The Corel5K dataset (Duygulu et al., 2002) has been the standard evaluation benchmark in the image annotation community for around a decade. It contains 5,000 images which are annotated with 260 labels and each image has up to 5 different labels (3.4 on average). This dataset is divided into 4,500 images for training and 500 images for testing.

IAPR-TC12. This dataset was introduced in (Grubinger et al., 2006) for cross-language information retrieval and it consists of 17,665 training images and 1,962 testing images. Each image is annotated with an average of 5.7 labels out of 291 candidate.

MIRFlickr-25K. The MIRFlickr-25K dataset has been recently introduced to evaluate keyword-based image retrieval methods. The set contains 25,000 images that were downloaded from Flickr and for each one of these images the tags originally assigned by the users are available (as well as EXIF information fields and other metadata such as GPS). It is a very challenging dataset since the tags are weak labels and not all of them are actually relevant to the image content. There are also many meaningless

Image Understanding by Socializing the Semantic Gap

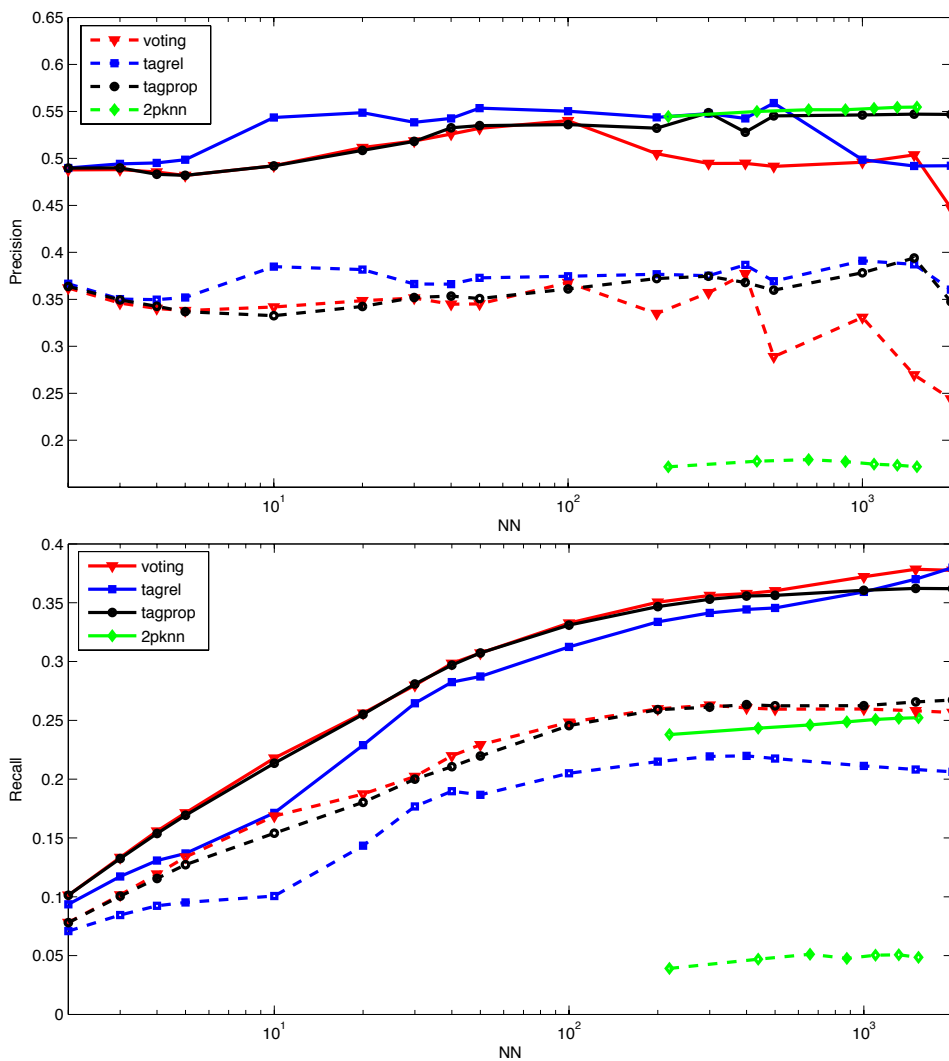


Figure 4.3: Precision and recall of all the methods on MIRFlickr-25k varying the number of nearest neighbors. Dashed lines represent baseline methods. Note that 2PKNN implicitly define the size of the neighborhood based only on the number of images per labels.

words. Therefore a pre-processing step was performed to filter out these tags. To this end we matched each tag with entries in Wordnet and only those tags with a corresponding item in Wordnet were retained. Moreover, we removed the less frequent tags, whose occurrence numbers are below 50. The result of this process is a vocabulary of 219 tags. The images are also manually annotated for 18 concepts (i.e. labels) that are used to evaluate the automatic annotation performances. As in (Verbeek et al., 2010), the dataset is divided into 12,500 images for training and 12,500 images for testing.

4.4.2 Evaluation Measures

We evaluate our models with standard performance measures, used in previous work on image annotation. The standard protocol in the field is to report Precision and Recall for fixed annotation length (Duygulu et al., 2002). Thus each image is annotated with the n most relevant labels (usually, as in this chapter, the results are obtained using $n = 5$). Then, the results are reported as mean precision \mathbf{P} and mean recall \mathbf{R} over the ground-truth labels; $\mathbf{N}+$ is often used to denote the number of labels with non-zero recall value. Note that each image is forced to be annotated with n labels, even if the image has fewer or more labels in the ground truth. Therefore we will not measure perfect precision and recall figures.

4.4.3 Results

As a first experiment we compare our method with the corresponding nearest neighbor voting schemes. It can be seen from Table 4.1 that our approach improves over baseline methods in every setting on all datasets. Precision is boosted notably, confirming the better separation of the classes in the semantic space (as previously discussed in Section 4.3). Also recall is improved by a large margin on Corel5K and MIRFlickr-25k. On IAPR-TC12 recall improvement is less pronounced. We believe this is due the different amount of textual annotation: IAPR-TC12 has an average of 5.7 tags per image (TPI) and up to 23 TPI while on Corel5K and MIRFlickr-25k the average TPI is respectively 3.4 and 4.7 with a maximum of 5 and 17 TPI respectively. Recalling that we are predicting $n = 5$ tags per image, recall is harder to improve on this dataset.

We conduct an evaluation of how the amount of neighbours affect the performance for both our method and the baseline on the challenging MIRFlickr-25k dataset. As can be seen from Figure 4.3 the KCCA variants (solid lines) of the four considered voting schemes systematically improve both precision and recall for any amount of nearest neighbors used. Note that in both cases, a similar pattern emerges due the natural instability of NN methods.

It is interesting to note that while recall gets better as the neighborhood gets bigger, saturating at near 2,000 neighbours, precision depends on the algorithm chosen. Basic voting and TagVote show an improvement until 200 neighbors and then begin decreasing; TagProp improves until saturates at around 900.

2PKNN misses a direct parameter to choose the dimension of the neighborhood, but it implicitly defines it by choosing at most M images per label. However, while it has a clear advantage on Corel5K and IAPR-TC12, both as a baseline and after the projection, it fails to achieve comparable performance on MIRFlickr-25K. We believe that this is due to the noisy and missing tags of MIRFlickr-25K, a notable difference on this more realistic and challenging dataset.

Comparing with the state of the art, on Tables 4.2 and 4.3, our method achieves better performance than all previous works while it is comparable with the state of the art method 2PKNN (Verma and Jawahar, 2012) on Corel5K. Our method performs slightly worse than 2PKNN in metric learning configuration. However, metric learning involves a learning procedure with many parameters that rise the complexity of optimization and undermines scalability.

Our method, once learned the semantic space, continues to work in what we call an open world setting. In this setting that is indeed more realistic, the amount of tags per image evolves over time. That is the case of big data from social media and, more in general, from the web.

We also report in Table 4.4 a comparison with the methods presented in (Guillaumin et al., 2009; Verbeek et al., 2010) using per-image average precision (iAP). This measure indicates how well a method identifies relevant concepts for a given image. Our method combining the 2PKNN voting scheme, without metric learning, with the semantic projection outperforms all the other methods.

Qualitative Analysis

In Figure 4.4 we present some anecdotal evidence for our method (from the MIRFlickr-25k dataset). It can be seen that TagProp and TagVote perform better in general for the baseline representation and our proposed KCCA variant. It has to be noted that for challenging images where visual features can be deceiving our cross-modal approach allows to retrieve more tags. As an example see the first two rows: a close-up of a flower and a cloudy sunset with a road. For the first one it is not surprising that visual features do not provide enough good neighbors to retrieve the *flower* tag. For the second one none of the baseline method can retrieve the *sunset* and *cloud* tags; we believe that this is due to the lack of color features. In this two cases it is clear that semantically induced neighbors in the common space can boost

	Previously reported results							ML		
	MBRM (Feng et al., 2004)	GS (Zhang et al., 2010)	JEC-15 (Guillaumin et al., 2009)	TagProp σ SD (Guillaumin et al., 2009)	RF-opt (Fu et al., 2012)	KSVM-VT (Verma and Jawahar, 2013)	2PKNN (Verma and Jawahar, 2012)	TagProp σ ML (Guillaumin et al., 2009)	2PKNN ML (Verma and Jawahar, 2012)	Our best result
P	24	32	29	41	44	47	49	46	54	59
R	23	29	19	30	31	29	32	35	37	30
N+	223	252	211	259	253	268	274	266	278	259

Table 4.3: This table shows the results of our method and related work on the IAPR-TC12 dataset (as reported in the literature).

	Previously reported results					ML	
	random	SVM v	SVM t	SVM v++	TagProp RK	TagProp ML	Our best result
iAP	5.6	44.2	32	45	46.3	47.3	50.8

Table 4.4: This table shows the results of our method and related work (Verbeek et al., 2010) on the MIRFlickr-25k dataset.

Image Understanding by Socializing the Semantic Gap

the accuracy.

Another challenging example is shown at row five: a *girl* is depicted behind an object that hides a part of the face. This image component do not have enough visual neighbors to retrieve its tags. With our representation we are able to retrieve *girl* and *portrait* in the first three voting schemes and also *people* in the TagProp voting scheme, though *face* and *woman* may be considered correct even if not present in the ground truth tags.

	Baselines				KCCA models			
	NN-voting	TagVote	TagProp	2PKNN	NN-voting	TagVote	TagProp	2PKNN
	dog graffiti people black art	dog graffiti animal people house	graffiti dog people face art	graffiti dog people face art	flower flowers pink green spring	flower flowers pink green red	flower flowers green pink white	graffiti dog people face art
	sky clouds water landscape trees	clouds sky landscape water trees	clouds sky water landscape trees	clouds sky water landscape trees	clouds sky landscape sunset blue	clouds sky sunset landscape cloud	clouds sky landscape sunset beach	clouds sky water landscape trees
	japan art water dog trees	japan zoo dog trees art	japan water dog park art	japan water dog park art	portrait girl tree street green	portrait girl woman tree trees	portrait girl green tree trees	japan water dog park art
	pink flower japan baby portrait	pink baby japan cake crochet	pink japan flower japanese vintage	pink japan flower japanese vintage	food chocolate cake fruit red	food cake chocolate dog crochet	food chocolate cake red fruit	pink japan flower japanese vintage
	japan people man street bicycle	japan man people bicycle animal	japan people animal kid eye	japan people animal kid eye	portrait girl girls hair face	portrait girl face woman hair	portrait girl face people woman	japan people animal kid eye
	street architecture beach white snow	street snow architecture beach home	beach street people portrait landscape	beach street people portrait landscape	beach sea clouds sky water	beach sea sunset ocean clouds	beach sea clouds ocean water	beach street people portrait landscape
	green garden people flower spring	green waterfall garden bird colours	green grass garden feet water	green grass garden feet water	dog animal zoo green dogs	dog animal animals puppy dogs	dog animal zoo dogs green	green grass garden feet water

Figure 4.4: Anecdotal results of the baseline methods and our proposed representation for a set of challenging images (MIRFlickr-25K dataset). The tags are ordered by their relevance scores.

4.5 Conclusions

We presented a cross-media model based on KCCA to perform tag assignment. We learn semantic projections for both textual and visual data. This

representation is able to provide better neighbors for voting algorithms. The experimental results show that our method makes consistent improvements over standard approaches based on a single-view visual representation as well as other previous work that also exploited tags. We report also experiments on a challenging dataset collected from Flickr and our results show that the performance of the proposed method is boosted even further in a realistic scenario such as the one provided by weakly-labelled images. Possible extensions of this work include the exploration of how richer textual and semantic cues from natural language annotations might improve our model.

Chapter 5

Evaluating Temporal Information in Social Images

Can we use the temporal gist of annotations in Web images to improve tasks such as annotation, indexing and retrieval? Typically visual content and text, are used to improve these tasks. A characteristic that has received less attention, so far, is the temporal aspect of social media production and tagging. This chapter gives a thorough analysis of the temporal aspects of two popular datasets commonly used for tasks such as tag ranking, tag suggestion and tag refinement, namely NUS-WIDE and MIR-Flickr-1M. The correlation of the time series of the tags with Google searches shows that for certain concepts web information sources may be beneficial to annotate social media.¹

5.1 Introduction

Typically visual content, text and metadata, such as geo-tags, are used to improve tasks such as annotation, indexing and retrieval of the huge quantities of media produced every day by the users of such systems. For instance, visual content similarity is used in (Li et al., 2009b) to perform tag suggestion and image retrieval, tag co-occurrence has been proposed in (Sigurbjörnsson and van Zwol, 2008) for tag suggestion, geo-tags have been used in (Sizov, 2010) for tag recommendation, content classification and clustering. A recent review of the state-of-the-art in areas related to web-based social communities and social media has been presented in (Sundaram et al., 2012), considering in particular the contribution of contextual and social aspects of media semantics to multimedia applications.

A characteristic that has received less attention, so far, is the temporal aspect of social media production. As noted in (Alonso et al., 2007), ex-

¹Parts of the work presented in this chapter have been published in Uricchio, T., Ballan, L., Bertini, M., and Del Bimbo, A. (2013, September). “Evaluating temporal information for social image annotation and retrieval”. In International Conference on Image Analysis and Processing (pp. 722-732). Springer, Berlin, Heidelberg. The publication is available at http://dx.doi.org/10.1007/978-3-642-41181-6_73.

Image Understanding by Socializing the Semantic Gap

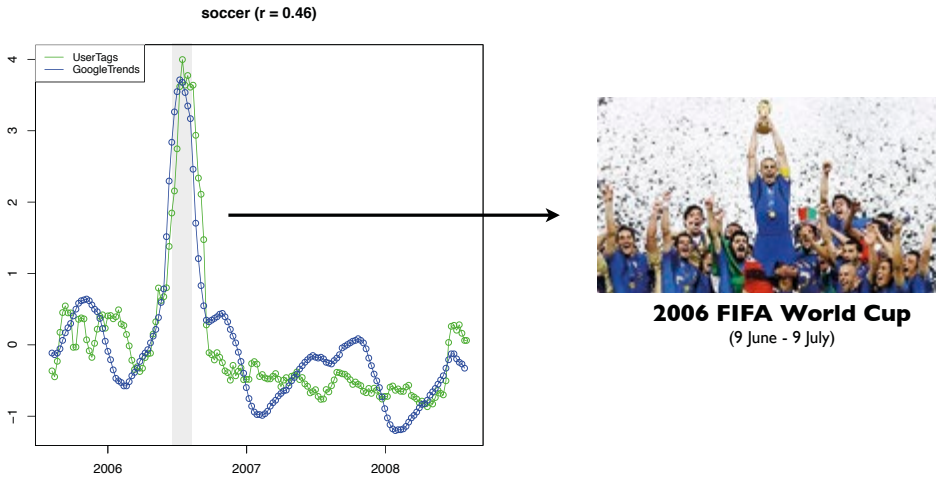


Figure 5.1: Time series of user tags and Google searches for “soccer” in NUS-WIDE dataset.

tracting time information from documents may improve several applications such as hit-list clustering and exploratory search. More recently, several researchers have shown that the temporal information associated to search engine queries (e.g. frequency of query keywords over time) can be used to predict trends and behaviors related to economics and medicine, such as claims for unemployment benefits (Choi and Varian, 2011), and detection of flu epidemics (Ginsberg et al., 2009).

In (Rattenbury et al., 2007) “burst” analysis techniques derived from signal processing are compared against a novel method to identify social events in the associated social media, using the tags and geo-localization information of Flickr images. In (Kim et al., 2010), the temporal evolution of topics in social image collections is proposed to perform subtopic outbreak detection and to classify noisy social images. The authors used a non-parametric approach in which images are represented using a similarity network, created using Sequential Monte Carlo, where images are the vertices and the edges connect the temporally related and visually similar images. Temporal dynamics of social image collections has been studied in (Kim and Xing, 2013) to improve search relevance at query time, addressing both a general case and personalized interest searches. The authors propose a unified statistical model based on regularized multi-task regression on multivariate point process, in which an image stream is considered an instance of a process and a regression problem is formulated to learn the relations between image occurrence probabilities and temporal factors that influence them (e.g. seasons).

Analysis of the temporal evolution of social media collections have been

proposed in (Jin et al., 2010) to predict political success and product sales; regression-based and diffusion-based models have been adapted to account for a Flickr-based index, combining images’ metadata and visual similarity, that models the popularity of politicians and products. The work presented in (Kim et al., 2012) re-casts the problem of image retrieval re-ranking as a prediction of which images will be more likely to appear on the web at a future time point. Both collective group level and individual user level cases are considered, using a multivariate point process to model a stream of input images, and using a stochastic parametric model to solve the relations between the occurrences of the images and factors such as visual clusters, user descriptors and month of the image.

All the datasets used in these works are based on custom selections of user-generated images selected from Flickr, and are not publicly available. The main contribution of this chapter is a thorough analysis of the temporal aspects of two “standard” datasets commonly used for tasks such as tag ranking, tag suggestion and tag refinement (Liu, Hua, Yang, Wang and Zhang, 2009)(Li et al., 2009b)(Zhu et al., 2010)(Liu, Yan, Hua and Zhang, 2011)(Uricchio et al., 2013): NUS-WIDE (Chua et al., 2009) and MIR-Flickr-1M (Huiskes et al., 2010). These datasets provide images and associated metadata, along with a ground-truth annotation of 81 and 18 tags, respectively. Analysis of the temporal evolution of both user tags and ground-truth tags allows to evaluate the social context (e.g. use of tags related to the semantics associated to social interaction, and not necessarily associated with image content) and visual content (e.g. use of tags that are more strictly related to image content). The correlation of the time series of the tags with Google searches (see Fig. 5.1) shows that for certain concepts web information sources may be beneficial to annotate social media.

5.2 Data Analysis Method

5.2.1 Datasets

To measure the impact of temporal information for image annotation purposes, we performed a quantitative analysis over two image datasets: NUS-WIDE (Chua et al., 2009) and MIR-Flickr-1M (Huiskes et al., 2010).

NUS-WIDE is a large scale dataset collected from Flickr. It contains 269,648 images, provided as multiple visual features and source URLs, with 5,018 tags of which 81 have been manually checked and can be considered ground-truth tags. Tab. 5.1 reports the classification of these tags according to their main WordNet category. In order to obtain all temporal metadata not contained in the set, we had to download again all the original images from Flickr. Unfortunately, some images are not available anymore, there-

fore we had to use a subset of 238,251 images that are still present on Flickr. We refer to this subset as NUS-WIDE-240K. Images are unbalanced with respect to time, having very different number of images per date. The time interval goes from year 1900 (old photo scans) to 2009, concentrating most of the images between 2005-2008.

MIR-Flickr-1M is also a large dataset crawled from Flickr which contains 1 million images, selected by their Flickr interestingness score (von Ahn and Dabbish, 2004)(Huiskes and Lew, 2008). Every image provided has full *Flickr metadata* which includes *taken* and *posted* timestamps, indicating when a photo was taken and when it was shared on Flickr. However, only about half of the images provide a valid “taken” timestamp, in particular only 584,892 are valid, as 330,454 have no timestamps and 84,654 have an invalid timestamp. Like NUS-WIDE-240K, images are unbalanced with respect to time. Images are concentrated around years 2007-2009. A ground-truth comprised of 18 tags is provided for the first 25,000 images only, that compose a subset called MIR-Flickr25K (Huiskes and Lew, 2008).

5.2.2 Temporal features

Given a set of images I , all taken in a set of dates D (as a daily interval), we denote as T the set of all tags used and U the set of all users. For every image $i \in I$ we denote $\text{tag}(i) \subseteq T$ the set of tags associated, $\text{day}(i) \in D$ the timestamp associated and $\text{user}(i) \in U$ the user who owns the image. We also consider two other time spans, a set of weeks W and a set of months M , easily computed by integrating over the interval of days considered. These can be thought as time series over the selected index set. For every set considered, we computed a set of features, as proposed in (Kim et al., 2012):

- **Images per day:** the number of relevant images which are *taken* in a day. More specifically, given a day $d \in D$, the number of images per day (IMD) is defined as

$$\text{IMD}(d) := |\{i \in I | \text{day}(i) = d\}| \quad (5.1)$$

Similarly we also define a feature for the number of images per week (IMW) and per month (IMM).

Object	12	Animal	13	Location	2	Substance	2
Action	5	Plant	4	Top	4	Time	2
Artifact	26	Event	4	Phenomenon	4	Person + Groups	3

Table 5.1: WordNet categories of NUS-WIDE ground-truth tags.

- **Images per day for a tag:** the number of relevant images associated with a tag which are *taken* in a day. More specifically, given a tag $t \in T$ and a day $d \in D$, the number of images with t per day (ITD) is defined as

$$\text{ITD}(t, d) := |\{i \in I \mid \text{day}(i) = d \wedge t \in \text{tag}(i)\}| \quad (5.2)$$

Similarly we also define a feature per week (ITW) and per month (ITM).

However, a phenomenon associated with a social source is that of *batch tagging*: a user may decide to upload an entire album of photos and, instead of carefully tagging each photo, he could simply opt to tag each photo with the same tags (e.g. tag the album instead of every single photo). This may result in a kind of noise with respect to the normal use of tags in time. In addition, the features defined above are sensitive to this kind of noise, producing noisy peaks over single days. To produce a more meaningful analysis we decide to collapse all images that are batch tagged into a single entry. A set of images are considered *batch tagged* if they are all uploaded by the same user on the same day and have the same set of tags. More specifically, given a user $\hat{u} \in U$, a day $\hat{d} \in D$ and a set of tags $\hat{t} \subseteq T$, a set of images $I_B = \{i_1, i_2, \dots, i_k\}$ are considered *batch tagged* if $\text{tag}(i) = \hat{t}$, $\text{user}(i) = \hat{u}$, $\text{day}(i) = \hat{d} \forall i \in I_B$.

5.2.3 Flickr Popularity Model

As described in (Jin et al., 2010), available images from the two datasets are only a sample of all images in Flickr. In addition, the number of images over time in Flickr are mostly variable, based on the popularity of the site itself. This slow change over time can be modeled as a trend over all tags, independent from any particular query. Unfortunately, no statistics are released publicly and other sources such as Alexa² or Google Trends³ are affected by the impact of news. Based on this preliminary analysis and supposing an uniform sampling in Flickr searches, we use the feature IMD to remove this background deviation by normalizing the ITD feature.

Given a tag $t \in T$ and a date $d \in D$ we compute:

$$\overline{\text{ITD}}(t, d) = \frac{\text{ITD}(t, d)}{\text{IMD}(d)} \quad (5.3)$$

This may also be considered as a frequentist probability distribution of tag t in day d with respect to all other tags considered, which is $p(t; d)$. Similarly we also compute $\overline{\text{ITW}}$ and $\overline{\text{ITM}}$ by considering a week and a

²Alexa Internet, Inc. <http://www.alexa.com>

³Google Trends. <http://www.google.com/trends>

month granularity, respectively. After collapsing all batch tagged images, the two datasets retain 179,128 images for NUS-WIDE-240K and 531,670 images for MIRFLICKR-1M respectively.

5.2.4 Processing

First of all we present a qualitative analysis by measuring the occurrence of tags in time. Given that NUS-WIDE-240K has the biggest ground truth of all datasets considered and that we are looking to discover the relations between tags and image content with respect to time, we choose to use it as the main reference. We use all the 81 manually checked tags as T set and consider four different information sources which are different in the kind of underlining latent process :

- From NUS-WIDE-240K, for all images, we consider the T set of tags using the **manually validated** tags which constitute the entire ground truth; we refer to this source as **NUS-GT**.
- From NUS-WIDE-240K, for all images, we consider the T set of tags using the **user tags** (e.g. the tags provided by the respective Flickr users); we refer to this source as **NUS-TAGS**.
- From MIRFLICKR-1M, for all images, we consider the T set of tags using the **user tags**; we refer to this source as **MIR-TAGS**.
- Beside image datasets, we also consider a source of temporal query information given by Google Trends. From Google Trends, we have downloaded all available query data for the T set of tags considered; we refer to this source as **GOO-TAGS**.

All sources are to be considered subject to different kinds of noise, in particular all images are highly unbalanced over time, resulting in days with hundreds of images and others with at most ten images. To reduce this effect, we choose to consider only the largest time span with at least 350 images per week. In addition the two image datasets differ in the time interval which has the most images. This forced us to use a reduced time interval that we choose as starting from 2005-06-01 and ending in 2008-08-01 for NUS-WIDE-240K (retaining 161,176 images from 179,128) and from 2007-01-01 to 2008-08-01 for MIR-Flickr-1M (retaining 110,064 images from 531,670). Those filters were processed with a combination of Python scripts and Google Refine⁴. After this we used the R package (Team, 2011) to plot and execute any successive analysis. A plotting of features of this data revealed an insufficient reduction in noise to be able to clearly visualize most characteristics pattern. To make the time series patterns more clear, we

⁴Google Refine. <http://code.google.com/p/google-refine>

computed a simple moving average over all time series, varying the windows size n from 2 to 10 weeks. For a day time series defined over a time span Ψ for a tag $t \in T$ is defined as:

$$ITD_n(t, d) = \frac{1}{n} \sum_{i=-n}^n \overline{ITD}(t, d+i) \quad \forall d \in \Psi \quad (5.4)$$

This has the effect to smooth the series, letting to visualize more clearly the trend. On the other hand, tags which have very sparse frequency tends to be worsened, so we adjusted the window size empirically, based on visualization clearness. The final time series are composed of 1,158 and 579 week samples respectively for NUS-WIDE-240K and MIR-Flickr-1M.

5.2.5 Correlation analysis

To exploit the underlying time process and to be able to improve image annotation using temporal information, we need a way to evaluate quantitatively the possible correlation between sources. This allows us to analyze if a series can be estimated by another one and how a generalized model may describe the original time series. To this end we compute a correlation measure over two series. First of all we standardize all time series: given a time series $X = \{x_i : i \in D\}$, we compute $x_i = \frac{x_i - \bar{X}}{s}$, where \bar{X} is the sample mean and s is the sample standard deviation. Even if sample mean and sample standard deviation are sensible to outliers, those are removed thanks to the filtering and smoothing procedure described above. To evaluate the correlation between two time series, we choose to use the *sample Pearson correlation coefficient*, often denoted as r . Given two time series X and Y of n samples, r is defined as the ratio between covariance and the product of X variance and Y variance:

$$r = \frac{\sum_{i=1}^n (x_i - \bar{X})(y_i - \bar{Y})}{\sqrt{\sum_{i=1}^n (x_i - \bar{X})^2} \sqrt{\sum_{i=1}^n (y_i - \bar{Y})^2}} \quad (5.5)$$

which is defined in $[-1, 1]$. Values towards the positive or negative end reveal a strong correlation between the two time series, changing only in the sign. We can reformulate it as the mean of the products of the standard scores, which permits us to use standardized time series $\hat{x}_i = \frac{x_i - \bar{X}}{s_X}$ and $\hat{y}_i = \frac{y_i - \bar{Y}}{s_Y}$:

$$r = \frac{1}{n-1} \sum_{i=1}^n \left(\frac{x_i - \bar{X}}{s_X} \right) \left(\frac{y_i - \bar{Y}}{s_Y} \right) = \frac{1}{n-1} \sum_{i=1}^n \hat{x}_i \hat{y}_i \quad (5.6)$$

Given that the strength of correlation is not dependent on the direction or the sign, we also computed r-square. Unfortunately the interpretation of

Image Understanding by Socializing the Semantic Gap

a correlation coefficient depends heavily on the context and purposes that can't be easily defined at this stage of work. However several works like (Cohen, 1988) offered some guidelines which can be used to interpret our analysis, that are reported in Tab. 5.2.

Correlation	None	Small	Medium	Strong
Positive	0.0 to 0.09	0.1 to 0.3	0.3 to 0.5	0.5 to 1.0
Negative	-0.09 to 0.0	-0.3 to -0.1	-0.5 to -0.3	-1.0 to -0.5

Table 5.2: Guidelines for sample Pearson correlation coefficient.

5.3 Experiments and Discussion

In the following we will consider both the presence of the tags that have been added by the users that uploaded the images to Flickr (referring to them as “user tags”) and the tags that have been manually checked by the creators of NUS-WIDE as referring to visual content of images (referring to them as “ground-truth” tags). In fact, several studies have shown that tags are often ambiguous and personalized (Kennedy et al., 2006)(Sigurbjörnsson and van Zwol, 2008), and do not necessarily reflect the visual content of the image. As an example consider Fig. 5.2 and 5.3, showing the temporal usage of the tags “snow” and “soccer” in NUS-WIDE, along with the respective Google searches, as obtained from Google Trends. It can be observed that the peak in usage of the “soccer” tag - associated with the 2006 FIFA World Cup - reflects that in Google Trends, but the peak is much less pronounced in the ground truth tags; this indicates that for this tag the relationship between tags and image may exist because of how people react to social events, rather than uploading photos depicting that event on Flickr. On the other hand the peaks of both user and ground truth “snow” tag are corresponding to that of Google Trends: in this case the relationship may exist because it is more likely that people take pictures of snow scenes during winter, and this concept is less related to social aspects than to visual content of these images.

5.3.1 Temporal Evaluation

Considering time series composed of the frequencies of image tags (either user or ground-truth) and Google searches obtained from Google Trends, it is possible to observe that they exhibit the presence of different components, that may appear mixed together:

trend long term variation, that can be increasing, decreasing or also sta-

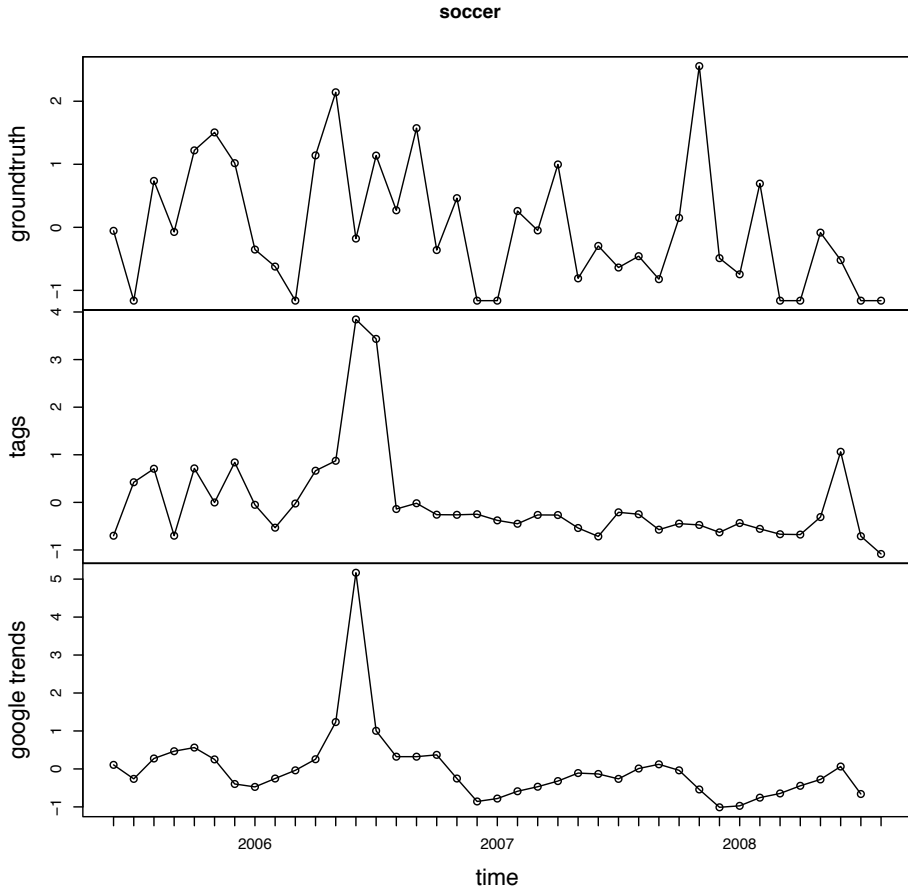


Figure 5.2: Frequency of “soccer” in NUS-GT, NUS-TAGS and GOO-TAGS: the peak of Google Trends and user tags in the summer of 2006 are related to the World Soccer Championship.

ble (see Fig. 5.4). Terms such as “computer” or “military” have this pattern;

cyclical variation repeated but not periodic variations. Tags like “sports” or “flags” have this pattern;

seasonal variation periodic variations, e.g. due to concepts associated with some regular event (see Fig. 5.4). Concepts related to seasons show this behavior, like “garden”, “snow”, “beach” or “frost”;

irregular variation random irregular variations, e.g. due to the sudden emergence of a topic (see Fig. 5.5), that appears as a burst of activity. Concepts that exhibit this pattern are related to social or natural events like “soccer”, “earthquake” and “protest”.

Image Understanding by Socializing the Semantic Gap

snow

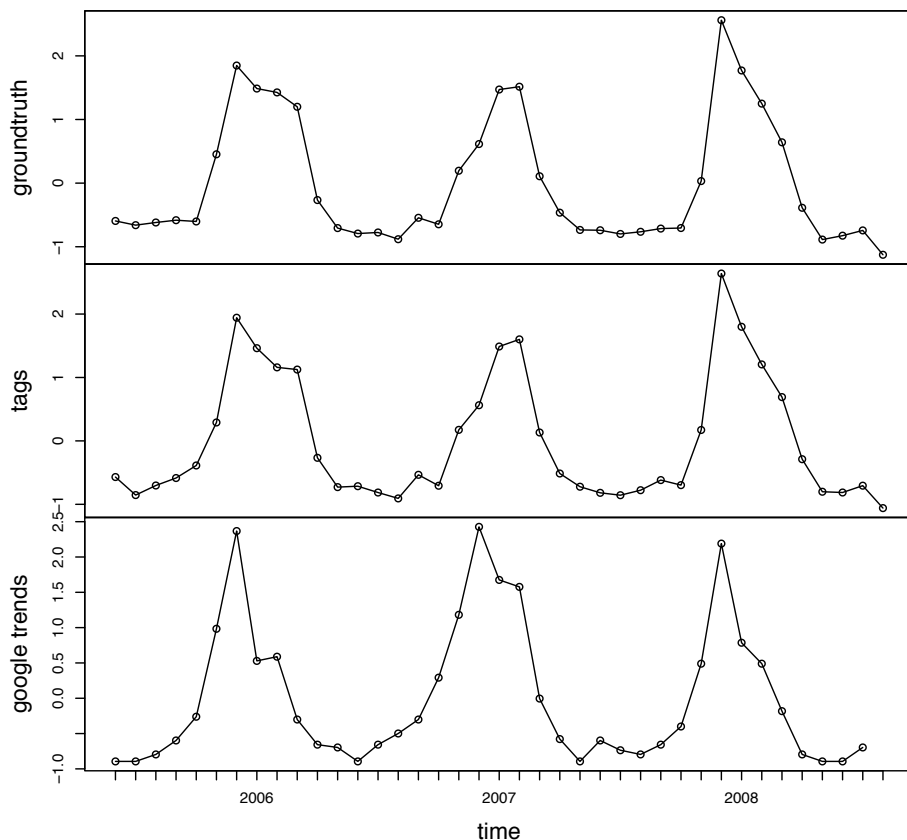


Figure 5.3: Frequency of “snow” in NUS-GT, NUS-TAGS and GOO-TAGS: the peaks are associated with winter seasons. Tag frequencies have been normalized by the number of images of the same day.

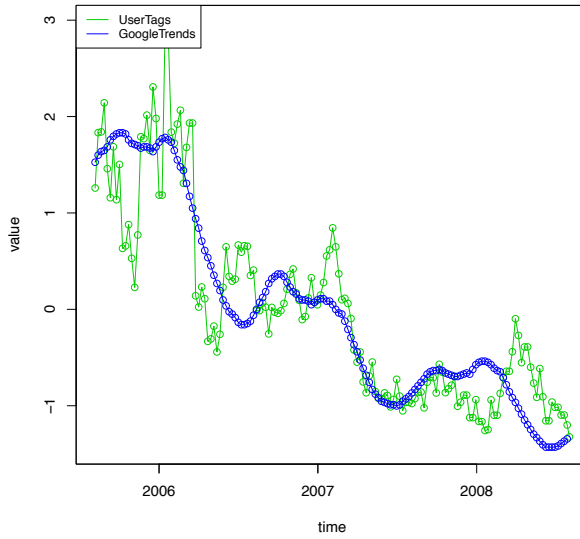
5.3.2 Correlation Analysis

Fig. 5.6 reports the outcome of correlation analysis of NUS-TAGS with NUS-GT, NUS-TAGS with GOO-TAGS and NUS-GT with MIR-TAGS. In particular it can be observed that the correlation of NUS-TAGS and NUS-GT has a vast majority of “Medium” and “Strong” values, while the correlation between user tags and Google searches is overall weaker and can be useful for a selected number of tags. The correlation between NUS-GT and MIR-TAGS has a large number of “Medium” and “Strong” values, suggesting that the temporal information of NUS-WIDE can be used in MIR-Flickr-1M.

Correlation analysis of NUS-TAGS with GOO-TAGS, followed by aver-

Tiberio Uricchio

computer ($r = 0.86$)



garden ($r = 0.55$)

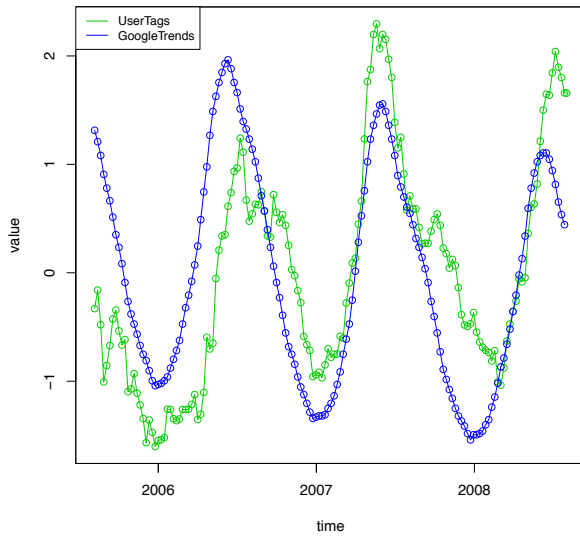


Figure 5.4: Time series patterns of NUS-TAGS and GOO-TAGS, averaged over 10 weeks. *i*) trend (computer); *ii*) seasonal (garden).

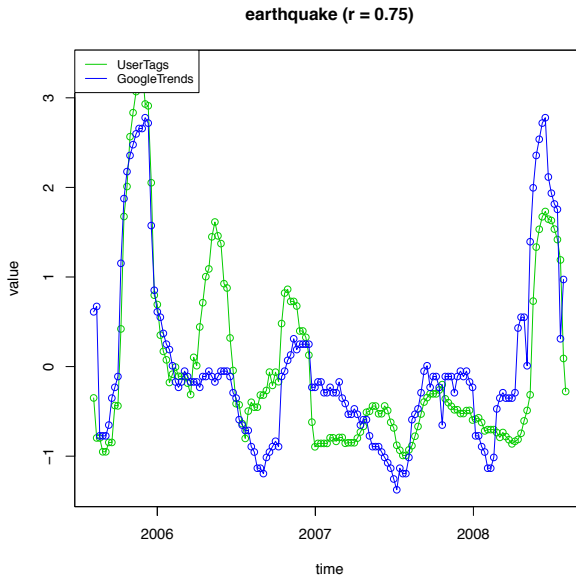


Figure 5.5: Time series patterns of NUS-TAGS and GOO-TAGS, averaged over 10 weeks. Episodic behavior (earthquake: peaks correspond to earthquakes in China and Pakistan).

aging of r-square values over tags classes (Fig. 5.7 left) shows that Plant, Event, Phenomenon and Action obtain the higher values. A second group of categories comprises Artifact, Person+Group, Animal, Object and Time. In general, the categories that obtain the best performances are benefitting from tags whose time series show seasonal behaviors (e.g. “snow”, “frost”, “grass”, “leaf”) or have a “burst” behavior associated with specific social events (e.g. “soccer”, “protest”, “earthquake”).

Correlation analysis of NUS-GT with GOO-TAGS (Fig. 5.7 right) shows that Plant and Phenomenon categories maintain their position among the best performing classes, because of the tags that exhibit a seasonal pattern. Instead the correlation of Event and Action categories is lower because the ground-truth tags that have an episodic pattern like “soccer”, “protest” and “earthquake” have a lower correlation. This is due to the fact that these tags are employed by users also when the content of the image is not visually related to the described event.

5.4 Conclusions

This chapter presented a thorough analysis of the temporal aspects of user annotations in two popular large-scale datasets. The correlation of the time series of the tags with Google searches showed that for certain concepts web information sources may be beneficial to annotate social media.

Tiberio Uricchio

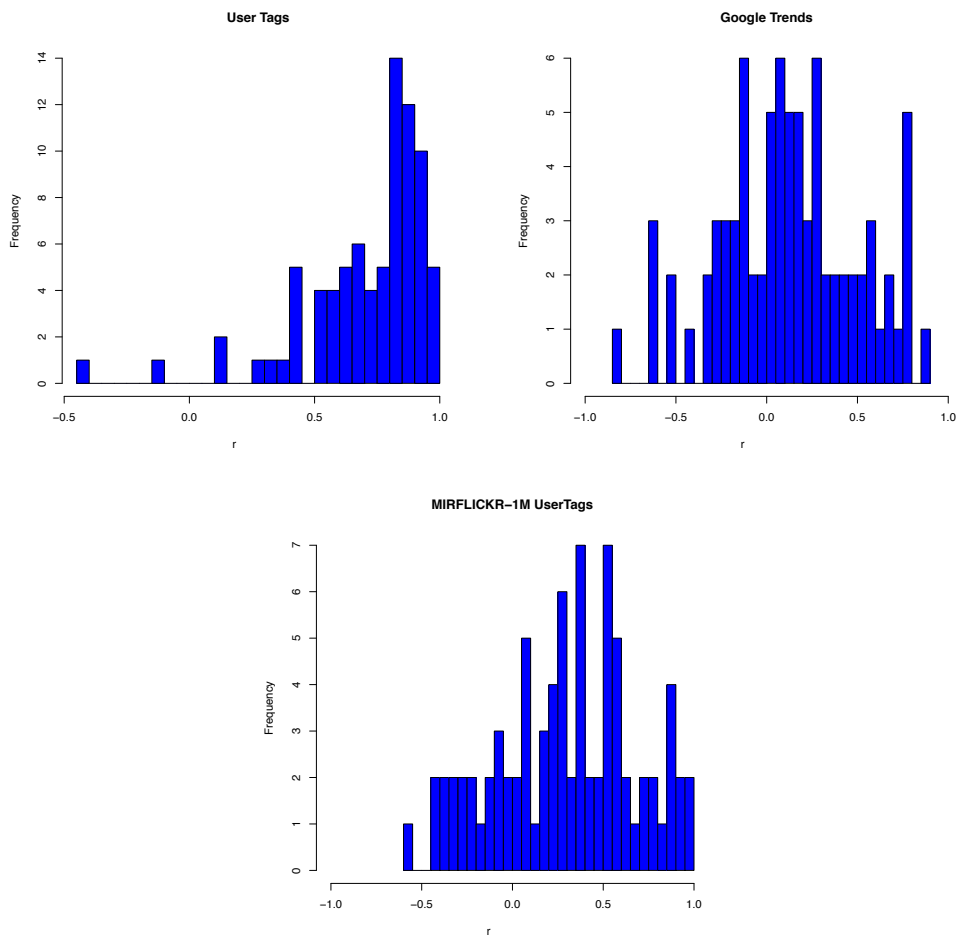
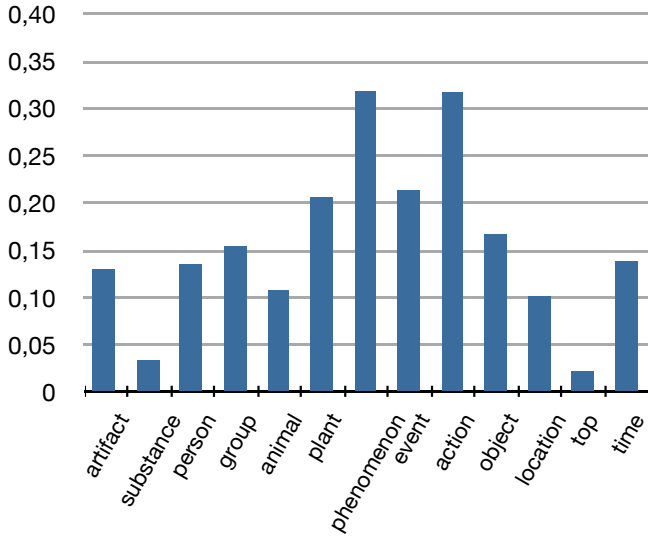


Figure 5.6: *i*) r values computed between NUS-TAGS and NUS-GT; *ii*) r values computed between NUS-TAGS and GOO-TAGS; *iii*) r values computed between NUS-GT and MIR-TAGS.

Image Understanding by Socializing the Semantic Gap

Avg. R-square per category (NUS-TAGS / GOO-TAGS)



Avg. R-square per category (NUS-GT / GOO-TAGS)

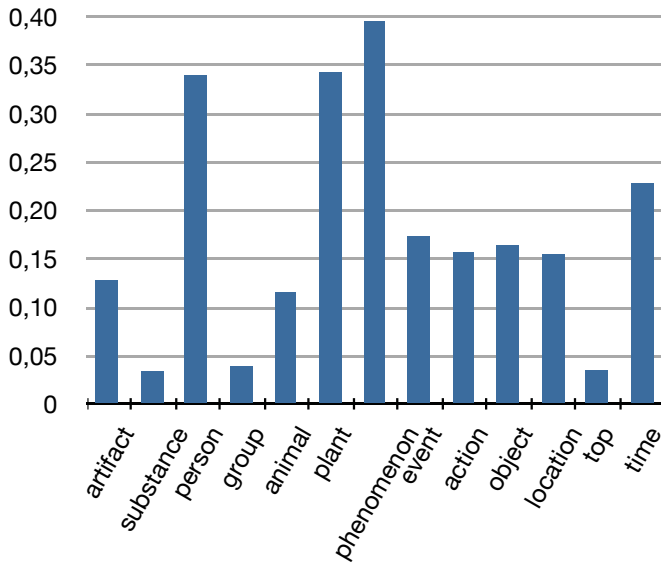


Figure 5.7: NUS-WIDE dataset: r-square averages for tags classes. *i)* NUS-TAGS correlation with GOO-TAGS; *ii)* NUS-GT correlation with GOO-TAGS.

Chapter 6

Multimodal Feature Learning for Sentiment Analysis

*In this chapter we investigate the use of a multimodal feature learning approach, using neural network based models such as Skip-gram and Denoising Autoencoders, to address sentiment analysis of micro-blogging content, such as Twitter short messages, that are composed by a short text and, possibly, an image. Motivated by the recent advances of unsupervised learning of language models and visual features based on neural networks models, we propose a novel architecture that incorporates these models and test it on several standard Twitter datasets. We show that the approach is efficient and obtains good classification results.*¹

6.1 Introduction

In the last few years micro-blogging services, in which users describe their current status by means of short messages, obtained a large success among users. Unarguably, one of the most successful services is Twitter², that is used worldwide to discuss about daily activities, to report or comment news, and to share information using messages (called ‘tweets’) composed by at most 140 characters. Since 2011 Twitter natively supports adding images to tweets, easing the creation of richer content. A study performed by Twitter³ has shown that adding images to tweets increases user engagement more than adding videos or hashtags.

Despite their brevity these messages often convey also the feeling and the point of view of the people writing them. The addition of images reinforces and clarifies these feelings (see Fig.6.1). Automatic analysis of the sentiment of these tweets, i.e. retrieving the opinion they express, has received a large

¹Parts of the work presented in this chapter have been published in Baecchi, C., Uricchio, T., Bertini, M., and Del Bimbo, A. (2016). “A multimodal feature learning approach for sentiment analysis of social network multimedia”. *Multimedia Tools and Applications*, 75(5), 2507-2525. The publication is available at <http://dx.doi.org/10.1007/s11042-015-2646-x>.

²Twitter reports to have 271 million monthly active users that send 500 million status updates per day - <https://about.twitter.com/company>

³<https://blog.twitter.com/2014/what-fuels-a-tweets-engagement>

Image Understanding by Socializing the Semantic Gap

attention from the scientific community. This is due to its usefulness in analyzing a large range of domains such as politics (Tumasjan et al., 2010) and business (Ghiassi et al., 2013). Sentiment analysis may encompass different scopes (Bravo-Marquez et al., 2013): *i*) polarity, i.e. categorize a sentiment as positive, negative or neutral; *ii*) emotion, i.e. assign a sentiment to an emotional category such as joy or sadness; *iii*) strength, i.e. determine the intensity of the sentiment.

So far, the vast majority of works have addressed only the textual data. In this chapter we address the classification of tweets, according to their polarity, considering both textual and visual information. We propose a novel schema that, by incorporating a language model based on neural networks, can efficiently exploit web-scale sources corpus and robust visual features obtained from unsupervised learning. The proposed method has been tested on several standard datasets, showing promising results.



Figure 6.1: Examples of tweets with images from the SentiBank Twitter dataset (Borth et al., 2013). *left*) positive sentiment tweet; *right*) negative sentiment tweet.

The chapter is organized as follows: Sect. 6.2 provides an overview of previous works; the proposed method is presented in Sect. 6.3, while experiments on four standard datasets and comparison with state-of-the-art approaches and baselines are reported in Sect. 6.4. Conclusions are drawn in Sect. 6.5.

6.2 Previous Work

Sentiment analysis in texts. Brevity, sentence composition and variety of topics are among the main challenges in sentiment analysis of tweets (and micro-blogs in general). In fact these texts are short, often they are not composed carefully as news or product reviews, and cover almost any conceivable topic. Several specific approaches for Twitter sentiment analysis have been proposed, typically using sentence-level classification with n -gram word models. Liu *et al.* (Liu et al., 2012) concatenate tweets of the same class (polarity) in large documents, from which a language model is derived and then classify tweets through maximum likelihood estimation, using both supervised and unsupervised data for training; the role of unsupervised data is to deal with words that do not appear in the vocabulary that can be built from a small supervised dataset. In (Bifet and Frank, 2010) three approaches to sentiment classification are compared: Multinomial Naïve Bayes (MNB), Hinge Loss with Stochastic Gradient Descent and Hoeffding Tree; the authors report that MNB outperforms the other approaches. In (Deitrick and Hu, 2013) unigram and bigram features have been used to train Naïve Bayes classifiers, where bigrams help to account for negation of words. Saif *et al.* (Saif et al., 2013) have evaluated the use of a Max Entropy classifier on several Twitter sentiment analysis datasets. Since using n -grams on tweet data may reduce classification performance due to the large number of infrequent terms in tweets, some authors have proposed to enrich the representation using micro-blogging features such as hashtags and emoticons as in (Barbosa and Feng, 2010), or using semantic features as in (Saif et al., 2012).

Neural networks language models. Recently, the scientific community has addressed the problem of learning vector representations of words that can represent information like similarity or other semantic and syntactic relations, obtaining better results than using the best n -gram models. The use of neural networks to perform this task is motivated by recent works addressing the scalability of training. In this formulation every word is represented in a distributional space where operations like concatenation and averaging are used to predict other words in context, trained by the use of stochastic gradient descent and backpropagation. In the work of (Bengio et al., 2006), a model is trained based on the concatenation of several words to predict the next word: every word is mapped into a vector space where similar words have similar vector representations. A successive work uses multitask techniques (Collobert and Weston, 2008) to jointly train several tasks showing improvements in generalization. A fast hierarchical language model was proposed in (Mnih and Hinton, 2009), attacking the main draw-

back of needing long training and testing times. The use of unsupervised additional words was proposed by (Turian et al., 2010) showing further improvements using word features learned in advance to a supervised NLP task. Recently Mikolov *et al.* (Mikolov, Sutskever, Chen, Corrado and Dean, 2013) have proposed several improvements on Hierarchical Softmax (Mnih and Hinton, 2009) and Negative Sampling (Gutmann and Hyvärinen, 2012) and introduced the Skip-gram model (Mikolov, Yih and Zweig, 2013), reducing further the computational cost, and showing fast training on corpora of billions of words (Mikolov, Sutskever, Chen, Corrado and Dean, 2013). More recently, researchers also extended these models, trying to achieve paragraph and document level representations (Le and Mikolov, 2014).

Micro-blog multimedia analysis. Most of the works dealing with analysis of the multimedia content of micro-blogs have dealt with content summarization and mining, image classification and annotation. Geo-tagged tweet photos are used in (Yanai, 2012; Kaneko et al., 2013) to visually mine events using both textual and visual information. The system presented in (Serra et al., 2013) provides tools for content curation, creation of personalized web sites and magazines through topic detection of tweets and selection of representative associated multimedia. A system for exploration of events based on facets related to who, when, what, why and how of an event, has been presented in (Wang, Cui, Xie, Chen, Zhu and Yang, 2012), using a Bilateral Correspondence model (BC-LDA) for image and words. A multi-modal extension of LDA has been proposed in (Bian et al., 2013) to discover sub-topics in microblogs, in order to create a comprehensive summarization.

An algorithm for photo tag suggestion using Twitter and Wikipedia are used in (McParlane and Jose, 2014) to annotate social media related to events, exploiting the fact that tweets about an event are typically tweeted during its development. Classification of tweets' images in visually-relevant and visually-irrelevant, i.e. images that are correlated or not to the text of the tweet, has been studied in (Chen et al., 2013), using a combination of text, context and visual features.

Zhao *et al.* (Zhao et al., 2012) have studied the effects of adding multimedia to tweets within Sina Weibo, a Chinese equivalent of Twitter, finding that adding images boosts the popularity of tweets and authors, and extends the lifespan of tweets.

Sentiment analysis in social images. Sentiment analysis of visual data has received so far less attention than that of text data and, in fact, only a few small datasets exist, such as the International Affective Picture System (IAPS) (Lang et al., 1999) and the Geneva Affective Picture Database (GAPED) (Dan-Glauser and Scherer, 2011). The former provides ratings of

emotion (in terms of pleasure, arousal and dominance) for 369 images, while the latter provides 520 images associated to negative sentiment, 89 neutral and 121 positive images. Another related direction is given by works on aesthetics: surveys are provided in (Wang and He, 2008; Joshi et al., 2011). However, none of these datasets deal with social media.

A few works have addressed the problem of multimedia sentiment analysis of social network data. Borth *et al.* (Borth et al., 2013) have recently presented a large-scale visual sentiment ontology and associated set of detectors, consisting of 3,244 pairs of nouns and adjectives (ANP), based on Plutchik’s Wheel of Emotions (Plutchik, 2001). Detectors are trained using Flickr images, represented using a combination of global (e.g. color histogram and GIST) and local (e.g. LBP and BoW) features. The paper provides also two publicly available image datasets obtained from Flickr and from Twitter. The system proposed in (Cao et al., 2014) for the classification of Sina Weibo statuses exploits the ANP detectors proposed in (Borth et al., 2013), fusing them with text sentiment analysis based on 3 features: *i*) sentiment words from HowNet (Chinese equivalent to WordNet), *ii*) semantic tags and *iii*) rules of sentence construction, to cope with rhetorical questions, negations and exclamatory sentences.

Cross-media bag-of-words, combining bag of text words with bag of image words obtained from the SentiBank detectors of (Borth et al., 2013), has been proposed in (Wang, Cao, Li, Li and Ji, 2014) for sentiment analysis of microblog messages obtained from Sina Weibo. Yang *et al.* (Yang, Cui, Zhu, Zhao, Shi and Yang, 2014) have proposed a hybrid link graph for images of social events, weighting links based on textual emotion information, visual similarity and social similarity. A ranking algorithm to discover emotionally representative images in microblog statuses is then presented. The work of Chen *et al.* (Chen, Chen, Hsu, Liao and Chang, 2014), distinguishes between the intended publisher effect and the sentiment that is induced in the viewer (‘viewer affect concept’) and aims at predicting the latter. The goals are to recommend appropriate images and suggest image comments.

6.3 The Proposed Method

Recent works have shown (Mikolov et al., 2011) that neural network based language models significantly outperform N-gram models; similarly, the use of neural networks to learn visual features and classify images has shown that they can achieve state-of-the-art results on several standard datasets and international competitions (Krizhevsky et al., 2012). The proposed method builds on these advances.

We start by describing the well-known text based approach *Continuous Bag-Of-Words* (CBOW) model (Mikolov, Yih and Zweig, 2013) that is the

Image Understanding by Socializing the Semantic Gap

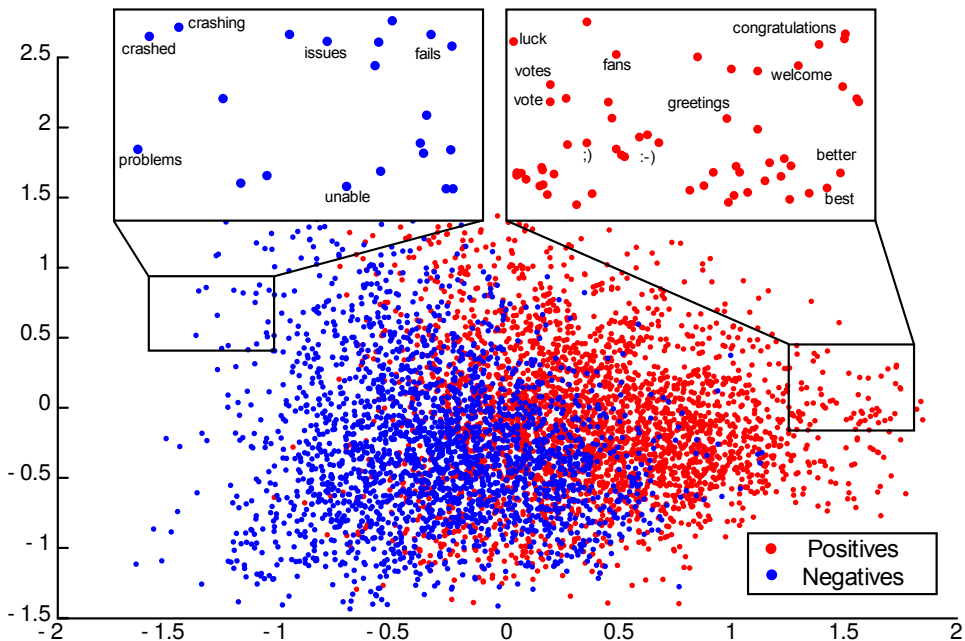


Figure 6.2: Visualization of CBOW word vectors trained on tweets of the SemEval-2013 dataset. Blue points are single words classified as negative, while red ones are positive. Semantically similar words are near (e.g. ‘crashing’ and ‘crashed’, ‘better’ and ‘best’) and share the same polarity.

base of our scheme, then we present our model for polarity classification problem. Finally, we show a further extension of the model to incorporate visual information, based on a Denoising Autoencoder (Vincent et al., 2008), that allows the same unsupervised capabilities on images as CBOW-based methods on text.

6.3.1 Textual information

Mikolov *et al.* (Mikolov, Yih and Zweig, 2013) showed that in the CBOW model, words with similar meaning are mapped to similar positions in a vector space. Thus, distances may carry a meaning, allowing to formulate questions in the vector space using simple algebra (e.g. the result of $\text{vector}(\text{‘king’}) - \text{vector}(\text{‘man’}) + \text{vector}(\text{‘woman’})$ is near $\text{vector}(\text{‘queen’})$). Another property is the very fast training, that allows to exploit large-scale unsupervised corpora such as web sources (e.g. Wikipedia).

Continuous Bag-Of-Words model. In this framework, each word is mapped to a unique vector represented by a column in a word matrix W of Q length. Every column is indexed by a correspondent index from a dictionary V_T . Given a sequence of words w_1, w_2, \dots, w_K , CBOW model with hierarchical

softmax aims at maximizing the average log probability of predicting the central word w_t given the context represented by its M -window of words, i.e. the M words before and after w_t :

$$\frac{1}{K} \sum_{t=M}^{K-M} \log p(w_t | w_{t-M}, \dots, w_{t-1}, w_{t+1}, \dots, w_{t+M}) \quad (6.1)$$

The output $f \in \mathbb{R}^{|V_T|}$ for the model is defined as:

$$f_{w_t} = [W_{t-M}, \dots, W_{t-1}, W_{t+1}, \dots, W_{t+M}]^T G \quad (6.2)$$

where W_i is the column of W corresponding to the word w_i and $G \in \mathbb{R}^{P \times |V_T|}$. Both W and G are considered as weights and have to be trained, resulting in a dual representation of words. Typically the columns of W are taken as final word features. An output probability is then obtained by using the softmax function on the output of the model:

$$p(w_t | w_{\text{context}}) = \frac{e^{f_{w_t}}}{\sum_i e^{f_{w_i}}} \quad (6.3)$$

where $w_{\text{context}} = (w_{t-M}, \dots, w_{t-1}, w_{t+1}, \dots, w_{t+M})$. When considering a high number of labels, it can be computed more efficiently by employing a hierarchical variation (Mnih and Hinton, 2009), requiring to evaluate $\log_2(|V_T|)$ words instead of $|V_T|$.

In (Mikolov, Yih and Zweig, 2013), an additional task named *Negative Sampling* is considered, where a word w_l is to be classified as related to the given context or not, i.e. $p(w_l | w_{\text{context}})$:

$$u_{w_l} = \sigma([W_{t-M}, \dots, W_l, \dots, W_{t+M}]^T N_s) \quad (6.4)$$

where $N_s \in \mathbb{R}^Q$ and σ is the logistic function. Depending on w_l as the actual w_t word or a randomly sampled one, u_{w_l} has a target value of respectively 1 or 0.

The CBOW-LR method. Our model, denoted as CBOW-LR, is an extension of CBOW with negative sampling, specialized on the task of sentiment classification. An important difference from approaches that directly use a CBOW representation, or from (Turian et al., 2010), is that our model learns representation and classification concurrently. Considering that multi-task learning can improve neural networks performance (Turian et al., 2010), the idea is to use two different contributions accounting for semantic and sentiment polarity, respectively.

Given a corpus of tweets \mathbf{X} where each tweet is a sequence of words w_1, w_2, \dots, w_K , we aim at classifying tweets as positive or negative, and

learn word vectors $W \in \mathbb{R}^{Q \times |V_T|}$ with properties related to the sentiment carried by words, while retaining semantic representation. Semantic representation can be well-represented by a CBOW model, while sentiment polarity has limited presence or is lacking. Note that polarity supervision is limited and possibly weak, thus a robust semi-supervised setting is preferred: on the one hand, a model of sentiment polarity can use the limited supervision available, on the other hand the ability to exploit a large corpus of unsupervised text, like CBOW, can help the model to classify previously unseen text. This is explicitly accounted in our model by considering two different components:

i) inspired by (Mikolov, Yih and Zweig, 2013), we consider a feature learning task on words by classifying sentiment polarity of a tweet. A tweet is represented as a set of M -window of words that we denote as \mathcal{G} . Each window \mathcal{G} is represented as a sum of their associated word vectors W_i , and a polarity classifier based on logistic regression is applied accordingly:

$$y(\mathcal{G}) = \sigma(C^T(\sum_{W_i \leftarrow w_i \in \mathcal{G}} W_i) + b_s) \quad (6.5)$$

Here the notation $W_i \leftarrow w_i \in \mathcal{G}$ refers to selecting the i -th column of W by matching the w_i word from \mathcal{G} . The matrix $C \in \mathbb{R}^Q$ and the vector $b_s \in \mathbb{R}$ are parameters of a logistic regression, while a binary cross entropy is applied as loss function for every window \mathcal{G} . This is applied for every tweet T labeled with \bar{y}_T in the training set and results in the following cost:

$$C_{\text{sent}} = \sum_{(T, \bar{y}_T)} \sum_{\mathcal{G} \in T} -\bar{y}_T \log(y(\mathcal{G})) - (1 - \bar{y}_T) \log(1 - y(\mathcal{G})) \quad (6.6)$$

However, differently from a standard logistic regression, the representation matrix W is also a parameter to be learned. A labeled sentiment dataset is required to learn this task.

ii) we explicitly represent semantics by adding a task similar to negative sampling, without considering the hierarchical variation. The idea is that a CBOW model may also act as a regularizer and provide an additional semantic knowledge of word context. Given a window \mathcal{G} , a classifier has to predict if a word w_l fits in it. To this end, an additional cost is added:

$$C_{\text{sem}} = \sum_T \sum_{\mathcal{G} \in T} \sum_{(r_l, w_l) \in \mathcal{F}} (r_l - u_{w_l})^2 \quad (6.7)$$

where \mathcal{F} is a set of words w_l with their associated target r_l , derived from a training text sequence. This is the core of negative sampling: \mathcal{F} always contains the correct word w_l for the considered context \mathcal{G} ($r_l = 1$) and $K - 1$ random sampled words from V_T ($r_l = 0$). It is indeed a sampling as $K < |V_T| - 1$ of the remain wrong words. Note that differently from the previous

task, this is unsupervised, not requiring labeled data; moreover tweets can belong to a different corpus than that used in the previous component. This allows to perform learning on additional unlabeled corpora, to enhance word knowledge beyond that of labeled training words.

Finally, concurrent learning is obtained by forging a total cost, defined by the sum of the two parts, opportunely weighted by a $\lambda \in [0, 1]$, and minimized with SGD:

$$C_{\text{CBOW-LR}} = \lambda \cdot C_{\text{sent}} + (1 - \lambda) \cdot C_{\text{sem}} \quad (6.8)$$

Fig. 6.2 visualizes the word vectors learned by our model. Note the tendency of separating the opposite polarities and the fact that similar words are close to each other.

At prediction time, for each word in a tweet T we consider its M -window \mathcal{G} and we compute (6.5) for each window, summing the results:

$$\text{Pred}(T) = \sum_{\mathcal{G} \in T} \left(y(\mathcal{G}) - 0.5 \right) \quad (6.9)$$

If $\text{Pred}(T) < 0$ the tweet is labeled as negative, otherwise it is considered positive. It is worth noticing that at prediction time the method does not consider a word as positive or negative in its own, but it uses also its context to classify its sentiment and how strong it is. Thus the same word can be classified differently if used in different contexts.

6.3.2 Textual and Visual Information

The CBOW-LR model presented in Sect. 6.3.1 can be extended to account for visual information, such as that of images associated to tweets or status messages. Popular image representations are the Visual Bag-Of-Words Model (Grauman and Darrell, 2005; Lazebnik et al., 2006; Li, Mei, Kweon and Hua, 2011), Fisher Vector (Perronnin, Liu, Sánchez and Poirier, 2010) and its improved version (Perronnin, Sánchez and Mensink, 2010; Baecchi et al., 2014). However, as shown recently in (Chatfield et al., 2014; Krizhevsky et al., 2012), neural network based models have been shown to widely outperform these previous models. So, to fit with the CBOW representation discussed in the previous section, we choose to exploit the images by using a representation similar to the one used for the textual information, i.e. a representation obtained from the whole training set by means of a neural network. Moreover, likewise for the text, unsupervised learning can be performed. For these reasons, inspired also by works such as (Vincent et al., 2008), we choose to extend our network with a single-layer Denoising Autoencoder, to take its middle level representation as our image descriptor. As for the textual version, the inclusion of this additional task allows

our method to concurrently learn a textual representation and a classifier on text polarity and its associated image.

Denoising Autoencoder. In general, an Autoencoder (also called Autoassociator (Bengio, 2009)) is a kind of neural network trained to encode the input into some representation (usually of lower dimension) so that the input can be reconstructed from that representation. For this type of network the output is thus the input itself. Specifically, an Autoencoder is a network that takes as input a K -dimensional vector x and maps it to a hidden representation h through the mapping:

$$h = \sigma(P_e x + b_e) \quad (6.10)$$

where σ is the sigmoid function (but any other non-linear activation function can be used), P_e and b_e are respectively a matrix of encoding weights and a vector of encoding biases. At this point, h is the coded representation of the input, and has to be mapped back to x . This second part is called the reconstruction z of x (being z of the same dimension and domain of x). In this step a similar transformation as in Eq. 6.10 is used:

$$z = \sigma(P_d h + b_d) \quad (6.11)$$

where P_d and b_d are respectively a matrix of decoding weights and a vector of decoding biases. One common choice is to constrain $P_d = P_e^T$; in this configuration the Autoencoder is said to have ‘tied weights’. The motivation for this is that tied weights are used as a regularizer, to prevent the Autoencoder to learn the identity matrix when the dimension of the hidden layer is big enough to memorize the whole input; another important advantage is that the network has to learn fewer parameters. With this configuration, Eq. (6.11) becomes:

$$\hat{z} = \sigma(P_e^T h + b_d) \quad (6.12)$$

Learning is performed by minimizing the cross-entropy between the input x and the reconstructed input z :

$$L(x, z) = - \sum_{k=1}^K \left(x_k \log z_k + (1 - x_k) \log (1 - z_k) \right) \quad (6.13)$$

using stochastic gradient descent and backpropagation.

In this scenario h is similar to a lossy compression of x , that should capture the coordinates along the main directions of variation of x . To further improve the network, the input x can be ‘perturbed’ to another slightly different image, \tilde{x} , so that the network will not adapt too much to the given inputs but will be able to better generalize over new samples. This forms the Denoising variant of the Autoencoder. To do this, the input is corrupted

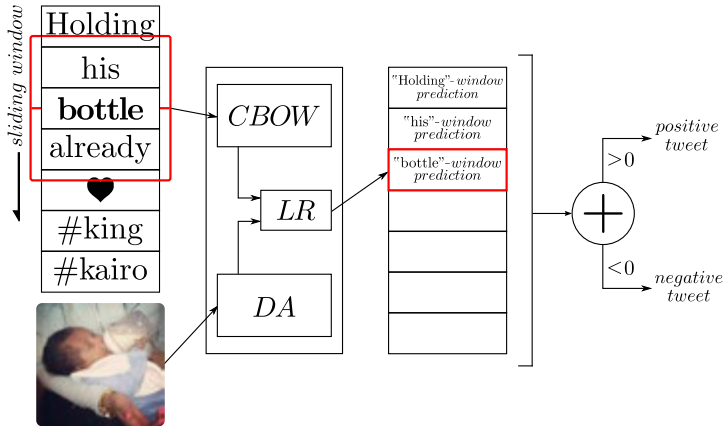


Figure 6.3: The process of polarity prediction of a tweet with its associated image performed by our model. On the left, one tweet text window (in red) at a time is fed into the CBOW model to get a textual representation. Likewise, the associated image is fed into the denoising autoencoder (DA). The two representations are concatenated and a polarity score for the window is obtained from the logistic regression (LR). Finally, each window polarity is summed into a final tweet polarity score.

by randomly setting some of the values to zero (Bengio, 2009). This way the Denoising Autoencoder will try to reconstruct the image including the missing parts. Another benefit of the stochastic corruption is that, when using a hidden layer bigger than the input layer, the network does not learn the identity function (which is the simplest mapping between the input and the output) but instead it learns a more useful mapping, since it is trying to also reconstruct the missing part of the image.

The CBOW-DA-LR method. The model used to deal with textual and visual information, denoted as CBOW-DA-LR, is an extension of CBOW-LR with the addition of a new task based on a Denoising Autoencoder (DA) applied to images, aiming at obtaining a mid-level representation. In this final form, the descriptor obtained from the DA, together with the continuous word representation, represents the new descriptor for a window of words in a tweet and is concurrently used to learn a logistic regressor. Given a tweet, for each window, we compute the continuous word representation and the image descriptor associated with the tweet. Each window in a tweet will be associated with the same image descriptor as the image for the tweet is always the same.

Fig. 6.3 shows an exemplification of the prediction process for a tweet with its accompanying image. While the image gets a fixed representation for the entire process, the text is represented one window at a time through a sliding window process. Each window is processed independently to get a local polarity score. To get the overall tweet polarity, each window polarity

is summed into a final score and classified according to its sign.

This can be formalized as follows: if we define $h_{\mathcal{G}}$ as the encoding of the image associated to the window \mathcal{G} of the tweet T , then Eq. (6.5) becomes:

$$y(\mathcal{G}) = \sigma \left(C^T \left(\left(\sum_{W_i \leftarrow w_i \in \mathcal{G}} W_i \right) \parallel (h_{\mathcal{G}}) \right) + b_s \right) \right) \quad (6.14)$$

where \parallel is the concatenation operator, i.e. the encoded representation of the image is concatenated to the continuous word representation of the window, forming a new vector whose size is the sum of the size of the continuous word space and the size of the encoding representation of the image.

As stated before, the Autoencoder can be pre-trained in the same fashion as the continuous word representation. Any set of unlabeled images can be used to train the network before the actual training on the tweets.

The DA will be a component of our model and, like the two previous components CBOW and LR, it has its own cost function. Similar to Eq. (6.13), it is:

$$C_{\text{image}} = - \sum_{k=1}^K \left(\tilde{x}_k \log \hat{z}_k + (1 - \tilde{x}_k) \log (1 - \hat{z}_k) \right) \quad (6.15)$$

Since we are aiming at concurrent learning the textual and image representations, the three components are combined together in a single final cost of CBOW-DA-LR. Starting from the previously defined Eq. (6.8) for CBOW and Eq. (6.7) for LR, the cost becomes:

$$C_{\text{CBOW-DA-LR}} = \lambda_1 \cdot C_{\text{sent}} + \lambda_2 \cdot C_{\text{sem}} + \lambda_3 \cdot C_{\text{image}} \quad (6.16)$$

where $\lambda_1, \lambda_2, \lambda_3$ weight the contribution of each task. The model can be trained by minimizing $C_{\text{CBOW-DA-LR}}$ with stochastic gradient descend. Symbolic derivatives can be easily obtained by using an automatic differentiation algorithm (e.g. Theano (Bastien et al., 2012)). After training, Eq. (6.9) can be used to predict the label of the tweet in the same manner as it is used when we do not consider the image descriptor.

6.4 Experiments

The datasets. To evaluate the proposed approach we have used four datasets obtained from Twitter:

i) Sanders Corpus⁴, consists of 5,513 manually labelled tweets on 4 topics (Apple, Google, Microsoft and Twitter). Of these, after removing missing

⁴<http://sananalytics.com/lab/twitter-sentiment/>

tweets, retweets and duplicates, only 3,625 remain. The dataset does not specify a train and a test subset, so to evaluate the performance the whole set is randomly divided multiple times into subsets each time each one with the same size and the mean performance is reported;

ii) Sentiment140⁵ (Go et al., 2009) consists of a 1.6 million tweet training set collected and weakly annotated by querying positive and negative emoticons, considering a tweet positive if it contains a positive emoticon like “ :) ” and negative if, likewise, it contains a negative emoticon like “ :(”; the dataset also comprises a manually annotated test set of 498 tweets obtained querying names of products, companies and people;

iii) SemEval-2013⁶ provides a training set of 9,684 tweets of which only 8,208 are not missing at the time of writing and a test set of 3,813 tweets, selected querying a mixture of entities, products and events; the dataset is part of the SemEval-2013 challenge for sentiment analysis and also comprises of a development set of 1,654 (of which only 1,413 available at the time of writing) that can be used as an addendum to the training set or as a validation set;

iv) SentiBank Twitter Dataset⁷, consists of 470 positive and 133 negative tweets with images, related to 21 topics, annotated using Mechanical Turk; the dataset has been partitioned by the authors into 5 subsets, each of around 120 tweets with the respective images, to be used for a 5-fold cross-validation.

In this work we consider the binary positive/negative classification, thus we have removed neutral/objective tweets from the corpora when necessary. This approach follows that of (Go et al., 2009) and (Liu et al., 2012), and is motivated by the difficulty to obtain training data for this class; it has to be noted that even human annotators tend to disagree whether a tweet has a negative/positive polarity or it is neutral (Jiang et al., 2011). Performance is reported in terms of Accuracy. The evaluation for SemEval is performed using F_1 , since this is the metric originally used in this dataset.

For the Sanders dataset, as described earlier, there is no definition of an actual test set nor of a training set. For these reasons we choose to follow the experimental setup of (Liu et al., 2012), where experiments on Sanders dataset have been performed varying the number of training tweets between 32 to 768. For each test, first the number of training tweets is selected, then half of them are randomly chosen from all the positive tweets and the other half are chosen from the negative ones. Finally, the remaining tweets are used as test set. Since there could be some variation from a random set to another, for each test 10 different runs are evaluated and the mean is taken

⁵<http://help.sentiment140.com/for-students>

⁶<http://www.cs.york.ac.uk/semeval-2013/task2/>

⁷<http://www.ee.columbia.edu/ln/dvmm/vso/download/sentibank.html>

as the result of the selected test. Results with this dataset are reported with the notation “Sanders@ n ”, where n is the number of training tweets selected.

The evaluation of the SentiBank dataset has been performed preserving the structure given by the authors so that the results could be comparable. The dataset is divided into 5 subsets for 5-fold cross-validation. Each at a time a subset is considered as test set while the other 4 are considered as training set; 5 runs are performed and in the end the mean of the 5 results is computed and considered the resulting value given by the method for the dataset. Considering the high imbalance between positive and negative tweets of this dataset we report also the F_1 score in addition to Accuracy.

We have evaluated the proposed method through a set of 5 experiments: in the first one we evaluate the performance of the proposed CBOW-LR text model comparing it against the standard CBOW model. Then we assess the performance of these models after pre-training them with large scale Twitter corpora. In a third experiment we compare the proposed approach against a baseline and two state-of-the-art methods. In the final experiment we compare the proposed CBOW-DA-LR text+image model against a state-of-the-art method on a publicly available dataset composed by tweets with images. In all these experiments we empirically fixed $K = 5$ and $Q = 100$. In the last experiment we evaluate the effects of K and Q parameters w.r.t. the classification performance on all the datasets. Regarding λ in the first three experiments and $\lambda_1, \lambda_2, \lambda_3$ in the last one, we tested several combinations and found a good setting by fixing $\lambda = 0.5$ and $\lambda_1 = \lambda_2 = \lambda_3 = 0.33$, respectively. Also the image DA was implemented with ‘tied weights’ to reduce overfitting. Its dimensionality was tested in the range [200, 1000] and found it better performing by fixing it to 500. To perform the optimization using stochastic gradient descent, we employed Theano (Bastien et al., 2012) to automatically compute the derivatives.

Exp. 1: Comparison with baselines. Tab. 6.1 compares our proposed method (CBOW-LR) with two baselines: RAND-LR and CBOW+SVM. The purpose is twofold: *i*) since we are learning features crafted for the specific task, we compare our method with randomly generated features. RAND-LR learns a logistic regression classifier on random word features (i.e. we set $\lambda = 1$ in eq. 6.8); *ii*) we verify the superiority of CBOW-LR learned features against a standard unsupervised CBOW representation. The CBOW+SVM baseline employs SVM with standard pre-trained CBOW representation on the specific dataset.

Performance figures show that the proposed method consistently outperforms both baselines, thus our method learns useful representations with some improvement over CBOW.

Dataset	(proposed)		
	CBOW-LR	RAND-LR	CBOW+SVM
Sentiment140	83.01	61.56	79.39
SemEval-2013 (F_1)	72.57	53.01	71.32
Sanders @ 32	62.55	58.38	59.89
Sanders @ 256	74.91	63.69	67.91
Sanders @ 768	82.69	65.53	73.03

Table 6.1: Comparison between our method and two baselines. Performance is reported in terms of accuracy except for SemEval-2013, where is used the F_1 measure. Sanders@n indicates the number of training tweets used for the experiments on that dataset.

Exp. 2: Exploiting CBOW training on large scale data. Tab. 6.2 compares our proposed method with two baselines when exploiting large scale training data for the CBOW representation. We pre-trained a CBOW model using the 1.6 million tweets of Sentiment140 and used the learned features (termed CBOW_S) with two standard learning algorithms. CBOW_S+LR employs the logistic regression while CBOW_S+SVM uses the SVM classifier. In contrast to the baselines, our model $\text{CBOW}_S\text{-LR}$ employs the pre-trained CBOW_S features as initialization for the W matrix. Comparing Tab. 6.2 with Tab. 6.1 shows that CBOW_S+SVM baseline benefit from the use of pre-learned CBOW_S . This is visible especially on the Sanders dataset, as more rich representation is built. Note that when CBOW_S+SVM is applied to Sentiment140 dataset it corresponds to CBOW+SVM, since CBOW_S description is trained on Sentiment140; therefore the result is the same.

While both CBOW_S+SVM and CBOW_S+LR are unable to modify the word vector representation, our model $\text{CBOW}_S\text{-LR}$ is able to retain the full richness of the initial representation and improve it on two datasets.

Exp. 3: Comparison with FSLM and ESLAM. In this experiment we have compared both textual variants of our approach, one with CBOW trained using the dataset on which the method is applied and one using CBOW_S , with two state-of-the-art methods: FSLM and ESLAM, proposed in (Liu et al., 2012). FSLM uses a fully supervised probabilistic language model, learned concatenating all the tweets of the same class to form synthetic documents. ESLAM extends FSLM exploiting noisy tweets, based on the presence of ‘positive’ and ‘negative’ emoticons, to smooth the language model. Inclusion of manually labelled data with the unsupervised noisy data gives the power to deal with unforeseen text that is not easily handled by fully supervised methods. Fig. 6.4 shows the Accuracy while varying the number of training tweets of the Sanders dataset. The proposed

Image Understanding by Socializing the Semantic Gap

Dataset	(proposed) CBOW _S -LR	CBOW _S +LR	CBOW _S +SVM
Sentiment140	83.84	76.32	79.39
Semeval-2013 (F_1)	72.23	73.73	71.48
Sanders @ 32	66.28	66.90	66.65
Sanders @ 256	76.33	71.14	73.69
Sanders @ 768	82.98	75.43	76.44

Table 6.2: Comparison between our method and two baselines, using an initialization based on CBOW pre-trained aside with 1.6 million tweets of Sentiment140. Performance is reported in terms of accuracy except for SemEval-2013, where is used the F_1 measure. Sanders@n indicates the number of training tweets used for the experiments on that dataset.

approach has a much lower performance when using only 32 or 64 tweets for training. However, it can be observed that as the number of training data increases so does the performance of the proposed method, that outperforms that of ESLAM when using 768 tweets for training. In general the proposed method outperforms FSLM. The fact that ESLAM outperforms the proposed method when using smaller training data can be explained by the fact that CBOW models, as Skip-Gram and feature learning methods, require large training datasets.

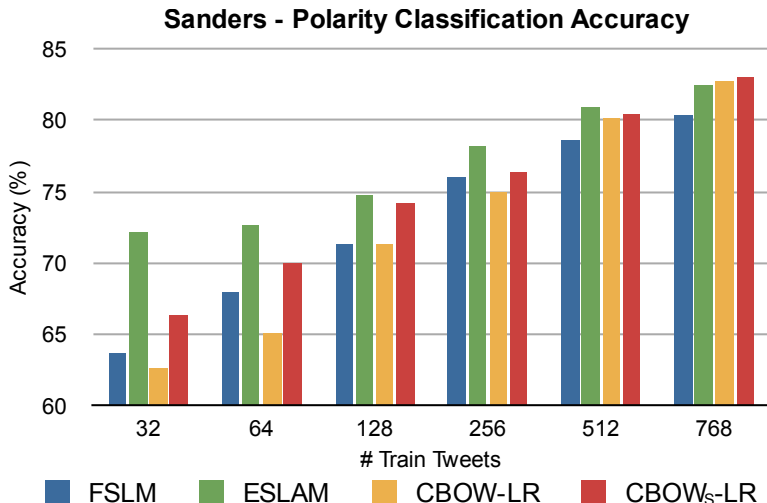


Figure 6.4: Comparison between our method with FSLM and ESLAM (Liu et al., 2012) on Sanders dataset, while varying the number of training tweets.

Data	Method	SentiBank (AC)	SentiBank (F_1)
	Random	47	42
<i>Text</i>	SentiStrength (Thelwall et al., 2010)	58	51
	CBOw+SVM	72	50
	^(proposed) CBOw-LR	75	52
<i>Image</i>	SentiBank (Borth et al., 2013)	71	51
	^(proposed) DA-LR	69	51
<i>Text+Image</i>	SentiStrength (Thelwall et al., 2010) + SentiBank (Borth et al., 2013)	72	n.a.
	^(proposed) CBOw-DA-LR	79	57

Table 6.3: Comparison between our method (on single and combined modalities) with baselines and state-of-the-art approaches on SentiBank Twitter Dataset.

Exp. 4: Exploiting textual and visual data. In this experiment we have evaluated the performance of three versions of our proposed approach – CBOw-LR for text, DA-LR for visual data, and CBOw-DA-LR for both text and visual information – with different baselines and state-of-the-art approaches.

CBOw-LR has been compared with SentiStrength (Thelwall et al., 2010) and the CBOw+SVM baseline used in Exp. 1 and Exp. 2. DA-LR has been compared with SentiBank (Borth et al., 2013) classifiers. CBOw-DA-LR has been compared with the approach proposed by the authors of the SentiBank Twitter dataset (Borth et al., 2013), that uses SentiStrength (Thelwall et al., 2010) API⁸ for text classification and SentiBank classifiers as mid-level visual features, with a logistic regression model. As the dataset is imbalanced, we also compare these approaches with an additional baseline based on random classification, i.e. we assign a random polarity to each test tweet. We used the code provided by the authors of the methods, except for the SentiStrength+SentiBank case, for which we report the result published in (Borth et al., 2013). Results reported in Tab. 6.3 show that not only CBOw-LR outperforms both the baseline and SentiStrength, but also the multimodal SentiStrength+SentiBank approach. When using only visual information SentiBank obtains a better performance than DA-LR. Considering the text+image case it can be observed that the proposed multimodal CBOw-DA-LR method improves upon single modalities (CBOw-LR and DA-LR) and outperforms SentiStrength+SentiBank by a larger margin, proving that images hold meaningful informations regarding the polarity of text, and thus can be exploited to improve overall Accuracy and F_1 .

⁸<http://sentistrength.wlv.ac.uk/>

Exp. 5: Parameters analysis. Fig. 6.5 shows accuracy and F_1 of our model when varying K and Q parameters on Sanders, SemEval-2013 and SentiBank datasets. The performance on SentiBank is practically not affected by these parameters. The same set of parameters results in the best performance on all the datasets. The values of K and Q are in line with those obtained to train CBOV models on Wikipedia by Mikolov *et al.* .

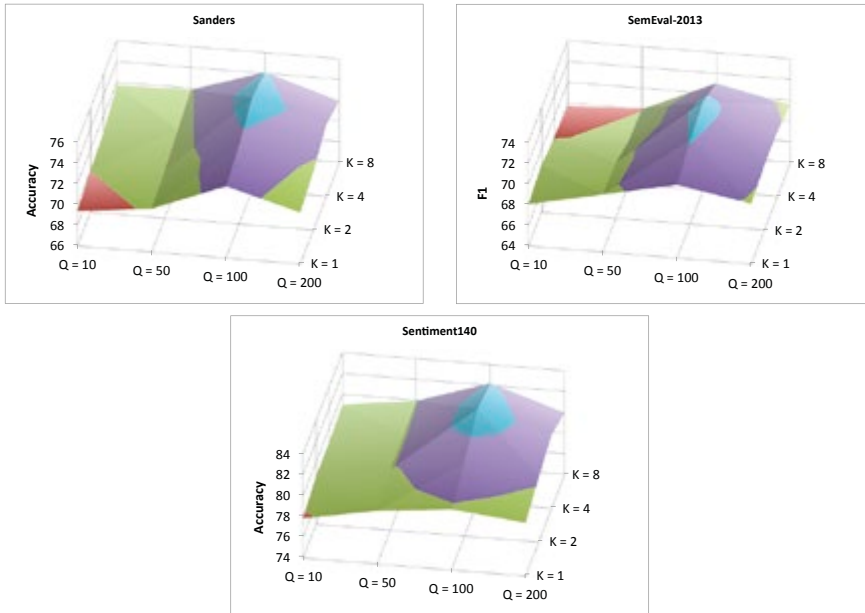


Figure 6.5: Performance of the proposed method when varying K and Q parameters on Sanders, SemEval-2013 and Sentiment140 datasets.

6.5 Conclusions

In this chapter we have presented a method for sentiment analysis of social network multimedia, presenting an unified model that considers both textual and visual information.

Regarding textual analysis we described a novel semi-supervised model CBOV-LR, extending the CBOV model, that learns concurrently vector representation and a sentiment polarity classifier on short texts such as that of tweets. Our experiments show that CBOV-LR can obtain improved accuracy on polarity classification over CBOV representation on the same quantity of text. When considering a large unsupervised corpus of tweets as additional training data for CBOV, a further improvement is shown, with our model being able to improve the overall accuracy. Comparison with the

state-of-the-art methods FSLM and ESLAM shows promising results.

The CBOW-LR model has been expanded to account for visual information using a Denoising Autoencoder. The unified model (CBOW-DA-LR) works in an unsupervised and semi-supervised manner, learning text and image representation, as well as the sentiment polarity classifier for tweets containing images. The unified CBOW-DA-LR model has been compared with SentiBank, a state-of-the-art approach on a publicly available Twitter dataset, obtaining a higher classification accuracy.

Chapter 7

Popularity Prediction with Sentiment and Context Features

Images in social networks share different destinies: some are going to become popular while others are going to be completely unnoticed. In this chapter we propose to use visual sentiment features together with three novel context features to predict a concise popularity score of social images. Experiments on large scale datasets show the benefits of proposed features on the performance of image popularity prediction. Exploiting state-of-the-art sentiment features, we report a qualitative analysis of which sentiments seem to be related to good or poor popularity.¹

7.1 Introduction

In the last decade users of social networks such as Flickr and Facebook have uploaded tens of billions of photos, often adding accompanying metadata by tagging and by providing a short description. Users interact with each other by forming groups of shared interests, following the status streams of each other, and by commenting the photos that have been shared. Inevitably, in the huge quantity of available media, some of these images are going to become very popular, while others are going to be totally unnoticed and end up in oblivion. Often, media may be popular because it conveys sentiments or it has a rich meaning in the social context it is put. In fact, sentiments have been known to affect popularity of visual media since the widespread watch of television programs (Diener and DeFour, 1978). Also, it was recently found to be related to popularity in tweets (Bae and Lee, 2012). Being able to predict the popularity of a media may have a profound impact on several essential applications such as content retrieval and annotation, but also in other fields such as advertising and content

¹Parts of the work presented in this chapter have been published in Gelli, F., Uricchio, T., Bertini, M., Del Bimbo, A., and Chang, S. F. (2015, October). “Image popularity prediction in social media using sentiment and context features”. In Proceedings of the 23rd ACM international conference on Multimedia (pp. 907-910). ACM. The publication is available at <http://dx.doi.org/10.1145/2733373.2806361>.

Image Understanding by Socializing the Semantic Gap

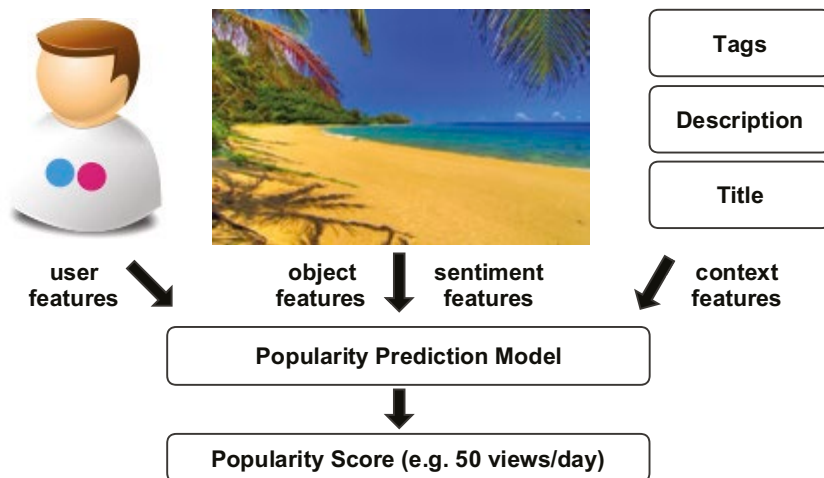


Figure 7.1: The idea of our approach to popularity prediction of images.

distribution (Figueiredo et al., 2014).

In this chapter, we address the problem of predicting the popularity of an image posted in a social network, considering different scenarios that are typical of different situations. Despite the recent crop of literature that studies the question of what makes an image popular (Khosla et al., 2014; Totti et al., 2014; McParlane et al., 2014), none of these works addresses the question of how much the visual sentiment is influencing the popularity of media. As social context has been widely found important to predict media popularity (Khosla et al., 2014), we show how to further improve popularity estimation by using a knowledge base to supplement the understanding of semantics in textual metadata.

The main contributions of this chapter are:

- we propose to employ state-of-the-art visual sentiment features (Borth et al., 2013; Chen, Borth, Darrell and Chang, 2014) to perform image popularity prediction;
- we propose three new textual features based on a knowledge base, to better model the semantic description of an image, in addition to the social context features proposed in (Khosla et al., 2014; McParlane et al., 2014);
- we show qualitative results of which sentiments seem to be related to a good or poor popularity.

To the best of our knowledge, this is the first work understanding specific visual concepts that positively or negatively influence the eventual popularity of images, beyond just numerical prediction of photo popularity.

Experiments performed on large scale datasets illustrate several benefits of the two types of proposed features, and show how their combination impacts effectively on the performance of popularity prediction.

7.2 Related work

Popularity Prediction Recently, a significant effort has been spent on investigating popularity of social media content. Regarding image popularity, the majority of works agree that social features have the greatest predictive power (Khosla et al., 2014; McParlane et al., 2014; Totti et al., 2014). Visual content features are less powerful than social ones in terms of predictive power, but they are useful when no user metadata is present (e.g. no tags or description) or to address scenarios such as the case in which no social interactions have been recorded before posting the image (e.g. because the user has just joined the social network). Previous works vary in terms of popularity score definition (e.g. image views, reshares, mean views over a period) but they all share the same basic pipeline: they extract several content and context related features and successively employ a regressor to compute the popularity score.

In (Khosla et al., 2014), Khosla *et al.* investigate both low-level features such as color, GIST, LBP, and content features such as the object predictions and network activations of a state-of-the-art CNN image classifier (Krizhevsky et al., 2012). Together with user and image context features, they show promising results. McParlane *et al.* (McParlane et al., 2014) propose to use image content, context features and user context to predict popularity. Their analysis is limited to a cold start scenario, i.e. where there exist no or little textual or interaction data. Totti *et al.* (Totti et al., 2014) investigate the use of aesthetics features such as blur, aspect ratio and color channel statistics together with the output of 85 object classifiers as content features.

Visual Sentiment A few works have addressed the problem of multimedia sentiment analysis of social network images. Starting from the 24 basic emotions of Plutchik’s Wheel of Emotions (Plutchik, 2001), Borth *et al.* (Borth et al., 2013) have recently presented a large-scale visual sentiment ontology termed SentiBank. They train 3,244 detectors on pairs of nouns and adjectives (ANPs) based on a combination of global and local features. Based on the recent breakthrough of convolutional networks for classification (Krizhevsky et al., 2012), Chen *et al.* (Chen, Borth, Darrell and Chang, 2014) used a CNN to replace SVM in the approach of Borth *et al.* (Borth et al., 2013), obtaining an improved accuracy on ANPs.

The authors in (Chen, Yu, Chen, Cui, Chen and Chang, 2014) proposed

an hierarchical system able to handle sentiment concept classification and localization on objects. They found individual concept detector of SentiBank (Borth et al., 2013) less reliable for object-based concepts.

Chen *et al.* (Chen, Chen, Hsu, Liao and Chang, 2014) studied the correlation between the intended publisher sentiment and the actual induced in the viewer (‘viewer affect concept’). They aim to recommend appropriate images for the publisher by predicting in advance the induced sentiment in the viewer.

7.3 The Proposed Method

Our proposed method is based on two hypotheses: *i*) the popularity of an image can be fueled by the inherent visual sentiments conveyed; *ii*) semantic descriptions of an image is also important for its popularity, since it makes it easier to be found or looked at.

7.3.1 Measuring Popularity

It is difficult to precisely define a single score as measure of popularity, and several ways have been proposed to measure it. Khoshla *et al.* (Khosla et al., 2014) used the number of views on Flickr as the principal metric. McParlane *et al.* (McParlane et al., 2014) consider both the number of views and the number of comments for each image as they have been found correlated in video popularity (Chatzopoulou et al., 2010). However they only aim to predict two classes of popularity: high or low.

In this work we follow Khoshla *et al.* (Khosla et al., 2014) and consider the number of views on Flickr as popularity metric. To cope with the large variation of views, we divide the popularity metric by the difference of time between the user upload and our retrieval, then we apply the log function.

7.3.2 Visual Sentiment Features

To discover which visual emotions are roused from the visualization of an image, a visual sentiment concept classification is performed based on the Visual Sentiment Ontology (VSO). The ontology, consisting in a collection of 3,244 Adjective-Noun-Pairs (ANPs), has been defined by Borth *et al.* (Borth et al., 2013). In particular we used DeepSentiBank (Chen, Borth, Darrell and Chang, 2014): a convolutional neural network pre-trained from (Krizhevsky et al., 2012) has been fine-tuned to classify images in one of a subset of 2,096 ANPs. Similarly to its previous version (Borth et al., 2013), this tool provides a mid-level representation of an image.

For each image we extract two descriptors that we term respectively

SentANPs and FeatANPs: the ANPs prediction layer of 2,096d and the rectified activations of the 7th fully connected layer of 4,096d.

7.3.3 Object Features

Since image popularity is related also to the visual content of the image, we extract the convolutional neural networks features, initially proposed in (Khosla et al., 2014). A very deep CNN with 16 layers (Chatfield et al., 2014) was used to extract for each image the final output containing 1,000 objects from ILSVRC 2014 challenge (termed ObjOut) and the 4,096d representation of the 7th rectified fully connected layer (termed ObjFC7).

7.3.4 Context Features

Image context information such as tags and description contains important cues that may reflect on the number of views that an image obtains. Entities like people, locations or tourist attractions can affect popularity as *i)* people may be more interested in photographs referring some particular subject; *ii)* the presence of tags and description, the submission of a photo to some groups, etc. make it easier to be found by other users. The extraction of entities from image context strongly depends on the nature of the text, i.e. tags and textual description; due to the different nature of these channels, two different approaches are proposed.

Entity Extraction from Tags Starting from image tags, we define two new context features that we term TagType and TagDomain. They both rely on Freebase, a large collaborative ontology containing millions of interconnected topics. Given a tag, a search for a *Freebase topic* is performed: if the tag is related to some topics, the most popular one is picked, according to Freebase popularity ranking. Meaningless tags that do not have a match in Freebase topics are ignored, thus they do not act as a nuisance. When a Freebase topic is retrieved, another query is performed to extract its *Freebase types* with the “notable” property and its *Freebase domain*. While *types* are mostly specific (e.g. Person, Author) *domains* cover broader areas (e.g. Film, Music).

Due to the vast number of types in the ontology, a smaller specific type knowledge base is introduced. We first randomly sampled 10k tags from MIR-Flickr dataset vocabulary (Huiskes et al., 2010) and used them to extract Freebase types. We select the 100 most frequent types as our specific knowledge base.

The extraction of TagType feature for an image is then straightforward: each tag is used to query Freebase for a notable type. We count the matches to the 100 selected types and obtain a 100d histogram as final feature.

Regarding the TagDomain feature, we take the full list of 78 domains pre-defined by Freebase curators and count the tag matches, similarly as TagType. Thus, the eventual TagDomain feature result in a 78d histogram.

Entity Extraction from description Differently from the concise tags, image descriptions allow users to comprehensively detail their images in natural language. We seek to recognize subjects and objects of this text to detail context. Hence, we adopt a well known CRF-based language model to perform Named Entity Recognition (NER) (Finkel et al., 2005). We used the pre-trained 7-class model for MUC that is able to recognize Time, Location, Organization, Person, Money, Percent, Date. We count the occurrences for each class and build a 7d feature that we term NER_7 .

7.3.5 User Features

Previous works have found that the number of views that a photograph is going to obtain depends not only on the image itself and its context information, but also on the author data. In this work we used the same user features proposed by Khosla *et al.* (Khosla et al., 2014): among these features the most related one to popularity is the mean views of the images of the user, as it represents the popularity of the user himself.

7.3.6 Popularity prediction

In order to predict popularity as a concise score, we used an off-the-shelf Support Vector Machine. As we are working with large-scale dataset, we used a L2 regularized L2 loss Support Vector Regression (SVR) from LIBLINEAR package due to its scalability with large sparse data and huge number of instances compared to a kernelized version.

7.4 Experiments

As different scenarios show different aspects of popularity, we structure our experimental setups similarly to those of Khosla *et al.* (Khosla et al., 2014), using Flickr social network. Two datasets were used to represent two different scenarios:

- *One-Per-User (OPU)*: we randomly selected 250k images from the VSO Flickr Dataset (Borth et al., 2013). This dataset represents the scenario of a Flickr search, where images belong to different users.
- *User Specific (US)*: 25 users from the VSO Flickr Dataset are selected at random to constitute 25 different trials. For each one, 10k images

are randomly selected. This dataset represent the scenario of a user that wants to select which of his pictures should be uploaded to attract the attention of other users.

In each experiment, we extract and concatenate the selected features. We freely provide the extracted features on our website. Multidimensional features are L2 normalized, while scalar attributes are scaled in the $[0, 1]$ range. We split every dataset in training and evaluation: half was randomly chosen as training set, while the remaining images were equally split in validation and testing set. The C of SVM was set in the range $[0.001 - 100]$.

After the prediction, testing images are ranked in descending popularity scores and compared to the correct ranking obtained by the ground truth scores. The correlation between these two lists r and s is computed using *Spearman’s rank correlation* that ranges in $[-1, 1]$:

$$\rho = \frac{\sum_i (r_i - \bar{r})(s_i - \bar{s})}{\sqrt{\sum_i (r_i - \bar{r})^2} \sqrt{\sum_i (s_i - \bar{s})^2}} \quad (7.1)$$

a score of 1 (or -1) corresponds to perfect (inverse) correlation, while 0 corresponds to random ranks.

7.4.1 Results

Experiments have been carried out for visual features, context ones and visual + context + user combination. We train a model with each single feature to show its predictive power. Then, we combine the features and compare a model with all of them against baselines implemented following the method of Khosla *et al.* (Khosla et al., 2014) i.e. without our novel features. Results are reported in terms of *Spearman’s rank correlation* and, for the User Specific dataset, the average scores between the 25 users are reported.

Visual Features Visual content features include visual sentiment and object detections (Sec. 7.3.2, 7.3.3). The latter ones are used in this case as a baseline, including ObjOut and ObjFC7.

Dataset	SentANPs	FeatANPs	ObjOut	ObjFC7	Baseline	All
OPU	0.28	0.32	0.13	0.30	0.30	0.36
US	0.31	0.40	0.27	0.40	0.40	0.43

Table 7.1: Visual Features Results

Results are reported in Table 7.1: sentiment features are comparable with object features. As ANPs are learned starting from a similar network

Image Understanding by Socializing the Semantic Gap

for classification, this suggests the existence of some correlation between them. Nevertheless, SentANPs is higher than ObjOut, suggesting that ANPs are better for popularity prediction than purely object classification. Our features are able to improve overall prediction in both scenarios.

Context Features The performance of the proposed context features (Sec. 7.3.4) is compared with a baseline composed by the number of tags, the length of title and description (Table 7.2).

Dataset	TagType	TagDomain	NER ₇	TagNum	TitleLen	DescLen	Baseline	All
OPU	0.42	0.36	0.50	0.55	0.22	0.48	0.61	0.63
US	0.44	0.37	0.13	0.23	0.17	0.20	0.33	0.54

Table 7.2: Context Features Results

Our features are comparable with other context-based ones in the OPU scenario. In the US scenario, all the features except TagType and TagDomain lose predictive power due to the limited context of a single user. This is because our features are able to better model semantically the single photos, regardless of the single user. When combined, our feature boost correlation to 0.54 from 0.33 of the baseline.

Visual + Context + User In this experiment we combined visual, context and user features along with the total combination with and without our novel features. User features are added to resemble a state of the art pipeline. Each modality is singularly tested and finally combined together. Results are reported in Table 7.3. Note that User Features can't be used for the User Specific scenario as each model is trained for a single user.

Dataset	Method	Visual Content	Image Context	User Features	All
OPU	proposed	0.36	0.63	0.72	0.76
	baseline	0.30	0.61	0.72	0.74
US	proposed	0.43	0.54	n/a	0.61
	baseline	0.40	0.33	n/a	0.50

Table 7.3: Visual + Context + User Features Results

User Features produce the highest correlation in the OPU scenario, confirming that popularity is highly related to the popularity of the author (Khosla et al., 2014). Despite this, the combination of the three modalities is helpful, boosting correlation from 0.72 to 0.74. Our features further improve upon this, bringing the value to 0.76. In the User Specific dataset, the improvement from the baseline is more pronounced, where a correlation of 0.61 vs 0.50 is obtained.

7.4.2 Qualitative Analysis

We investigate which specific ANP and semantic metadata correlated the most with the number of views of images. This analysis is performed for the One-Per-User scenario, as it aims to be as generic as possible. Fig. 7.2(a) shows the trained SVR weights for each of the 2089 ANPs, in descending order. According to the figure we split the visual sentiments in three categories.

A first group include those ANPs that have a positive impact on image popularity (e.g. *sexy legs*, *beautiful eyes*, *heavy rain*). The rapid drop evinces that a very short number of ANPs corresponds to strongly popular images in the training dataset. Then, we observe that some visual sentiments obtain very low weights, near zero: that ANPs are almost irrelevant to the number of views (e.g. *sunny trees*, *dry forest*). Finally a third group includes ANPs that are associated to a sufficiently negative score: the detection of those push an image towards unpopularity (e.g. *creepy eyes*, *silly clown*).

Extending our analysis to the 28 basic emotions of the Plutchick wheel, we found out that our model marked as unpopular those images that arouse emotions such as *annoyance* or *serenity*, while high scores are likely to be returned in case of sentiments as *amazement* or *ecstasy*. These last emotions derive from ANPs containing the adjective *sexy*, resulting in 10 occurrences in the top 35 visual emotions. A similar analysis on the 100 semantic entities is shown in Fig. 7.2(b). This plot has a similar trend compared with that of visual sentiment, but for the extreme values: in this case the negatively weighted types (e.g. *religious practice* and *software genre*) have more prominent values than the positively weighted ones (e.g. *garment* and *film character*).

7.5 Conclusions

In this chapter we proposed to employ state-of-the-art visual sentiment features and three new context features to address the problem of predicting whether an image posted on a social network may became popular. We are the first to show a qualitative analysis of which sentiments (as ANPs) are correlated to popularity. Our experiments suggest that some sentiments have a correlation with popularity, still smaller than user features. However, together with our novel context features, they have good prediction power, especially when user features are unavailable as in the User Specific scenario.

Image Understanding by Socializing the Semantic Gap

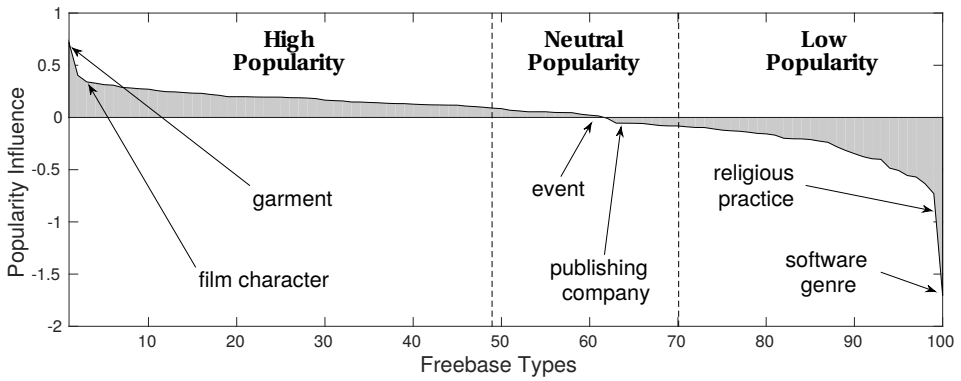
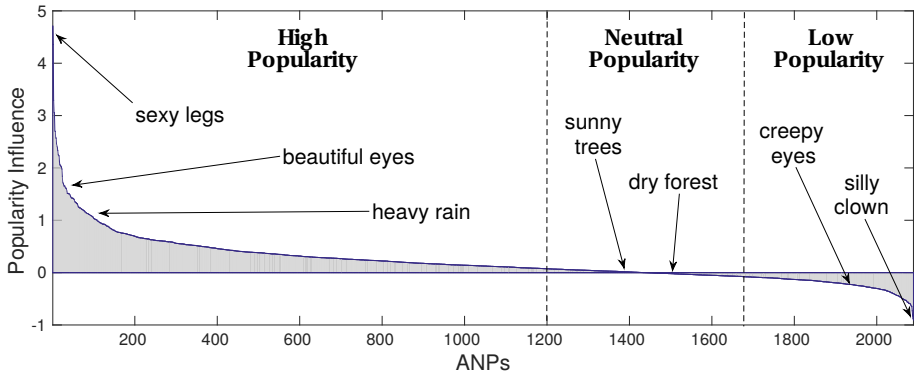


Figure 7.2: Influence of Multimedia Concepts on Popularity: weights of the 2089 ANP visual sentiment concepts (*top*); weights of the 100 Freebase Types extracted from contextual image tags (*bottom*).

Chapter 8

Conclusion

This chapter summarizes the contribution of the thesis and discusses avenues for future research.

8.1 Summary of Contribution

After presenting a structured survey of related work on social tagging and retrieval, we detailed a novel experimental protocol that we used to test and analyze eleven key methods. Established the state of the art, we proposed several models and methods to achieve objective annotation of images. Finally we moved to subjective annotation of sentiments aroused in a viewer and the expected popularity of an image.

In particular, we first presented in Chapter 2 a survey on image tag assignment, refinement and retrieval, with the hope of illustrating connections and difference between the many methods and their applicabilities, and consequently helping the interested audience to either pick up an existing method or devise a method of their own given the data at hand. Based on the key observation that all works rely on tag relevance learning as the common ingredient, exiting works, which vary in terms of their methodologies and target tasks, are interpreted in a unified framework. Consequently, a two-dimensional taxonomy has been developed, allowing us to structure the growing literature in light of what information a specific method exploits and how the information is leveraged in order to produce their tag relevance scores.

Having established the common ground between methods, a new experimental protocol was introduced in Chapter 3 for a head-to-head comparison between the state-of-the-art. A selected set of eleven representative works were implemented and evaluated for tag assignment, refinement, and/or retrieval.

Nearest neighbors methods proved to be the best overall performing method for assignment in Chapter 3. Hence, we proposed a novel technique in Chapter 4 that reduce the semantic gap in that class of methods. We presented a cross-media model based on KCCA for tag assignment. The key

idea was learning a semantic space, where visual and textual data were represented as blended unified features. This representation is able to provide better neighbors for nearest neighbor algorithms. The experimental results showed that our method makes consistent improvements over standard approaches based on a single-view visual representation as well as other previous work that also exploited tags. The properties of tested methods found in Chapter 3 remain still valid in the semantic space, although with an improved capability of retrieving better neighbors. Hence a better performance is obtained.

Considering the influence of real world events in tagging behavior, in Chapter 5 we briefly analyzed the correlations between user tags, news and the objective relevance of concepts. The results suggest that analyzing the time series of tags may be beneficial to annotate social media.

Moving on to subjective information extraction, in Chapter 6 and 7 we explored the related tasks of sentiment analysis in tweets and the popularity estimation of images in social networks. In Chapter 6 we have presented a method for sentiment analysis of social network multimedia, capable of learning both textual and visual features in an unified fashion. Our model CBOW-LR, extending the CBOW model, learns concurrently a vector representation and a sentiment polarity classifier on short texts. Comparing to previous work, our representation explicitly includes the sentiment of words and maintains good performance. By adding images to the mix, a further extension CBOW-DA-LR was presented. This semi-supervised model concurrently learns text and image representation, as well as the sentiment polarity classifier for tweets containing images. Experiments with large unsupervised corpus of tweets show promising results compared to the state-of-the-art.

Chapter 7 presented a novel approach to predict whether an image posted on a social network may become popular. The approach uses a combination of state-of-the-art visual sentiment features and three novel context features to reduce the semantic gap. The experiments reported suggest that some sentiments have a correlation with popularity. Moreover, our novel context features have good prediction power, especially when user features are unavailable. We also presented the first study that show a qualitative analysis of which sentiments (as ANPs) are correlated to popularity.

8.2 Direction of future work

Much remains to be done. Several exciting recent developments open up new opportunities for the future. First, extraction of objective information can profit from recent developments of deep learning. Employing novel deep learning based visual features is likely to boost the performance of an-

notations method that employ visual features. What is scientifically more interesting is to devise a learning strategy that is capable of jointly exploiting tag, image, and user information in a much more scalable manner than currently feasible. The importance of the filter component, which refines socially tagged training examples in advance to learning, is underestimated. Having a number of collaboratively labeled resources publicly available, research on joint exploration of social data and these resources is important. This connects to the most fundamental aspect of content-based image retrieval in the context of sharing and tagging within social media platforms: to what extent a social tag can be trusted remains open. Image retrieval by multi-tag query is another important yet largely unexplored problem. For a query of two tags, it is suggested to view the two tags as a single bi-gram tag (Li et al., 2012; Nie et al., 2012; Borth et al., 2013), which is found to be superior to late fusion of individual tag scores. Nonetheless, due to the increasing sparseness of n-grams, how to effectively answer generic queries of more than two tag is challenging. Exploiting further modalities remain still a largely unexplored area of research. In Chapter 5 we investigated the correlation of tags with the ground truth and events gathered from news by considering the time dimension. Although of limited scope, the study found that objective tags have a strong correlation to both content and context, giving a promising direction for improving content understanding. Possible extensions of this work include the exploration of how richer textual and semantic cues from natural language annotations might improve our models. Compared to extracting objective information, subjective information extraction is still young and full of exciting directions. We are still far from getting reliable estimations of sentiments in visual content. Current features are handcrafted on psychological or empirical studies but they are inherently affected by the semantic gap. Automatically learning features alike to approaches used in deep learning could bring considerable improvements in recognizing feelings despite the hard interpretability of filters. We barely scratched the surface in Chapter 6. Similarly, the prediction of popularity is still relying in basic handcrafted features. Although the social network aspects are well known to be related to popularity, visual content and context analysis is still needed when aiming to maximize popularity of a content. An underestimated factor is the peculiarity of different cultures in having different values and thus interest and feelings. Social networks can provide a world playground for study these aspects.

We see contributions of this field as essential to other related fields such as that of computer vision and artificial intelligence. The last two years were marked by a surge of deep convolutional models that showed remarkable improvement on vision tasks such as object recognition and image captioning. However, their limit is related to the strong supervision they need for train-

ing. Due to the cost of scaling these approaches, we expect an increased interest in unsupervised and semi-supervised learning, ultimately reaching social networks as an essential source of media.

“One way to resolve the semantic gap comes from sources outside the image ...”, Smeulders *et al.* wrote at the end of their seminal paper (Smeulders et al., 2000). While what such sources would be was mostly unknown by that time, it is now becoming evident that the many images shared and tagged in social media platforms are promising to resolve the semantic gap. By adding new relevant tags, refining the existing ones or directly addressing retrieval, the access to the semantic of the content has been much improved. This is achieved only when appropriate care is taken to attack the unreliability of social tagging.

Appendix A

Publications

This research activity has led to several publications in international journals and conferences. These are summarized below.¹

International Journals

1. **T. Uricchio**, L. Ballan, L. Seidenari, A. Del Bimbo, “Automatic Image Annotation via Label Transfer in the Semantic Space”, In *Pattern Recognition*, Volume 71, November 2017, Pages 144-157, DOI: 10.1016/j.patcog.2017.05.019.
2. X. Li*, **T. Uricchio***, L. Ballan, M. Bertini, C.G.M. Snoek, A. Del Bimbo, “Socializing the Semantic Gap: A Comparative Survey on Image Tag Assignment, Refinement and Retrieval”, *ACM Computing Surveys (CSUR)*, Volume 49 Issue 1, July 2016, DOI: 10.1145/2906152 (* indicates equal contribution).
3. L. Ballan*, M. Bertini*, **T. Uricchio***, A. Del Bimbo*, “Data-driven approaches for social image and video tagging”. In *Multimedia Tools and Applications, Feb 2015, Volume 74, Issue 4, pp. 1443-1468*. DOI: 10.1007/s11042-014-1976-4 *equal contribution.
4. C. Baecchi, **T. Uricchio**, M. Bertini, A. Del Bimbo, “A multimodal feature learning approach for sentiment analysis of social network multimedia”. In *Multimedia Tools and Applications.*, Volume 75, March 2016, Issue 5, pp. 2507-2525. DOI: 10.1007/s11042-015-2646-x.

International Conferences and Workshops

Tutorials

1. X. Li*, **T. Uricchio***, L. Ballan, M. Bertini, C.G.M. Snoek, A. Del Bimbo, “Image Tag Assignment, Refinement and Retrieval”. In *Proc. of ACM Conference on Multimedia Conference (ACM MM)*, Brisbane, Australia, 2015. *equal contribution.
2. X. Li*, **T. Uricchio***, L. Ballan, M. Bertini, C.G.M. Snoek, A. Del Bimbo, “Image Tag Assignment, Refinement and Retrieval”. In *Proc. of Computer Vision and Pattern Recognition (CVPR)*, Las Vegas, USA, 2016, (* indicates equal contribution).

¹The author’s bibliometric indices at the end of his PhD were the following *H*-index = 5, total number of citations = 43, i10-index = 1 (source: Google Scholar on November 28, 2015).

Image Understanding by Socializing the Semantic Gap

3. X. Li*, **T. Uricchio***, L. Ballan, M. Bertini, C.G.M. Snoek, A. Del Bimbo, “Image Tag Assignment, Refinement and Retrieval”. In *Proc. of International Conference on Image Analysis and Processing (ICIAP)*, Catania, Italy, 2017, (* indicates equal contribution).

Conferences and Workshops

1. F. Gelli, **T. Uricchio**, M. Bertini, A. Del Bimbo, S-F. Chang, “Image Popularity Prediction in Social Media Using Sentiment and Context Features”, In *Proc. of ACM Conference on Multimedia Conference (ACM MM)*, Brisbane, Australia, 2015.
2. L. Ballan*, **T. Uricchio***, L. Seidenari, A. Del Bimbo, “A Cross-media Model for Automatic Image Annotation”. In *Proc. of ACM International Conference on Multimedia Retrieval (ICMR)*, Glasgow, United Kingdom, 2014, *equal contribution.
3. **T. Uricchio**, L. Ballan, M. Bertini, and A. Del Bimbo, “Evaluating Temporal Information for Social Image Annotation and Retrieval”. In *Proc. of International Conference on Image Analysis and Processing (ICIAP)*, Napoli, Italy, 2013.
4. **T. Uricchio**, L. Ballan, M. Bertini, and A. Del Bimbo, “An Evaluation of Nearest-Neighbor Methods for Tag Refinement”. In *Proc. of IEEE International Conference on Multimedia & Expo (ICME)*, San Jose, CA, USA, 2013.
5. **T. Uricchio**, L. Ballan, M. Bertini, and A. Del Bimbo, “MICC-UNIFI at Image-CLEF 2013 Scalable Concept Image Annotation”. In *Proc. of Conference and Labs of the Evaluation Forum (CLEF)*, Valencia, Spain, 2013.
6. **T. Uricchio***, M. Bertini*, L. Seidenari, A. Del Bimbo, “Fisher Encoded Convolutional Bag-of-Boxes for Efficient Image Annotation and Retrieval”. *Proc. of International Conference on Computer Vision Workshops (ICCVW)*, Santiago, Chile, 2015, *equal contribution.
7. L. Ballan, M. Bertini, **T. Uricchio**, and A. Del Bimbo, “Social Media Annotation”. In *Proc. of IEEE International Workshop on Content-Based Multimedia Indexing (CBMI)*, Veszprem, Hungary, 2013.

Acknowledgments

This thesis would not have been possible without the help and support of many people. First, I would like to acknowledge the efforts and input of my supervisors, Prof. Alberto Del Bimbo and Prof. Marco Bertini, who were of great help during my research. I thank Telecom Italia and my industrial tutor Carlo Alberto Licciardi for their support of my work.

Many people contributed to the development of this research. The discussions with Dr. Lamberto Ballan were extremely important to me and the success of this work. Thank you for your patience and insightful suggestions. Special thanks to Prof. Cees G.M. Snoek, Dr. Xirong Li, Dr. Lorenzo Seidenari, Dr. Claudio Baecchi and Francesco Gelli who collaborated on several parts of my research work. I will be always grateful to you all. Props out to Prof. Paolo Frasconi who inspired me with his visionary look at research. His passion has always encouraged me to take bolder roads.

Many many thanks to all my colleagues of the Media Integration and Communication Center (MICC): Dr. Irene Amerini, Prof. Andrew Bagdanov, Dr. Federico Bartoli, Federico Becattini, Giuseppe Becchi, Enrico Bondi, Matteo Bruni, Dr. Maxime Devanne, Dr. Dario Di Fina, Dr. Simone Ercoli, Andrea Ferracani, Claudio Ferrari, Leonardo Galteri, Dr. Svebor Karaman, Dr. Giuseppe Lisanti, Dr. Iacopo Masi, Dr. Federico Pernici, Daniele Pezzatini, Andrea Salvi, Dr. Francesco Turchini. In these years, their enthusiasm and their support was extremely important to me during the highs and especially in the lows.

Thanks to my long-standing friends Elisa, Filippo, Francesco, Giulia, Laura, Leonardo, Massimo, Riccardo, Stefano, Yasamin. You are very important to me. Finally, I don't know how I would have made it through without the support of Valentina and my family. I thank them deeply for all the love and understanding.

Bibliography

- Alonso, O., Gertz, M. and Baeza-Yates, R. (2007), ‘On the value of temporal information in information retrieval’, *SIGIR Forum* **41**(2), 35–41.
- Andrews, S., Tsochantaridis, I. and Hofmann, T. (2003), Support vector machines for multiple-instance learning, in ‘Proc. of NIPS’, pp. 561–568.
- Atrey, P., Hossain, M., El Saddik, A. and Kankanhalli, M. (2010), ‘Multimodal fusion for multimedia analysis: a survey’, *Multimedia Systems* **16**(6), 345–379.
- Bae, Y. and Lee, H. (2012), ‘Sentiment analysis of Twitter audiences: Measuring the positive or negative influence of popular twitterers’, *JASIST* **63**(12), 2521–2535.
- Bacchi, C., Turchini, F., Seidenari, L., Bagdanov, A. D. and Bimbo, A. D. (2014), Fisher vectors over random density forests for object recognition, in ‘Proc. of International Conference on Pattern Recognition (ICPR)’.
- Ballan, L., Bertini, M., Uricchio, T. and Del Bimbo, A. (2014), ‘Data-driven approaches for social image and video tagging’, *Multimedia Tools and Applications* **74**(4), 1443–1468.
- Ballan, L., Uricchio, T., Seidenari, L. and Bimbo, A. D. (2014), A cross-media model for automatic image annotation, in ‘Proc. of ACM ICMR’, pp. 73–80.
- Barbosa, L. and Feng, J. (2010), Robust sentiment detection on Twitter from biased and noisy data, in ‘Proc. of International Conference on Computational Linguistics (COLING)’.
- Barnard, K., Duygulu, P., Forsyth, D., De Freitas, N., Blei, D. M. and Jordan, M. I. (2003), ‘Matching words and pictures’, *JMLR* **3**, 1107–1135.
- Bastien, F., Lamblin, P., Pascanu, R., Bergstra, J., Goodfellow, I., Bergeron, A., Bouchard, N., Warde-Farley, D. and Bengio, Y. (2012), ‘Theano: new features and speed improvements’, *arXiv preprint arXiv:1211.5590*.
- Bengio, Y. (2009), ‘Learning deep architectures for AI’, *Foundations and Trends in Machine Learning* **2**(1), 1–127.
- Bengio, Y., Schwenk, H., Senécal, J.-S., Morin, F. and Gauvain, J.-L. (2006), Neural probabilistic language models, in ‘Innovations in Machine Learning’, Springer, pp. 137–186.
- Bian, J., Yang, Y. and Chua, T.-S. (2013), Multimedia summarization for trending topics in microblogs, in ‘Proc. of the ACM International Conference on Information & Knowledge Management (CIKM)’, pp. 1807–1812.
- Bifet, A. and Frank, E. (2010), Sentiment knowledge discovery in Twitter streaming data, in ‘Proc. of International Conference on Discovery Science (DS)’.
- Bird, S., Loper, E. and Klein, E. (2009), *Natural Language Processing with Python*, O’Reilly Media Inc.
- Blei, D., Ng, A. and Jordan, M. (2003), ‘Latent Dirichlet Allocation.’, *Journal of Machine Learning Research* **3**, 993–1022.
- Borth, D., Ji, R., Chen, T., Breuel, T. and Chang, S.-F. (2013), Large-scale visual sentiment ontology and detectors using adjective noun pairs, in ‘Proc. of ACM International Conference on Multimedia (MM)’, pp. 223–232.
- Bravo-Marquez, F., Mendoza, M. and Poblete, B. (2013), Combining strengths, emotions and polarities for boosting Twitter sentiment analysis, in ‘Proc. of ACM International Workshop on Issues of Sentiment Discovery and Opinion Mining (WISDOM)’.
- Candès, E., Li, X., Ma, Y. and Wright, J. (2011), ‘Robust principal component analysis?’,

Image Understanding by Socializing the Semantic Gap

- Journal of the ACM* **58**(3), 11.
- Cao, D., Ji, R., Lin, D. and Li, S. (2014), ‘A cross-media public sentiment analysis system for microblog’, *Multimedia Systems (MS)* pp. 1–8.
- Carneiro, G., Chan, A. B., Moreno, P. J. and Vasconcelos, N. (2007), ‘Supervised learning of semantic classes for image annotation and retrieval’, *IEEE TPAMI* **29**(3), 394–410.
- Chatfield, K., Simonyan, K., Vedaldi, A. and Zisserman, A. (2014), Return of the devil in the details: Delving deep into convolutional nets, in ‘Proc. of BMVC’.
- Chatzopoulou, G., Sheng, C. and Faloutsos, M. (2010), A first step towards understanding popularity in YouTube, in ‘Proc. of INFOCOM’.
- Chen, L., Xu, D., Tsang, I. and Luo, J. (2012), ‘Tag-based image retrieval improved by augmented features and group-based refinement’, *IEEE Transactions on Multimedia* **14**(4), 1057–1067.
- Chen, T., Borth, D., Darrell, T. and Chang, S.-F. (2014), ‘DeepSentiBank: Visual sentiment concept classification with deep convolutional neural networks’, *arXiv:1410.8586*
- Chen, T., Lu, D., Kan, M.-Y. and Cui, P. (2013), Understanding and classifying image tweets, in ‘Proc. of ACM International Conference on Multimedia (MM)’, pp. 781–784.
- Chen, T., Yu, F. X., Chen, J., Cui, Y., Chen, Y.-Y. and Chang, S.-F. (2014), Object-based visual sentiment concept analysis and application, in ‘Proc. of ACM MM’.
- Chen, Y.-Y., Chen, T., Hsu, W. H., Liao, H.-Y. M. and Chang, S.-F. (2014), Predicting viewer affective comments based on image content in social media, in ‘Proc. of ACM International Conference on Multimedia Retrieval (ICMR)’, pp. 233:233–233:240.
- Choi, H. and Varian, H. (2011), Predicting the present with Google Trends, Technical report, Google.
- Chua, T.-S., Tang, J., Hong, R., Li, H., Luo, Z. and Zheng, Y.-T. (2009), Nus-wide: A real-world web image database from national university of singapore, in ‘Proc. of ACM Conf. on Image and Video Retrieval (CIVR’09)’.
- Cilibiasi, R. and Vitanyi, P. (2004), ‘The Google similarity distance’, *IEEE Transactions on Knowledge and Data Engineering* **19**(3), 370–383.
- Cohen, J. (1988), *Statistical power analysis for the behavioral sciences*, Routledge Academic.
- Collobert, R. and Weston, J. (2008), A unified architecture for natural language processing: Deep neural networks with multitask learning, in ‘Proc. of International Conference on Machine Learning (ICML)’.
- Dan-Glauser, E. and Scherer, K. (2011), ‘The geneva affective picture database (gaped): a new 730-picture database focusing on valence and normative significance’, *Behavior Research Methods* **43**(2), 468–477.
- Datta, R., Joshi, D., Li, J. and Wang, J. (2008), ‘Image retrieval: ideas, influences, and trends of the new age’, *ACM Computing Surveys* **40**(2), 5:1–5:60.
- Deitrick, W. and Hu, W. (2013), ‘Mutually enhancing community detection and sentiment analysis on Twitter networks’, *Journal of Data Analysis and Information Processing* **1**(3), 19:29.
- Deng, J., Dong, W., Socher, R., Li, L., Li, K. and Fei-Fei, L. (2009), ImageNet: A large-scale hierarchical image database, in ‘Proc. of CVPR’, pp. 248–255.
- Diener, E. and DeFour, D. (1978), ‘Does television violence enhance program popularity?’, *JPSP* **36**(3), 333.
- Dodge, J., Goyal, A., Han, X., Mensch, A., Mitchell, M., Stratos, K., Yamaguchi, K., Choi, Y., Daumé, III, H., Berg, A. and Berg, T. (2012), Detecting visual text, in ‘Proc. of NAACL’, pp. 762–772.
- Duan, K., Crandall, D. J. and Batra, D. (2014), Multimodal learning in loosely-organized web images, in ‘Proc. of CVPR’, pp. 2465–2472.
- Duan, L., Li, W., Tsang, I. and Xu, D. (2011), ‘Improving web image search by bag-based reranking’, *IEEE Transactions on Image Processing* **20**(11), 3280–3290.
- Duygulu, P., Barnard, K., de Freitas, J. F. G. and Forsyth, D. A. (2002), Object recognition as machine translation: Learning a lexicon for a fixed image vocabulary, in ‘Proc. of ECCV’.
- Everingham, M., Eslami, S., Gool, L. V., Williams, C., Winn, J. and Zisserman, A. (2015),

- ‘The PASCAL visual object classes challenge - a retrospective’, *International Journal of Computer Vision* **111**(1), 98–136.
- Fan, R.-E., Chang, K.-W., Hsieh, C.-J., Wang, X.-R. and Lin, C.-J. (2008), ‘LIBLINEAR: A library for large linear classification’, *Journal of Machine Learning Research* **9**, 1871–1874.
- Feng, S. L., Manmatha, R. and Lavrenko, V. (2004), Multiple bernoulli relevance models for image and video annotation, in ‘Proc. of CVPR’.
- Feng, S., Lang, C. and Li, B. (2012), Towards relevance and saliency ranking of image tags, in ‘Proc. of ACM MM’, pp. 917–920.
- Feng, Z., Feng, S., Jin, R. and Jain, A. (2014), Image tag completion by noisy matrix recovery, in ‘Proc. of ECCV’, pp. 424–438.
- Figueiredo, F., Almeida, J. M., Gonçalves, M. A. and Benevenuto, F. (2014), ‘On the dynamics of social media popularity: A YouTube case study’, *TOIT* **14**(4), 24.
- Finkel, J. R., Grenager, T. and Manning, C. (2005), Incorporating non-local information into information extraction systems by Gibbs sampling, in ‘Proc. of ACL’.
- Freund, Y., Iyer, R., Schapire, R. and Singer, Y. (2003), ‘An efficient boosting algorithm for combining preferences’, *Journal of Machine Learning Research* **4**, 933–969.
- Fu, H., Zhang, Q. and Qiu, G. (2012), Random forest for image annotation, in ‘Proc. of ECCV’.
- Gao, Y., Wang, M., Zha, Z.-J., Shen, J., Li, X. and Wu, X. (2013), ‘Visual-textual joint relevance learning for tag-based social image search’, *IEEE Transactions on Image Processing* **22**(1), 363–376.
- Ghiassi, M., Skinner, J. and Zimbra, D. (2013), ‘Twitter brand sentiment analysis: A hybrid system using n-gram analysis and dynamic artificial neural network’, *Expert Systems with Applications* **40**(16), 6266–6282.
- Ginsberg, J., Mohebbi, M. H., Patel, R. S., Brammer, L., Smolinski, M. S. and Brilliant, L. (2009), ‘Detecting influenza epidemics using search engine query data’, *Nature* **457**(7232), 1012–1014.
- Ginsca, A., Popescu, A., Ionescu, B., Armagan, A. and Kanellos, I. (2014), Toward an estimation of user tagging credibility for social image retrieval, in ‘Proc. of ACM MM’, pp. 1021–1024.
- Go, A., Bhayani, R. and Huang, L. (2009), Twitter sentiment classification using distant supervision, Technical report, CS224N Project Report, Stanford.
- Golder, S. and Huberman, B. (2006), ‘Usage patterns of collaborative tagging systems’, *Journal of Information Science* **32**(2), 198–208.
- Golub, G. and Van Loan, C. (2012), *Matrix computations*, Vol. 3, JHU Press.
- Gong, Y., Ke, Q., Isard, M. and Lazebnik, S. (2013), ‘A multi-view embedding space for internet images, tags, and their semantics’, *IJCV* **in press**.
- Grangier, D. and Bengio, S. (2008), ‘A discriminative kernel- based approach to rank images from text queries’, *IEEE TPAMI* **30**(8), 1371–1384.
- Grauman, K. and Darrell, T. (2005), The pyramid match kernel: Discriminative classification with sets of image features, in ‘Proc. of International Conference on Computer Vision (ICCV)’.
- Grubinger, M., Clough, P., Muller, H. and Deselaers, T. (2006), The IAPR TC-12 benchmark: a new evaluation resource for visual information systems, in ‘Proc. of LREC’.
- Guillaumin, M., Mensink, T., Verbeek, J. and Schmid, C. (2009), TagProp: Discriminative metric learning in nearest neighbor models for image auto-annotation, in ‘Proc. of ICCV’, pp. 309–316.
- Gupta, M., Li, R., Yin, Z. and Han, J. (2010), ‘Survey on social tagging techniques’, *SIGKDD Explorations Newsletter* **12**(1), 58–72.
- Gutmann, M. U. and Hyvärinen, A. (2012), ‘Noise-contrastive estimation of unnormalized statistical models, with applications to natural image statistics’, *The Journal of Machine Learning Research (JMLR)* **13**(1), 307–361.
- Hardoon, D. R. and Shawe-Taylor, J. (2003), KCCA for different level precision in content-based image retrieval, in ‘Proc. of IEEE CBMI’.
- Hardoon, D. R., Szedmak, S. and Shawe-Taylor, J. (2004), ‘Canonical correlation analysis:

Image Understanding by Socializing the Semantic Gap

- An overview with application to learning methods', *Neural Computation* **16**(12), 2639–2664.
- Huiskes, M. J. and Lew, M. S. (2008), The MIR Flickr retrieval evaluation, in 'Proc. of ACM MIR'.
- Huiskes, M. J., Thomee, B. and Lew, M. S. (2010), New trends and ideas in visual concept detection: the MIR Flickr retrieval evaluation initiative, in 'Proc. of ACM MIR', pp. 527–536.
- Hwang, S. J. and Grauman, K. (2012), 'Learning the relative importance of objects from tagged images for retrieval and cross-modal search', *IJCV* **100**(2), 134–153.
- Jabeen, F., Khusro, S., Majid, A. and Rauf, A. (2015), 'Semantics discovery in social tagging systems: A review', *Multimedia Tools and Applications* **In press**.
- Järvelin, K. and Kekäläinen, J. (2002), 'Cumulated gain-based evaluation of IR techniques', *ACM Transactions on Intelligent Systems and Technology* **20**(4), 422–446.
- Jégou, H., Douze, M. and Schmid, C. (2011), 'Product quantization for nearest neighbor search', *IEEE Transactions on Pattern Analysis and Machine Intelligence* **33**(1), 117–128.
- Jiang, L., Yu, M., Zhou, M., Liu, X. and Zhao, T. (2011), Target-dependent Twitter sentiment classification, in 'Proc. of ACL Annual Meeting of the Association for Computational Linguistics: Human Language Technologies (HLT)'.
- Jiang, Y.-G., Ngo, C.-W. and Chang, S.-F. (2009), Semantic context transfer across heterogeneous sources for domain adaptive video search, in 'Proc. of ACM MM', pp. 155–164.
- Jin, X., Gallagher, A., Cao, L., Luo, J. and Han, J. (2010), The wisdom of social multimedia: using Flickr for prediction and forecast, in 'Proc. of ACM MM', pp. 1235–1244.
- Jin, Y., Khan, L., Wang, L. and Awad, M. (2005), Image annotations by combining multiple evidence & Wordnet, in 'Proc. of ACM MM', pp. 706–715.
- Joachims, T. (1999), Transductive inference for text classification using support vector machines, in 'Proc. of ICML', pp. 200–209.
- Johnson, J., Ballan, L. and Fei-Fei, L. (2015), Love thy neighbors: Image annotation by exploiting image metadata, in 'Proc. of ICCV'.
- Joshi, D., Datta, R., Fedorovskaya, E., Luong, Q.-T., Wang, J., Li, J. and Luo, J. (2011), 'Aesthetics and emotions in images', *IEEE Signal Processing Magazine (MSP)* **28**(5), 94–115.
- Kalayeh, M. M., Idrees, H. and Shah, M. (2014), NMF-KNN: Image annotation using weighted multi-view non-negative matrix factorization, in 'Proc. of CVPR', pp. 184–191.
- Kaneko, T., Harada, H. and Yanai, K. (2013), Twitter visual event mining system, in 'Proc. of IEEE International Conference on Multimedia and Expo Workshops (ICMEW)', pp. 1–2.
- Kennedy, L. S., Chang, S.-F. and Kozintsev, I. (2006), To search or to label? Predicting the performance of search-based automatic image classifiers, in 'Proc. of ACM MIR', pp. 249–258.
- Kennedy, L. S., Slaney, M. and Weinberger, K. (2009), Reliable tags using image similarity: mining specificity and expertise from large-scale multimedia databases, in 'Proc. of ACM MM Workshop on Web-scale Multimedia Corpus', pp. 17–24.
- Khosla, A., Das Sarma, A. and Hamid, R. (2014), What makes an image popular?, in 'Proc. of WWW'.
- Kim, G., Fei-Fei, L. and Xing, E. P. (2012), Web image prediction using multivariate point processes, in 'Proc. of ACM SIGKDD', pp. 1068–1076.
- Kim, G. and Xing, E. (2013), Time-sensitive web image ranking and retrieval via dynamic multi-task regression, in 'Proc. of ACM WSDM', pp. 163–172.
- Kim, G., Xing, E. P. and Torralba, A. (2010), Modeling and analysis of dynamic behaviors of web image collections, in 'Proc. of ECCV', pp. 85–98.
- Krizhevsky, A., Sutskever, I. and Hinton, G. E. (2012), Imagenet classification with deep convolutional neural networks, in 'Proc. of Neural Information Processing Systems (NIPS)', pp. 1097–1105.
- Kuo, Y.-S., Cheng, W.-H., Lin, H.-T. and Hsu, W. (2012), 'Unsupervised semantic feature discovery for image object retrieval and tag refinement', *IEEE Transactions on*

- Multimedia* **14**(4), 1079–1090.
- Lan, T. and Mori, G. (2013), A max-margin riffled independence model for image tag ranking, in ‘Proc. of CVPR’, pp. 3103–3110.
- Lang, P. J., Bradley, M. M. and Cuthbert, B. N. (1999), ‘International affective picture system (iaps): Technical manual and affective ratings’.
- Lavrenko, V., Manmatha, R. and Jeon, J. (2003), A model for learning the semantics of pictures, in ‘Proc. of NIPS’.
- Lazebnik, S., Schmid, C. and Ponce, J. (2006), Beyond bags of features: Spatial pyramid matching for recognizing natural scene categories, in ‘Proc. of Conference on Computer Vision and Pattern Recognition (CVPR)’.
- Le, Q. V. and Mikolov, T. (2014), Distributed representations of sentences and documents, in ‘Proc. of International Conference on Machine Learning (ICML)’.
- Lee, S., De Neve, W. and Ro, Y. (2013), ‘Visually weighted neighbor voting for image tag relevance learning’, *Multimedia Tools and Applications* **72**(2), 1363–1386.
- Li, L.-J. and Fei-Fei, L. (2010), ‘OPTIMOL: Automatic online picture collection via incremental model learning’, *IJCV* **88**(2), 147–168.
- Li, M. (2007), Texture moment for content-based image retrieval, in ‘Proc. of ICME’, pp. 508–511.
- Li, T., Mei, T., Kweon, I.-S. and Hua, X.-S. (2011), ‘Contextual bag-of-words for visual categorization’, *IEEE Transaction on Circuits and Systems for Video Technology (TCSVT)* **21**(4), 381–392.
- Li, W., Duan, L., Xu, D. and Tsang, I. (2011), Text-based image retrieval using progressive multi-instance learning, in ‘Proc. of ICCV’, pp. 2049–2055.
- Li, X. (2015), ‘Tag relevance fusion for social image retrieval’, *Multimedia Systems* **In press**.
- Li, X., Gavves, E., Snoek, C., Worring, M. and Smeulders, A. (2011), Personalizing automated image annotation using cross-entropy, in ‘Proc. of ACM MM’, pp. 233–242.
- Li, X. and Snoek, C. (2013), Classifying tag relevance with relevant positive and negative examples, in ‘Proc. of ACM MM’, pp. 485–488.
- Li, X., Snoek, C. and Worring, M. (2009a), Annotating images by harnessing worldwide user-tagged photos, in ‘Proc. of ICASSP’, pp. 3717–3720.
- Li, X., Snoek, C. and Worring, M. (2009b), ‘Learning social tag relevance by neighbor voting’, *IEEE Transactions on Multimedia* **11**(7), 1310–1322.
- Li, X., Snoek, C. and Worring, M. (2010), Unsupervised multi-feature tag relevance learning for social image retrieval, in ‘Proc. of ACM CIVR’, pp. 10–17.
- Li, X., Snoek, C., Worring, M., Koelma, D. and Smeulders, A. (2013), ‘Bootstrapping visual categorization with relevant negatives’, *IEEE Transactions on Multimedia* **15**(4), 933–945.
- Li, X., Snoek, C., Worring, M. and Smeulders, A. (2012), ‘Harvesting social images for bi-concept search’, *IEEE Transactions on Multimedia* **14**(4), 1091–1104.
- Li, X., Uricchio, T., Ballan, L., Bertini, M., Snoek, C. G. and Del Bimbo, A. (2015), ‘Socializing the semantic gap: A comparative survey on image tag assignment, refinement and retrieval’, *arXiv preprint arXiv:1503.08248*.
- Li, Z., Liu, J. and Lu, H. (2013), ‘Nonlinear matrix factorization with unified embedding for social tag relevance learning’, *Neurocomputing* **105**, 38–44.
- Li, Z., Liu, J., Zhu, X., Liu, T. and Lu, H. (2010), Image annotation using multi-correlation probabilistic matrix factorization, in ‘Proc. of ACM MM’, pp. 1187–119.
- Lin, H.-T., Lin, C.-J. and Weng, R. (2007), ‘A note on Platt’s probabilistic outputs for support vector machines’, *Machine Learning* **68**(3), 267–276.
- Lin, Z., Ding, G., Hu, M., Wang, J. and Ye, X. (2013), Image tag completion via image-specific and tag-specific linear sparse reconstructions, in ‘Proc. of CVPR’, pp. 1618–1625.
- Liu, D., Hua, X.-S., Wang, M. and Zhang, H.-J. (2010), Image retagging, in ‘Proc. of ACM MM’, pp. 491–500.
- Liu, D., Hua, X.-S., Yang, L., Wang, M. and Zhang, H.-J. (2009), Tag ranking, in ‘Proc. of WWW’, pp. 351–360.

- Liu, D., Hua, X.-S. and Zhang, H.-J. (2011), ‘Content-based tag processing for internet social images’, *Multimedia Tools and Applications* **51**(2), 723–738.
- Liu, D., Yan, S., Hua, X.-S. and Zhang, H.-J. (2011), ‘Image retagging using collaborative tag propagation’, *IEEE Transactions on Multimedia* **13**(4), 702–712.
- Liu, J., Li, M., Liu, Q., Lu, H. and Ma, S. (2009), ‘Image annotation via graph learning’, *Pattern Recognition* **42**(2), 218–228.
- Liu, J., Li, Z., Tang, J., Jiang, Y. and Lu, H. (2014), ‘Personalized geo-specific tag recommendation for photos on social websites’, *IEEE Transactions on Multimedia* **16**(3), 588–600.
- Liu, J., Zhang, Y., Li, Z. and Lu, H. (2013), ‘Correlation consistency constrained probabilistic matrix factorization for social tag refinement’, *Neurocomputing* **119**(7), 3–9.
- Liu, K.-L., Li, W.-J. and Guo, M. (2012), Emoticon smoothed language models for Twitter sentiment analysis., in ‘Proc. of AAAI Conference on Artificial Intelligence (CAI)’.
- Liu, Y., Wu, F., Zhang, Y., Shao, J. and Zhuang, Y. (2011), Tag clustering and refinement on semantic unity graph, in ‘Proc. of ICDM’, pp. 417–426.
- Ma, H., Zhu, J., Lyu, M.-T. and King, I. (2010), ‘Bridging the semantic gap between image contents and tags’, *IEEE Transactions on Multimedia* **12**(5), 462–473.
- Maji, S., Berg, A. and Malik, J. (2008), Classification using intersection kernel support vector machines is efficient, in ‘Proc. of CVPR’, pp. 1–8.
- Makadia, A., Pavlovic, V. and Kumar, S. (2008), A new baseline for image annotation, in ‘Proc. of ECCV’.
- Makadia, A., Pavlovic, V. and Kumar, S. (2010), ‘Baselines for image annotation’, *International Journal of Computer Vision* **90**(1), 88–105.
- McAuley, J. and Leskovec, J. (2012), Image labeling on a network: using social-network metadata for image classification, in ‘Proc. of ECCV’, pp. 828–841.
- McParlane, P. J. and Jose, J. (2014), Exploiting Twitter and Wikipedia for the annotation of event images, in ‘Proc. of ACM SIGIR International Conference on Research & Development in Information Retrieval’, pp. 1175–1178.
- McParlane, P. J., Moshfeghi, Y. and Jose, J. M. (2014), Nobody comes here anymore, it’s too crowded; predicting image popularity on Flickr, in ‘Proc. of ACM ICMR’.
- McParlane, P., Whiting, S. and Jose, J. (2013a), Improving automatic image tagging using temporal tag co-occurrence, in ‘Proc. of MMM’, pp. 251–262.
- McParlane, P., Whiting, S. and Jose, J. (2013b), On contextual photo tag recommendation, in ‘Proc. of ACM SIGIR’, pp. 965–968.
- Mei, T., Rui, Y., Li, S. and Tian, Q. (2014), ‘Multimedia search reranking: A literature survey’, *ACM Computing Surveys* **46**(3), 38.
- Metzler, D. and Manmatha, R. (2004), An inference network approach to image retrieval, in ‘Proc. of ACM CIVR’.
- Michalski, R. (1983), ‘A theory and methodology of inductive learning’, *Artificial intelligence* **20**(2), 111–161.
- Mikolov, T., Deoras, A., Kombrink, S., Burget, L. and Cernocky, J. H. (2011), Empirical evaluation and combination of advanced language modeling techniques, in ‘Proc. of Interspeech’.
- Mikolov, T., Sutskever, I., Chen, K., Corrado, G. S. and Dean, J. (2013), Distributed representations of words and phrases and their compositionality, in ‘Proc. of Neural Information Processing Systems (NIPS)’.
- Mikolov, T., Yih, W.-t. and Zweig, G. (2013), Linguistic regularities in continuous space word representations, in ‘Proc. of NAACL-HLT’, pp. 746–751.
- Mnih, A. and Hinton, G. E. (2009), A scalable hierarchical distributed language model, in ‘Proc. of Neural Information Processing Systems (NIPS)’.
- Monay, F. and Gatica-Perez, D. (2004), PLSA-based image auto-annotation: Constraining the latent space, in ‘Proc. of ACM Multimedia’.
- Moore, G. E. (1965), ‘Cramming more components onto integrated circuits’, **38**.
- Nie, L., Yan, S., Wang, M., Hong, R. and Chua, T.-S. (2012), Harvesting visual concepts for image search with complex queries, in ‘Proc. of ACM MM’, pp. 59–68.
- Niu, Z., Hua, G., Gao, X. and Tian, Q. (2014), Semi-supervised relational topic model for

- weakly annotated image recognition in social media, in ‘Proc. of CVPR’, pp. 4233–4240.
- Pereira, J. C., Coviello, E., Doyle, G., Rasiwasia, N., Lanckriet, G., Levy, R. and Vasconcelos, N. (2014), ‘On the role of correlation and abstraction in cross-modal multimedia retrieval’, *IEEE Transactions on Pattern Analysis and Machine Intelligence* **36**(3), 521–535.
- Perronnin, F., Liu, Y., Sánchez, J. and Poirier, H. (2010), Large-scale image retrieval with compressed fisher vectors, in ‘Proc. of Computer Vision and Pattern Recognition (CVPR)’.
- Perronnin, F., Sánchez, J. and Mensink, T. (2010), Improving the fisher kernel for large-scale image classification, in ‘Proc. of European Conference on Computer Vision (ECCV)’.
- Plutchik, R. (2001), ‘The nature of emotions’, *American Scientist* **89**(4), 344–350.
- Qi, G.-J., Aggarwal, C., Tian, Q., Ji, H. and Huang, T. (2012), ‘Exploring context and content links in social media: A latent space method’, *IEEE Transactions on Pattern Analysis and Machine Intelligence* **34**(5), 850–862.
- Qian, X., Hua, X.-S., Tang, Y. and Mei, T. (2014), ‘Social image tagging with diverse semantics’, *IEEE Transactions on Cybernetics* **44**(12), 2493–2508.
- Qian, Z., Zhong, P. and Wang, R. (2015), ‘Tag refinement for user-contributed images via graph learning and nonnegative tensor factorization’, *IEEE Signal Processing Letters* **22**(9), 1302–1305.
- Rasiwasia, N., Costa Pereira, J., Coviello, E., Doyle, G., Lanckriet, G. R. G., Levy, R. and Vasconcelos, N. (2010), A new approach to cross-modal multimedia retrieval, in ‘Proc. of ACM Multimedia’.
- Rattenbury, T., Good, N. and Naaman, M. (2007), Towards automatic extraction of event and place semantics from flickr tags, in ‘Proc. of ACM SIGIR’, pp. 103–110.
- Richter, F., Romberg, S., Horster, E. and Lienhart, R. (2012), ‘Leveraging community metadata for multimodal image ranking’, *Multimedia Tools and Applications* **56**(1), 35–62.
- Russakovsky, O., Deng, J., Su, H., Krause, J., Satheesh, S., Ma, S., Huang, Z., Karpathy, A., Khosla, A., Bernstein, M., Berg, A. and Fei-Fei, L. (2015), ‘ImageNet Large Scale Visual Recognition Challenge’, *International Journal of Computer Vision*. In press.
- Saif, H., Fernandez, M., He, Y. and Alani, H. (2013), Evaluation datasets for Twitter sentiment analysis, in ‘Proc. of AI*IA Emotion and Sentiment in Social and Expressive Media (ESSEM)’.
- Saif, H., He, Y. and Alani, H. (2012), Semantic sentiment analysis of Twitter, in ‘Proc. of International Conference on the Semantic Web (ISWC)’.
- Sang, J., Xu, C. and Liu, J. (2012), ‘User-aware image tag refinement via ternary semantic analysis’, *IEEE Transactions on Multimedia* **14**(3), 883–895.
- Sang, J., Xu, C. and Lu, D. (2012), ‘Learn to personalized image search from the photo sharing websites’, *IEEE Transactions on Multimedia* **14**(4), 963–974.
- Sawant, N., Datta, R., Li, J. and Wang, J. (2010), Quest for relevant tags using local interaction networks and visual content, in ‘Proc. of ACM MIR’, pp. 231–240.
- Sawant, N., Li, J. and Wang, J. (2011), ‘Automatic image semantic interpretation using social action and tagging data’, *Multimedia Tools and Applications* **51**(1), 213–246.
- Sen, S., Lam, S., Rashid, A., Cosley, D., Frankowski, D., Osterhouse, J., Harper, F. and Riedl, J. (2006), tagging, communities, vocabulary, evolution, in ‘Proc. of CSCW’, pp. 181–190.
- Serra, G., Alisi, T., Bertini, M., Ballan, L., Del Bimbo, A., Goix, L. and Licciardi, C. (2013), STAMAT: A framework for social topics and media analysis, in ‘Proc. of IEEE International Conference on Multimedia and Expo Workshops (ICMEW)’, pp. 1–2.
- Sigurbjörnsson, B. and van Zwol, R. (2008), Flickr tag recommendation based on collective knowledge, in ‘Proc. of WWW’, pp. 327–336.
- Simonyan, K. and Zisserman, A. (2015), Very deep convolutional networks for large-scale image recognition, in ‘Proc. of ICLR’.
- Sizov, S. (2010), Geofolk: latent spatial semantics in web 2.0 social media, in ‘Proc. of ACM WSDM’, pp. 281–290.

Image Understanding by Socializing the Semantic Gap

- Smeulders, A., Worring, M., Santini, S., Gupta, A. and Jain, R. (2000), 'Content-based image retrieval at the end of the early years', *IEEE Transactions on Pattern Analysis and Machine Intelligence* **22**(12), 1349–1380.
- Srivastava, N. and Salakhutdinov, R. (2014), 'Multimodal learning with deep boltzmann machines', *Journal of Machine Learning Research* **15**(1), 2949–2980.
- Sun, A., Bhowmick, S., Nguyen, K. and Bai, G. (2011), 'Tag-based social image retrieval: An empirical evaluation', *Journal of the American Society for Information Science and Technology* **62**(12), 2364–2381.
- Sundaram, H., Xie, L., De Choudhury, M., Lin, Y.-R. and Natsev, A. (2012), 'Multimedia semantics: Interactions between content and community', *Proceedings of the IEEE* **100**(9), 2737–2758.
- Tang, J., Hong, R., Yan, S., Chua, T.-S., Qi, G.-J. and Jain, R. (2011), 'Image annotation by kNN-sparse graph-based label propagation over noisily tagged web images', *ACM Transactions on Intelligent Systems and Technology* **2**(2), 14:1–14:15.
- Tang, J., Yan, S., Hong, R., Qi, G.-J. and Chua, T.-S. (2009), Inferring semantic concepts from community-contributed images and noisy tags, in 'Proc. of ACM MM', pp. 223–232.
- Team, R. C. (2011), 'R: A language and environment for statistical computing. vienna, austria: R foundation for statistical computing; 2008'.
- Tenenbaum, J. B., De Silva, V. and Langford, J. C. (2000), 'A global geometric framework for nonlinear dimensionality reduction', *Science* **290**(5500), 2319–2323.
- Thelwall, M., Buckley, K., Paltoglou, G., Cai, D. and Kappas, A. (2010), 'Sentiment strength detection in short informal text', *Journal of the American Society for Information Science and Technology* **61**(12), 2544–2558.
- Totti, L. C., Costa, F. A., Avila, S., Valle, E., Meira Jr, W. and Almeida, V. (2014), The impact of visual attributes on online image diffusion, in 'Proc. of WebSci'.
- Truong, B., Sun, A. and Bhowmick, S. (2012), Content is still king: the effect of neighbor voting schemes on tag relevance for social image retrieval, in 'Proc. of ACM ICMR', pp. 9:1–9:8.
- Tucker, L. (1966), 'Some mathematical notes on three-mode factor analysis', *Psychometrika* **31**(3), 279–311.
- Tumasjan, A., Sprenger, T. O., Sandner, P. G. and Welpe, I. M. (2010), Predicting elections with Twitter: What 140 characters reveal about political sentiment., in 'Proc. of AAAI International Conference on Weblogs and Social Media (ICWSM)'.
- Turian, J., Ratinov, L. and Bengio, Y. (2010), Word representations: a simple and general method for semi-supervised learning, in 'Proc. of ACL Annual Meeting of the Association for Computational Linguistics'.
- Uricchio, T., Ballan, L., Bertini, M. and Del Bimbo, A. (2013), An evaluation of nearest-neighbor methods for tag refinement, in 'Proc. of ICME'.
- van de Sande, K., Gevers, T. and Snoek, C. (2010), 'Evaluating color descriptors for object and scene recognition', *IEEE Transactions on Pattern Analysis and Machine Intelligence* **32**(9), 1582–1596.
- Verbeek, J., Guillaumin, M., Mensink, T. and Schmid, C. (2010), Image annotation with TagProp on the MIRFLICKR set, in 'Proc. of ACM MIR', pp. 537–546.
- Verma, Y. and Jawahar, C. V. (2012), Image annotation using metric learning in semantic neighbourhoods, in 'Proc. of ECCV'.
- Verma, Y. and Jawahar, C. V. (2013), Exploring svm for image annotation in presence of confusing labels, in 'Proc. of BMVC'.
- Vincent, P., Larochelle, H., Bengio, Y. and Manzagol, P.-A. (2008), Extracting and composing robust features with denoising autoencoders, in 'Proc. of International Conference on Machine Learning (ICML)', pp. 1096–1103.
- von Ahn, L. and Dabbish, L. (2004), Labeling images with a computer game, in 'Proc. of ACM CHI'.
- Vreeswijk, D., van de Sande, K., Snoek, C. and Smeulders, A. (2012), All vehicles are cars: Subclass preferences in container concepts, in 'Proc. of ACM ICMR', pp. 8:1–8:7.
- Wang, C., Zhang, L., Jing, F. and Zhang, H.-J. (2006), Image annotation refinement using random walk with restarts, in 'Proc. of ACM MM', pp. 647–650.

- Wang, G., Hoiem, D. and Forsyth, D. (2009a), Building text features for object image classification, in ‘Proc. of CVPR’, pp. 1367–1374.
- Wang, G., Hoiem, D. and Forsyth, D. (2009b), Learning image similarity from Flickr groups using stochastic intersection kernel machines, in ‘Proc. of ICCV’, pp. 428–435.
- Wang, J., Zhou, J., Xu, H., Mei, T., Hua, X.-S. and Li, S. (2014), ‘Image tag refinement by regularized latent Dirichlet allocation’, *Computer Vision and Image Understanding* **124**(0), 61–70.
- Wang, M., Cao, D., Li, L., Li, S. and Ji, R. (2014), Microblog sentiment analysis based on cross-media bag-of-words model, in ‘Proc. of International Conference on Internet Multimedia Computing and Service (ICIMCS)’, pp. 76:76–76:80.
- Wang, M., Hua, X.-S. and Zhang, H.-J. (2010), ‘Towards a relevant and diverse search of social images’, *IEEE Transactions on Multimedia* **12**(8), 829–842.
- Wang, M., Ni, B., Hua, X.-S. and Chua, T.-S. (2012), ‘Assistive tagging: A survey of multimedia tagging with human-computer joint exploration’, *ACM Computing Surveys* **44**(4), 25:1–25:24.
- Wang, W. and He, Q. (2008), A survey on emotional semantic image retrieval, in ‘Proc. of IEEE International Conference on Image Processing (ICIP)’, pp. 117–120.
- Wang, Z., Cui, P., Xie, L., Chen, H., Zhu, W. and Yang, S. (2012), Analyzing social media via event facets, in ‘Proc. of ACM International Conference on Multimedia (MM)’, pp. 1359–1360.
- Wu, L., Hua, X.-S., Yu, N., Ma, W.-Y. and Li, S. (2008), Flickr distance, in ‘Proc. of ACM MM’, pp. 31–40.
- Wu, L., Jin, R. and Jain, A. (2013), ‘Tag completion for image retrieval’, *IEEE Transactions on Pattern Analysis and Machine Intelligence* **35**(3), 716–727.
- Wu, L., Yang, L., Yu, N. and Hua, X.-S. (2009), Learning to tag, in ‘Proc. of WWW’, pp. 361–370.
- Wu, P., Hoi, S. C.-H., Zhao, P. and He, Y. (2011), Mining social images with distance metric learning for automated image tagging, in ‘Proc. of ACM WSDM’, pp. 97–206.
- Wu, Z. and Palmer, M. (1994), Verb semantic and lexical selection, in ‘Proc. of ACL’, pp. 133–138.
- Xu, H., Wang, J., Hua, X.-S. and Li, S. (2009), Tag refinement by regularized LDA, in ‘Proc. of ACM MM’, pp. 573–576.
- Xu, X., Shimada, A. and Taniguchi, R. (2014), Tag completion with defective tag assignments via image-tag re-weighting, in ‘Proc. of ICME’, pp. 1–6.
- Yanai, K. (2012), World Seer: A realtime geo-tweet photo mapping system, in ‘Proc. of ACM International Conference on Multimedia Retrieval (ICMR)’, pp. 65:1–65:2.
- Yang, K., Hua, X.-S., Wang, M. and Zhang, H.-J. (2011), ‘Tag tagging: Towards more descriptive keywords of image content’, *IEEE Transactions on Multimedia* **13**(4), 662–673.
- Yang, Y., Cui, P., Zhu, W., Zhao, H. V., Shi, Y. and Yang, S. (2014), Emotionally representative image discovery for social events, in ‘Proc. of ACM International Conference on Multimedia Retrieval (ICMR)’, pp. 177:177–177:184.
- Yang, Y., Gao, Y., Zhang, H., Shao, J. and Chua, T.-S. (2014), Image tagging with social assistance, in ‘Proc. of ACM ICMR’, pp. 81–88.
- Yavlinsky, A., Schofield, E. and Rüger, S. (2005), Automated image annotation using global features and robust nonparametric density estimation, in ‘Proc. of ACM CIVR’.
- Zhang, S., Huang, J., Huang, Y., Yu, Y., Li, H. and Metexas, D. N. (2010), Automatic image annotation using group sparsity, in ‘Proc. of CVPR’.
- Zhao, X., Zhu, F., Qian, W. and Zhou, A. (2012), Impact of multimedia in Sina Weibo: Popularity and life span, in ‘Proc. of Chinese Semantic Web Symposium and the First Chinese Web Science Conference (CSWS & CWSC)’.
- Zhou, B., Jagadeesh, V. and Piramuthu, R. (2015), ConceptLearner: Discovering visual concepts from weakly labeled image collections, in ‘Proc. of CVPR’.
- Zhou, D., Huang, J. and Schölkopf, B. (2006), Learning with hypergraphs: Clustering, classification, and embedding, in ‘Proc. of NIPS’, pp. 1601–1608.
- Zhu, G., Yan, S. and Ma, Y. (2010), Image tag refinement towards low-rank, content-tag

Image Understanding by Socializing the Semantic Gap

- prior and error sparsity, *in* 'Proc. of ACM MM', pp. 461–470.
- Zhu, S., Ngo, C.-W. and Jiang, Y.-G. (2012), 'Sampling and ontologically pooling web images for visual concept learning', *IEEE Transactions on Multimedia* **14**(4), 1068–1078.
- Zhu, X., Nejdl, W. and Georgescu, M. (2014), An adaptive teleportation random walk model for learning social tag relevance, *in* 'Proc. of ACM SIGIR', pp. 223–232.
- Zhuang, J. and Hoi, S. (2011), A two-view learning approach for image tag ranking, *in* 'Proc. of ACM WSDM', pp. 625–634.
- Znaidia, A., Le Borgne, H. and Hudelot, C. (2013), Tag completion based on belief theory and neighbor voting, *in* 'Proc. of ACM ICMR', pp. 49–56.

PREMIO TESI DI DOTTORATO

ANNO 2007

- Bracardi M., *La Materia e lo Spirito. Mario Ridolfi nel paesaggio umbro*
Coppi E., *Purines as Transmitter Molecules. Electrophysiological Studies on Purinergic Signalling in Different Cell Systems*
Mannini M., *Molecular Magnetic Materials on Solid Surfaces*
Natali I., *The Ur-Portrait. Stephen Hero ed il processo di creazione artistica in A Portrait of the Artist as a Young Man*
Petretto L., *Imprenditore ed Università nello start-up di impresa. Ruoli e relazioni critiche*

ANNO 2008

- Bemporad F., *Folding and Aggregation Studies in the Acylphosphatase-Like Family*
Buono A., *Esercito, istituzioni, territorio. Alloggiamenti militari e «case Herme» nello Stato di Milano (secoli XVI e XVII)*
Castenasi S., *La finanza di progetto tra interesse pubblico e interessi privati*
Colica G., *Use of Microorganisms in the Removal of Pollutants from the Wastewater*
Gabbiani C., *Proteins as Possible Targets for Antitumor Metal Complexes: Biophysical Studies of their Interactions*

ANNO 2009

- Decorosi F., *Studio di ceppi batterici per il biorisanamento di suoli contaminati da Cr(VI)*
Di Carlo P., *I Kalasha del Hindu Kush: ricerche linguistiche e antropologiche*
Di Patti F., *Finite-Size Effects in Stochastic Models of Population Dynamics: Applications to Biomedicine and Biology*
Inzitari M., *Determinants of Mobility Disability in Older Adults: Evidence from Population-Based Epidemiologic Studies*
Macri F., *Verso un nuovo diritto penale sessuale. Diritto vivente, diritto comparato e prospettive di riforma della disciplina dei reati sessuali in Italia*
Pace R., *Identità e diritti delle donne. Per una cittadinanza di genere nella formazione*
Vignolini S., *Sub-Wavelength Probing and Modification of Complex Photonic Structures*

ANNO 2010

- Fedi M., *«Tuo lumine». L'accademia dei Risvegliati e lo spettacolo a Pistoia tra Sei e Settecento*
Fondi M., *Bioinformatics of genome evolution: from ancestral to modern metabolism. Phylogenomics and comparative genomics to understand microbial evolution*
Marino E., *An Integrated Nonlinear Wind-Waves Model for Offshore Wind Turbines*
Orsi V., *Crisi e Rigenerazione nella valle dell'Alto Khabur (Siria). La produzione ceramica nel passaggio dal Bronzo Antico al Bronzo Medio*
Polito C., *Molecular imaging in Parkinson's disease*
Romano R., *Smart Skin Envelope. Integrazione architettonica di tecnologie dinamiche e innovative per il risparmio energetico*

ANNO 2011

- Acciaioi S., *Il trompe-l'œil letterario, ovvero il sorriso ironico nell'opera di Wilhelm Hauff*
Bernacchioni C., *Sfingolipidi bioattivi e loro ruolo nell'azione biologica di fattori di crescita e citochine*
Fabbri N., *Bragg spectroscopy of quantum gases: Exploring physics in one dimension*
Gordillo Hervás R., *La construcción religiosa de la Hélade imperial: El Panhelenion*
Mugelli C., *Indipendenza e professionalità del giudice in Cina*
Pollastri S., *Il ruolo di TAF12B e UVR3 nel ciclo circadiano dei vegetali*
Salizzoni E., *Paesaggi Protetti. Laboratori di sperimentazione per il paesaggio costiero euro-mediterraneo*

ANNO 2012

- Evangelisti E., *Structural and functional aspects of membranes: the involvement of lipid rafts in Alzheimer's disease pathogenesis. The interplay between protein oligomers and plasma membrane physicochemical features in determining cytotoxicity*
- Bondi D., *Filosofia e storiografia nel dibattito anglo-americano sulla svolta linguistica*
- Petrucchi F., *Petri Candidi Decembrii Epistolarum iuveniliū libri octo. A cura di Federico Petrucchi*
- Alberti M., *La 'scoperta' dei disoccupati. Alle origini dell'indagine statistica sulla disoccupazione nell'Italia liberale (1893-1915)*
- Gualdani R., *Using the Patch-Clamp technique to shed light on ion channels structure, function and pharmacology*
- Adessi A., *Hydrogen production using Purple Non-Sulfur Bacteria (PNSB) cultivated under natural or artificial light conditions with synthetic or fermentation derived substrates*
- Ramalli A., *Development of novel ultrasound techniques for imaging and elastography. From simulation to real-time implementation*

ANNO 2013

- Lunghi C., *Early cross-modal interactions and adult human visual cortical plasticity revealed by binocular rivalry*
- Brancasi I., *Architettura e illuminismo: filosofia e progetti di città nel tardo Settecento francese*
- Cucinotta E., *Produzione poetica e storia nella prassi e nella teoria greca di età classica*
- Pellegrini L., *Circostanze del reato: trasformazioni in atto e prospettive di riforma*
- Locatelli M., *Mid infrared digital holography and terahertz imaging*
- Muniz Miranda F., *Modelling of spectroscopic and structural properties using molecular dynamics*
- Bacci M., *Dinamica molecolare e modelli al continuo per il trasporto di molecole proteiche - Coarse-grained molecular dynamics and continuum models for the transport of protein molecules*
- Martelli R., *Characteristics of raw and cooked fillets in species of actual and potential interest for italian aquaculture: rainbow trout (*oncorhynchus mykiss*) and meagre (*argyrosomus regius*)*

ANNO 2014

- Lana D., *A study on cholinergic signal transduction pathways involved in short term and long term memory formation in the rat hippocampus. Molecular and cellular alterations underlying memory impairments in animal models of neurodegeneration*
- Lopez Garcia A., *Los Auditoria de Roma y el Athenaeum de Adriano*
- Pastorelli G., *L'immagine del cane in Franz Kafka*
- Bussoletti A., *L'età berlusconiana. Il centro-destra dai poli alla Casa della Libertà 1994-2001*
- Malavolti L., *Single molecule magnets sublimated on conducting and magnetic substrates*
- Belingardi C., *Comunanze urbane. Autogestione e cura dei luoghi*
- Guzzo E., *Il tempio nel tempio. Il tombeau di Rousseau al Panthéon di Parigi*

ANNO 2015

- Lombardi N., *MEREA FaPS: uno Studio di Farmacovigilanza Attiva e Farmacoepidemiologia in Pronto Soccorso*
- Baratta L., *«A Marvellous and Strange Event». Racconti di nascite mostruose nell'Inghilterra della prima età moderna*
- Richichi I.A., *La teocrazia: crisi e trasformazione di un modello politico nell'Europa del XVIII secolo*
- Palandri L., *I giudici e l'arte. Stati Uniti ed Europa a confronto*
- Caselli N., *Imaging and engineering optical localized modes at the nano scale*
- Calabrese G., *Study and design of topologies and components for high power density dc-dc converters*
- Porzilli S., *Rilevare l'architettura in legno. Protocolli metodologici per la documentazione delle architetture tradizionali lignee: i casi studio dei villaggi careliani in Russia*

ANNO 2016

Martinelli S., *Study of intracellular signaling pathways in Chronic Myeloproliferative Neoplasms*

Abbado E., *“La celeste guida”. L’oratorio musicale a Firenze: 1632-1799*

Focarile P., *I Mannelli di Firenze. Storia mecenatismo e identità di una famiglia fra cultura mercantile e cultura cortigiana*

Nucciotti A., *La dimensione normativa dell’imprenditorialità accademica. Tre casi di studio sugli investigatori principali, i loro gruppi di ricerca e i fattori di innesco dell’imprenditorialità accademica*

Peruzzi P., *La inutilizzabilità della prestazione*

Lottini E., *Magnetic Nanostructures: a promising approach towards RE-free permanent magnets*

Uricchio T., *Image Understanding by Socializing the Semantic Gap*

